8-2010

CATALYSIS OF ETHANOL SYNTHESIS FROM SYNGAS

Jia Gao
Clemson University, jia@clemson.edu

CATALYSIS OF ETHANOL SYNTHESIS FROM SYNGAS

A Dissertation
Presented to
the Graduate School of
Clemson University

In Partial Fulfillment
of the Requirements for the Degree
Doctor of Philosophy
Chemical Engineer

---

by
Jia Gao
August 2010

Accepted by:
Dr. James G. Goodwin, Jr., Committee Chair
Dr. David A. Bruce
Dr. Christopher L. Kitchens
Dr. Shiou-Jyh Hwu

ABSTRACT

Catalytic synthesis of ethanol and other higher alcohols from CO hydrogenation has been a subject of significant research since the 1980s. The focus of this research is to establish a better fundamental insight into heterogeneous catalysis for CO hydrogenation reactions, in an attempt to design the best catalysts for ethanol synthesis.

It has been reported widely that promoted Rh-based catalysts can exhibit high selectivity to C_{2+} oxygenates during CO hydrogenation. The doubly promoted Rh-La-V/SiO_2 catalysts exhibited higher activity and selectivity for ethanol and other C_{2+} oxygenates than singly promoted catalysts. The better performance appears to be due to a synergistic promoting effect of the combined La and V additions through intimate contact with Rh.

The kinetic study carried out in this study shows that, in general, increasing H_2 pressure resulted in increased activities while increasing CO partial pressure had an opposite effect. Langmuir-Hinshelwood rate expressions for the formation of methane and of ethanol were derived and compared to the experimentally derived power law parameters. It was found that the addition of different promoters appeared to result in different rate limiting steps.

Strong metal-oxide interactions (SMOI) of Rh and vanadium oxide (as a promoter) supported on SiO_2 was studied. It was found by SSITKA (steady-state isotopic transient kinetic analysis) that the concentration of surface reaction intermediates decreased on $Rh/V/SiO_2$ as the reduction temperature increased, but the activities of the reaction sites

increased. The results suggest that Rh being covered by VO_x species is probably the main reason for the decreased overall activity induced by high reduction temperature, but more active sites appear to be formed probably at the Rh-VO_x interface.

The mechanism of C_1 and C_2 hydrocarbon and oxygenate formation during CO hydrogenation on Rh/SiO_2 was for the first time investigated in detail using multiproduct SSITKA. Based on SSITKA results, methanol and CH_4 appeared to be produced on different active sites. It is possible that C_2 products share at least one intermediate with CH_4, but not with methanol. Moreover, C_2 hydrocarbons are not likely to be formed from adsorbed acetaldehyde.

DEDICATION

I would like to dedicate my dissertation to my beloved parents, Xianmin Dou and Qi Gao, whose love, support and patience encouraged me all these years. Particularly, to my aunt, whose optimism and strong will in fighting serious illness gave me the courage to overcome any challenges in my life.

ACKNOWLEDGEMENTS

I would like to acknowledge and express my appreciation for the immeasurable support and guidance contributed by my advisor, Dr. James G. Goodwin, Jr. throughout this project. His high expectations to me and continuous encouragement are the power for me to conquer any difficulties in my work. Without his guidance, perseverance, and patience, I would have not finished this work. I also would like to thank Dr. Xunhua Mo, my academic mentor, who inspired the series of experiments described in this dissertation. Despite her busy schedule, she would always find the time guiding me in the lab to solve the tough and unexpected problems in experiments. Her creativity and wide-scope knowledge inspired me to take the experiment to unprecedented level. I wish to thank my committee members, Dr. David Bruce, Dr. Christopher Kitchens and Dr. Shiou-Jyh Hwu, not only for their input in the preparation of this dissertation, but also for the many hours of quality instruction they have provided to me in my graduate studies leading up to this point.

I would like to thank all the members of the Goodwin group who directly and indirectly provided helpful discussion and assistance. Additionally, I gratefully acknowledge U.S. Department of Energy for the financial supports and Dr. James Spivey at Louisiana State University for his contribution to this project.

TABLE OF CONTENTS

Table of Contents (Continued)

Page

Table of Contents (Continued)

Page

LIST OF TABLES

List of Tables (Continued)

LIST OF FIGURES

List of Figures (Continued)

CHAPTER ONE

INTRODUCTION

Ethanol, due to its low cost and low pollution emission in use, is a useful octane enhancer and may be a viable gasoline alternative and a solution to the energy crisis in the future. In order to meet the requirements of the domestic energy security and economic development, ethanol production in United States have been increasing significantly in recent years. However, more than 90% ethanol in United States is made through corn fermentation process, which is not energy efficient or environmentally friendly. Contrary to the enzyme process in fermentation, ethanol production from synthesis gas has better potential for large scale production with lower cost and higher energy efficiency.

Catalytic hydrogenation of carbon monoxide is one of the direct routes for converting synthesis gas to useful chemical compounds such as hydrocarbons and oxygenates. After nearly one hundred year of development, Fischer-Tropsch (FT) synthesis has been widely employed in hydrocarbon production from synthesis gas. Research efforts in FT synthesis have been aimed towards designing both active and selective catalysts. The process is unique in the field of heterogeneous catalysis in that the emphasis is not on producing a single desired product but rather avoiding several undesirable by-products.

Cobalt- and iron-based catalysts are employed most often in FT synthesis to produce hydrocarbons because of this relatively low costs and high activities. For cobalt-

based catalysts, the principal function of the support is to disperse cobalt and to produce stable cobalt metal particles after catalyst reduction and activation. Promoters are also added to improve catalyst activation, catalyst deactivation and hydrocarbon selectivity. Similar to cobalt-based catalysts, it is also meaningful to add promoters to iron-based catalysts in order to minimize methane, olefin and oxygenate selectivities. Thus, specific supports and promoters are preferred for FT synthesis when high per pass conversion, longer life-times, and higher selectivities to paraffinic products are needed.

It has been already found that Rh is the best catalyst to produce ethanol from CO hydrogenation. However, there are still numerous challenges using this catalyst such as low conversion, low ethanol selectivity and high cost of the catalysts.

The aim of this research was focused on modification of Rh-based catalysts for selective ethanol synthesis from synthesis gas. Based on the results of previous research, a number of promoters and supports were investigated in this research and it was found out that silica is the best support for Rh for high selectivity to ethanol and high metal dispersion. La and V were found to be effective promoters for boosting catalyst activity 3 times and adding both of them together resulted in an even greater increase in activity. The kinetics of CO hydrogenation has been studied in a wide range of reaction temperatures and partial pressures to clarify the discrepancies regarding the reaction mechanism. Different promoters have been elaborately evaluated and their promoting effects have been investigated at the site level by the application of SSITKA (Steady State Isotopic Transient Analysis).

CHAPTER TWO

BACKGROUND

Due to the energy crisis during an era of ever-growing energy consumption, meeting the energy demand in a way that minimizes environmental disruption is one of the central problems of the 21st century. Ethanol, as a major fuel additive and alternative fuel, has attracted increasing attention in recent years. Since corn ethanol results in net energy loss, considerable emphasis has been gra ethanol synthesis from synthesis gas.

2.1 Reasons for Ethanol

Ethanol, with the formula C_2H_5OH and molecular weight of 46.07, is a clear and colorless liquid with a boiling point of 78.5ºC and a density (at 20ºC) of 0.789 g/mL. There is nothing new with regard to the production of ethanol. Worldwide, the earliest example of ethanol synthesis, which referred to wine making, occurred between 7000 and 9000 years ago [1].

Production and demand for ethanol in the U.S. soared to new heights in recent years. According to data released by the Energy Information Administration (EIA) and the Renewable Fuels Association (RFA), production of ethanol in 2009 reached 10.7 billion gallons, an average of 945,000 barrels per day (b/d) or 29.3 million gallons per day. That is an increase of 16.3 percent compared to 2008. Likewise, demand for ethanol

has also increased. Demand for ethanol, also calculated by the RFA, reached 10.9 billion gallons, an average of 963,000 b/d. That is a surge of 14 percent over 2008 and two times more than that of 2004 [2].

Thus, even though it is known to all that the energy content of ethanol is lower than that of gasoline, the ethanol demand and production increased significantly recent years. There are several factors expediting this trend.

Firstly, an alternative energy source, ethanol is helpful in satisfying the increasing energy needs in society development. Nowadays, we are totally dependent on an abundant and uninterrupted supply of energy for living and working. It was reported that the increasing quality of life is clearly associated with increasing per capita electricity consumption [3]. Without energy, advanced economies cannot sustain their standard of living, developing and emerging economies will never attain the growth and quality of life to which we aspire cannot even be realized. Thus, looking for different kinds of energy is essential in maintaining the high speed of economic development.

Secondly, ethanol is an effective method to guarantee the security of the energy supply. By 1905, ethanol was emerging as the fuel of choice for automobiles among engineers and drivers, opinion being heavily swayed by fears about oil scarcity and rising gasoline prices. In the United States, there is an increasing dependence on imported energy to meet personal, transportation, and industrial needs. According to United States Department of Energy, the U.S. dependency on imported oil increased significantly over the past 60 years. The results of its statistical study are shown in Figure 2.1. Moreover, record oil and gas prices in 2009 underscore the need for energy independence by

eliminating that volatility in the market caused by instability and conflict in oil-producing parts of the world. As a domestic, renewable source of energy, ethanol can reduce the dependence on foreign oil and increase the United States' ability to control its own security and economic future by increasing the availability of domestic fuel supplies. For example, in 2006, the production and use of ethanol in the U.S. reduced oil imports by 170 million barrels, saving $11 billion from being sent to foreign and often hostile countries [4].

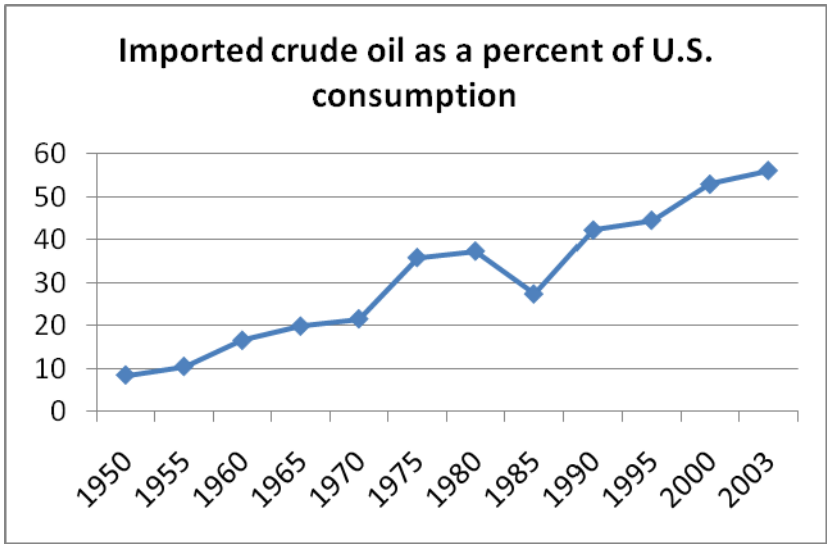

Figure 2.1 Imported Crude Oil as a Percent of US Consumption [1].

However, there are not only the energy, security, and economic benefits. The use of ethanol is also attractive for environmental sustainability. Since adding oxygen to fuel results in more complete fuel combustion thus reduces harmful tailpipe emissions. The 35% oxygen content in ethanol molecules makes it one of the best tools we have to fight

air pollution from vehicles. Ethanol is also added to replace the use of toxic gasoline components such as benzene, a carcinogen. Ethanol is attractive to industry for its unique characteristics such as being non-toxic, water soluble and quickly biodegradable.

Currently, ethanol blends commercially available are the 10% (E10) and 85% (E85) versions. The 2004 Volumetric Ethanol Excise Tax Credit made E85 eligible for a 51 cent/gallon tax break. There are various states (Pennsylvania, Main, Minnesota, and Kansas) that levy lower taxes on E85 to compensate for the lower mileage with this fuel. The 2005 Energy Policy Act established tax credits for the installation of a clean-fuel infrastructure, and state income tax credits for installing E85 fueling equipment have been introduced. Since 1995, flexible-fuel vehicles capable of using E85 have appeared. According to the RFA statistics study, usage of ethanol blends is highest in California - 46% of the total United States consumption [2].

2.2 Ethanol Production

2.2.1 Enzyme/Fermentation

Current fuel ethanol production in the United States comes almost exclusively from traditional grain fermentation processes using corn, although sorghum, wheat and barley have made small contributions. Corn ethanol production developed from wet milling of corn; data compiled in the mid-1990s indicates that more than 70% of the large ethanol facilities then used wet milling [5].

Wet mills process corn by a series of steeping, wet-grinding and fractionation steps which result in starch, oil, protein, fiber, corn gluten meal and corn gluten feed. Ethanol can be produced through fermentation of starch. The outline of corn wet milling and ethanol production is shown in Figure 2.2.

Together with the possibility of collecting CO_2 from the fermentation step as a salable commodity, the multiplicity of products gave wet milling flexibility in times of variable input and output prices, although requiring a higher initial capital investment. Unlike Brazilian sucrose-based ethanol, corn-based ethanol has been technology-driven, especially in the field of enzymes and improved yeast strains with high ethanol tolerance and may be capable of yielding relatively high amounts of ethanol in batch fermentations.

However, despite the advantages of high selectivity and domestically available resources, these processes are also characterized by low reaction rate, difficult product separation, and, especially, energetically inefficiency - there is nearly 70% more energy required to produce ethanol than the energy actually in ethanol. Moreover, it has been reported that in order to replace 10% of the gasoline consumption, corn ethanol would need to be produced on 12% of the total United States cropland. On the other hand, offsetting 10% CO_2 emissions from gasoline consumption would require a fourfold higher production of corn ethanol; that is from 48% of the total United States cropland [5]. Thus, even though ethanol provides a solution to the energy crisis, corn ethanol cannot be relied on.

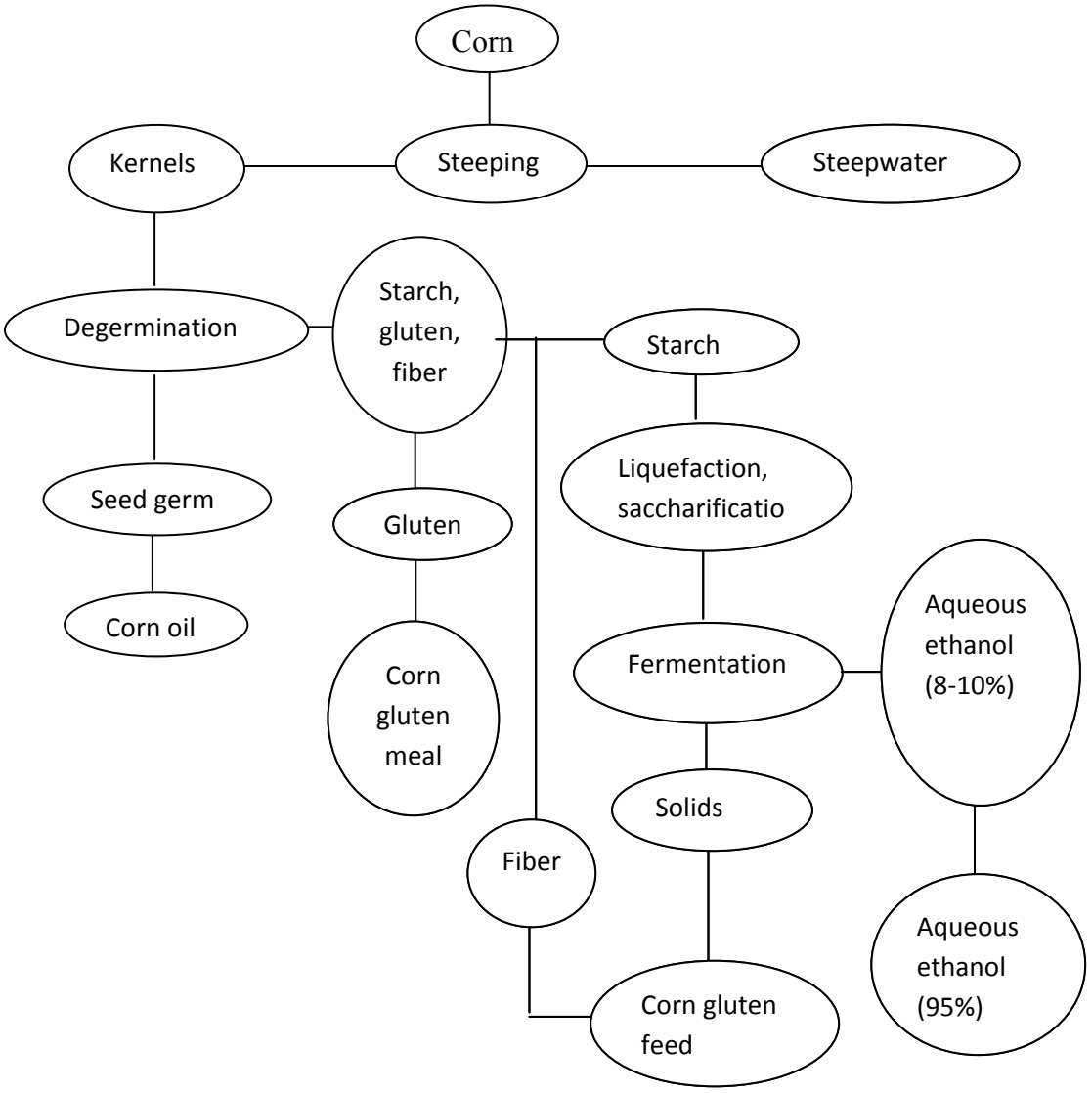

Figure 2.2 Outline of corn wet milling and ethanol production [5].

2.2.2. Via Synthesis Gas

Synthesis gas, also named syngas, is a mixture of various concentrations of carbon monoxide and hydrogen. It can be derived from natural gas, coal or biomass. This ethanol synthesis process from synthesis gas consists of three basic steps: first is

syngas production, second is the conversion of syngas to ethanol over a catalyst, and the last step is distillation to produce high purity ethanol. Unlike current fermentation processes, ethanol can be produced from syngas derived from a wide variety of sources including natural gas, coal bed methane, landfill gas and biomass.

Table 2.1 compared the costs of enzyme/fermentation and gasification/synthesis processes. The $2.33/gallon capital cost and $0.78/gallon production cost are based on estimates by Plant Process Equipment Inc, Houston, TX, (PPE's) using landfill gas and a plant with small scale 80 TPD capacity [6]:

Table 2.1 Cost Comparison [6]

	Enzyme/Fermentation	Gasification/Synthesis
Theoretical yield	114 gal/ton	230 gal/ton
Actual yield	70 gal/ton	114 gal/ton
Approx. capital cost/gallon/year	$4.45 (IEA 2002 est.)	$2.33 (PPE est.)
Approximate cost/gallon	$1.44 (IEA 2002 est.)	$0.78(PPE est.)

Since the cost of gasification is lower and the energy efficiency is higher than for the enzyme process, there is greater economy in ethanol production from the synthesis gas than from corn. It also has with more potential for large scale production. Moreover, this process could also create far greater green house gas reductions and carbon credits than the fermentation process.

2.2.3 Synthesis Gas Production for Ethanol Synthesis

The technology used to prepare synthesis gas used for CO hydrogenation can be separated into two main categories - reforming and gasification. The reforming process produces synthesis gas from gaseous or light liquid feedstock, while the gasification process produces synthesis gas from solid or heavy liquid feed stocks.

The most common feed used to produce synthesis gas for CO hydrogenation is coal, which is rich in carbon. This is because coal is the world's most abundant fossil fuel resource. To make a synthesis gas suitable for ethanol synthesis, coal needs to be gasified with steam and oxygen. There are several types of coal gasification technology that may be considered. In this study, the synthesis gas produced by Conoco-Philips' EGAS technology from coal is used as the basis for further conversion to ethanol. This technology has been commercially demonstrated, thus, the coal gasification and gas cleanup are elements of the process but were not investigated in this study.

2.3 Fischer-Tropsch Technology

2.3.1 Orientation

Fischer-Tropsch (FT) technology can be defined as the means used to convert synthesis gas containing hydrogen and carbon monoxide to hydrocarbon products. Discovered early in the last century along with many bulk chemical technologies, its development has been primarily due to the efficient use of coal, economical security and

military constraint in the first half of the century. After the Second World War, the research on FT synthesis was mostly driven by energy independence concerns while the world economy was mostly orientated to oil consumption. Several commercial scale plants have been built and some are currently in use. Because of the similarity to the catalytic conversion from synthesis gas to ethanol, understanding the well-developed FT technology is the first step for catalyst design in ethanol synthesis.

The FT reaction is carried out at 473-623 K and involves monometallic or bimetallic catalysts. Depending on catalyst, reactor and reaction conditions, FT synthesis can produce a wide range of hydrocarbons: light hydrocarbons, gasoline, diesel fuel and wax [7]. The Fischer-Tropsch process can be carried out at low temperatures (LTFT) to produce a syncrude with a large fraction of heavy, waxy hydrocarbons or it can be carried out at high temperatures (HTFT) to produce a light syncrude and olefins. The products by HTFT can be refined to environmentally friendly gasoline and diesel, solvents and olefins while by LTFT, the primary products can be refined to special waxes or if hydrocracked and/or isomerized, to produce excellent diesel, base stock for lube oils and a naphtha that is an ideal feedstock for cracking to light olefins. Moreover, selectivities are considered essential in the design of the FT section of a gas conversion plant. For a plant focusing on the production of middle distillates, the C_{5+} hydrocarbon selectivities should be as high as possible. If olefins or waxes are co-produced, then their selectivities should be optimized simultaneously.

Catalysts are the vital part in any FT process. Iron and cobalt catalysts are two different kinds of catalysts that have been employed widely in FT technology. Cobalt

catalysts are typically used in (natural) gas-to-liquids (GTL) technology, and suitable for converting H_2-rich, natural gas-derived synthesis gas since they have low intrinsic water gas shift (WGS) activity. On the other hand, iron catalysts are often used for converting coal-derived, CO-rich synthesis gas due to the fact that their high WGS activities adjust the H_2/CO ratio upward. However, for both kinds of catalysts, catalyst development remains an area of ongoing research and there is still room for further improvement.

2.3.2 Cobalt Catalysts

Usually cobalt catalysts are prepared by depositing cobalt on an oxide support, such as silica, alumina, titania or zinc oxide or a combination of these materials. There are significant and multiple roles the support plays in the design and catalytic performance of cobalt catalysts. The activity of supported cobalt catalysts for FT synthesis depends on the number of active sites on the surface of crystalline cobalt metal which is determined by the cobalt particle size, dispersion, loading, and degree of reduction [8]. The support can modify the catalytic activity and product selectivity by affecting strong metal-oxide interaction (SMOI), reducibility and dispersion of cobalt species to enhance the formation of desired cobalt species. Thus, the structure and chemical properties of the support are essential to supported cobalt catalysts in FT synthesis. For instance, in an investigation of silica-supported cobalt catalysts, Kababji et al. [9] concluded that the support surface area affects SMOI leading to the formation of cobalt silicate, which is considered inactive for FT synthesis. Moreover, it was also suggested that the properties of silica supports affect the product distribution with small

pore diameters (< 6 nm) increasing the rate of methane formation. On the other hand, it was concluded by Zhang et al. [10] that the addition of solvents during the preparation of FT synthesis catalysts can also influence the supported cobalt catalysts significantly. According to their study, using ethanol as solvent for the cobalt precursor promoted dispersion of the supported cobalt and a relatively higher reduction degree, resulting in high activity and stability of this catalyst. Meanwhile, adding acetic acid in the reaction also modified the catalyst surface and affected the FT reaction.

SMOI effects between cobalt and the support have been seen even high loadings of cobalt, i.e., higher than 20% by weight cobalt [11]. Moreover, it has been reported that at low loadings, cobalt clusters are more sensitive to support-influenced deactivation processes [12]. Thus, promoters are added in supported cobalt catalysts to enhance subsequent reduction that produced cobalt metal on the catalyst surface.

Ru and Pt are often employed as promoters, and it was found out by different research groups [13, 14] that they only act as a reduction promoter for cobalt in FT synthesis. It was proposed that Re leads to higher cobalt dispersion by preventing agglomeration of CoO_x particles during calcination treatment and oxidative regenerations [15, 16]. However, it was also suggested that noble metals can only be added in small amounts because higher noble metal/cobalt ratios may result in increased oxygenate selectivity [17]. In order to avoid the use of expensive noble metals, Jacobs et al. [18] studied the promoting effects of Group 11 metals (Cu, Ag, Au) to cobalt catalysts for FT synthesis. It was found out that Ag and Au improved the surface cobalt metal active site densities. Cu facilitated cobalt reduction but the increased fraction of reduced cobalt did

not translate in improved active site densities. It is possible that a fraction of Cu covers the surfaces of cobalt particles and results in a decrease in CO hydrogenation and an increase in light product selectivity. Thus, use of effective promoters is essential in cobalt catalyst design and both the type and loading of the promoters should be optimized for FT synthesis.

2.3.3 Iron Catalysts

Compared to cobalt-based catalysts, iron-based catalysts lead to more olefinic products and to lower methane selectivity over a wide range of temperatures and H_2/CO ratios derived from coal or biomass. Thus, iron-based catalysts provide an attractive complement to cobalt-based catalysts for FT synthesis even though cobalt catalysts are usually more active than iron-based catalysts at lower temperatures (470-490 K).

Similar to cobalt catalysts, the choice and level of promoters are also important in producing an iron-based catalyst with a low selectivity to methane and a high selectivity to heavy hydrocarbon products with the desired olefin and oxygenate content in the products. It has been discovered that iron catalysts promoted by some transition metal oxides like MnO, TiO_2 and V_2O_5 show unusually high selectivity for low alkenes and suppress methane formation [19-21]. On the other hand, it was also found out that some rare earth oxides like La_2O_3 and CeO_2 can be added to iron catalysts to promote catalytic activity, while methane selectivity decreases and light olefin selectivity increases [22]. By studying the promoting effects of Cu, Ru and K, Li et al. [23] discovered that the presence of Cu or Ru led to the nucleation of reduced iron species (Fe_3O_4, FeC_x), which

resulted in higher steady-state FT synthesis rates than for unpromoted catalysts and a larger number of CO binding sites on steady state catalysts, without changing the product selectivity. Interestingly, Soled et al. [24] found out that adding both K and Cu to Fe-Zn results in a higher reaction rate than when adding only Cu or K.

2.4 Catalyst Design for Ethanol Synthesis

2.4.1 CO Hydrogenation Mechanism

CO hydrogenation produces paraffins, olefins, and oxygenated products such as alcohols, aldehydes, ketones, acids, and esters. Extensive efforts have been focused on catalyst screening and mechanistic studies, aimed at developing highly selective catalysts for achieving a specific product distribution. By summarizing the results published before, Chuang et al. [25] linked together all the possible pathways of the mechanism in a network as shown in Figure 2.3.

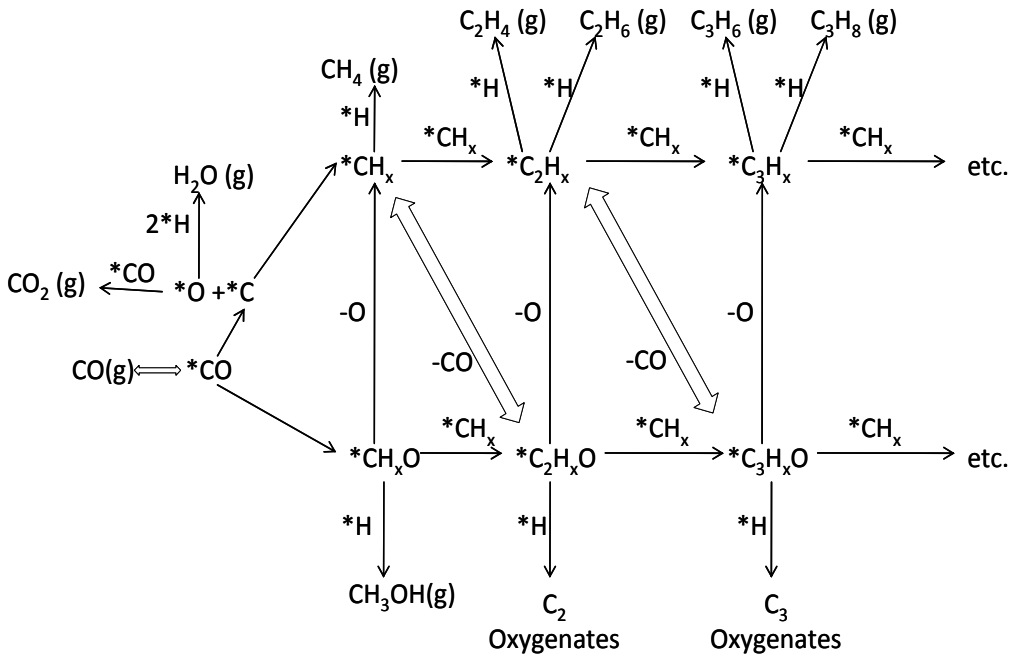

Figure 2.3 CO hydrogenation network [25].

The reaction on catalysts begins with CO dissociative adsorption and hydrogenation or hydrogen assisted adsorption and splitting to produce CH_x species, which then undergo

(i) hydrogenation to produce CH_4,

(ii) chain growth with another CH_x to produce C_2 hydrocarbons,

(iii) CO insertion to produce C_2 oxygenates. Methane and hydrocarbons are formed by the hydrogenation of (CH_x) species, suggesting that ethanol formation is favored by a catalyst that selectively promotes the CO dissociation and insertion reaction instead of the hydrogenation of the CH_x surface species.

2.4.2 Criteria for Catalyst Design

A number of criteria are required to be met before a catalyst can be selected for the ethanol production. The non-chemical requirements include the morphology, the mechanical strength and the cost of the catalyst. The three most important chemical requirements are:

(i) Activity.

(ii) Selectivity - the extent to which it produces the desired product rather than any others, in our research, the selectivity to ethanol is a crucial point.

(iii) Stability - how long it can be used before it becomes deactivated by poisons.

There are several factors influencing catalyst behaviors. First of all, the composition of the catalyst is especially important. On one hand, most active materials are not mechanically or thermally stable and the cost is always high. Thus, in order to achieve the optimal dispersion for the active component and stabilization against sintering, the support is need consisting of an ultra hard and chemically nonreactive material with a high melting point and a large surface area, such as SiO_2, TiO_2, Al_2O_3, carbon, etc. Promoters are also added to improve activity, selectivity, or useful lifetime of the catalyst. Second, the preparation methods, including the impregnation sequence and the calcination temperature have been shown to affect catalyst behavior. Third, the catalyst activity can be changed by the variation of the pretreatment and reaction conditions though the reasons for the influence is still in the discussion.

2.4.3 Rh-based Catalysts

Rh catalysts have been found so far to be the most selective catalysts for the synthesis of higher alcohols, especially in the production of ethanol [24-27]. The activity and selectivity of C_{2+} oxygenate synthesis of Rh catalysts has been attributed to the unique carbon monoxide adsorption behavior on Rh [26, 27].

Moreover, both the CO dissociation and insertion abilities of Rh can be adjusted by varying the additive and support compositions, which influence the catalyst in different ways. For example, Zn and Fe tend to block surface sites, which decreases CO adsorption; Mn, Ti and Zr enhance both the CO insertion and CO dissociation by interaction with the reactant molecules and reaction intermediates; the catalyst states can be modified by an electronic effect of additives such as alkali promoters, which increase the adsorption energy of the CO and as a result, decrease CO hydrogenation significantly. Figure 2.4 shows the effects of different supports and promoters on the supported Rh catalysts.

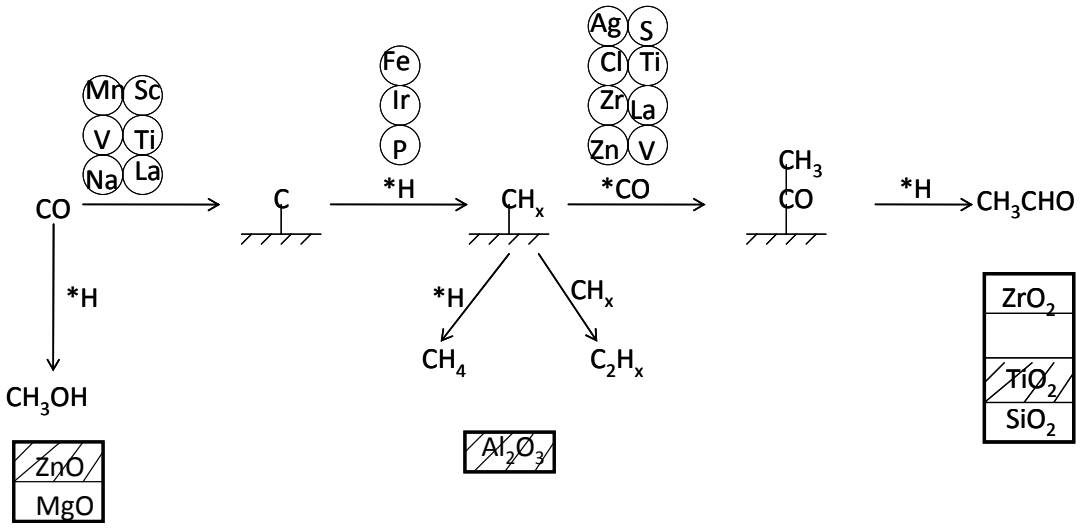

Figure 2.4 Support and promoter effects on C_2 oxygenate synthesis on the supported Rh catalysts. (M) indicates the promoter (i.e., Mn, Fe, Ag, etc.) which enhances the rate of the specific step; M denotes the support which promotes the formation of the specific product (e.g., ZnO promotes the formation of methanol) [25].

Gajardo et al. [28] found that the selectivity for ethanol decreased in the order: Rh/La_2O_3>Rh/TiO_2>Rh/SiO_2>Rh/Al_2O_3. The variation of alcohol selectivity has been attributed to the electron withdrawing/donating capability of an acidic/basic support, morphology of the metal, and effect of support on the reducibility of the metal.

Not only the composition, the preparation method, the calcination and reduction temperature influence the catalysts behavior significantly. For example, it was found that the lanthana particles are not formed in the La_2O_3/SiO_2 system, contrary to La_2O_3/Al_2O_3 system [29]. Instead, amorphous and embedded particles of a mixed silicate phase were observed, and this amorphous silicate phase was found to be soluble in acid media, which has significant influence to the catalysts by sequential preparation. Nevertheless, the exact mechanisms of these effects are still largely unknown.

2.5 Research Objective

The objective of this research was to develop a catalytic process for the selective conversion of coal-derived synthesis gas to ethanol. The process is shown in Figure 2.6.

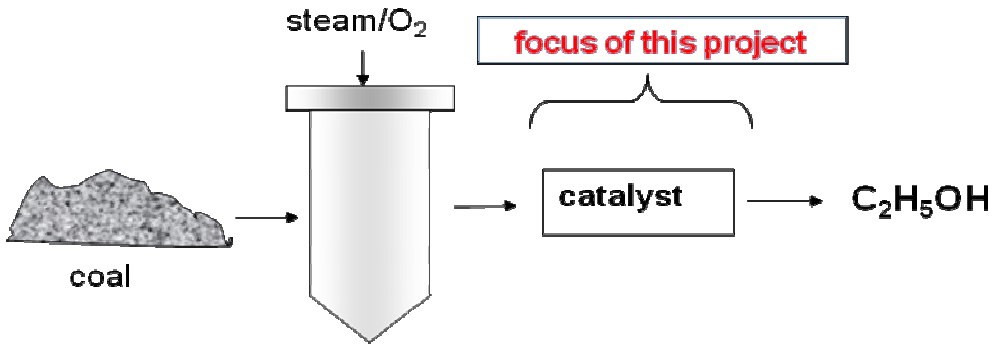

Figure 2.5 Conversion of coal to ethanol.

2.6 References

[1] http://en.wikipedia.org/wiki/Ethanol.

[2] http://www.ethanolrfa.org/industry/statistics/.

[3] http://www.bp.com/genericarticle.do?categoryId=98&contentId=7015967.

[4] http://www.ethanolrfa.org/resource/facts/economy/.

[5] D.M. Mousdale, Biofuels: Biotechnology, Chemistry, and Sustainable Development, Taylor & Francis Group, 2008, p. 21.

[6] http://thefraserdomain.typepad.com/energy/2006/06/new_ethanol_fro.html.

[7] A.P. Steynberg, M.E. Dry, Fischer-tropsch technology, Elsevier BV., Amsterdam, 2004, p. 19.

[8] B.G. Johnson, C.H. Bartholomew, D.W. Goodman, J. Catal. 128 (1991) 231.

[9] A.H. Kababji, B. Joseph, J.T. Wolan, Catal. Lett. 130 (2009) 72.

[10] Y. Zhang, Y. Liu, G. Yang, Y. Endo, N. Tsubaki, Catal. Today 142 (2009) 85.

[11] G. Jacobs, M.C. Ribeiro, W.P. Ma, Y.Y. Ji, S. Khalid, P.T.A. Sumodjo, B.H. Davis, Appl. Catal., A 361 (2009) 137.

[12] A.P. Steynberg, M.E. Dry, Fischer-tropsch technology, Elsevier BV., Amsterdam, 2004, p. 21.

[13] A. Kogelbauer, J.G. Goodwin, Jr., R. Oukaci, J. Catal. 160 (1996) 125.

[14] D. Schanke, S. Vada, E.A. Blekkan, A.M. Hilmen, A. Hoff, A. Holmen, J. Catal. 156 (1995) 85.

[15] E. Iglesia, Appl. Catal., A 161 (1997) 59.

[16] S. Vada, A. Hoff, E. Adnanes, D. Schanke, A. Holmen, Top. Catal. 2 (1995) 155.

[17] L. Guczi, T. Hoffer, Z. Zsoldos, S. Zyade, G. Maire, F. Garin, J Phys Chem-Us 95 (1991) 802.

[18] G. Jacobs, M.C. Ribeiro, W. Ma, Y. Ji, S. Khalid, P.T.A. Sumodjo, B.H. Davis, Appl. Catal. A: Gen 361 (2009) 137.

[19] J. Barrault, C. Forquy, V. Perrichon, Appl. Catal. 5 (1983) 119.

[20] H. Arai, K. Mitsuishi, T. Seiyama, Chem. Lett. (1984) 1291.

[21] U. Lochner, H. Papp, M. Baerns, Appl. Catal. 23 (1986) 339.

[22] K. Chen, Q. Yan, Appl. Catal. A 158 (1997) 215.

[23] S. Li, S. Krishnamoorthy, A. Li, G.D. Meitzner, E. Iglesia, J. Catal. 206 (2002) 202.

[24] S.L. Soled, E. Iglesia, S. Miseo, B.A. Derites, R.A. Fiato, Top. Catal. 2 (1995) 193.

[25] S.S.C. Chuang, R.W. Stevens, Jr., R. Khatri, Top. Catal. 32 (2005) 225.

[26] R.P. Underwood, A.T. Bell, Appl. Catal. 34 (1987) 289.

[27] R.P. Underwood, A.T. Bell, Appl. Catal. 21 (1986) 157.

[28] P. Gajardo, E.F. Gleason, J.R. Katzer, A.W. Sleight, Stu. Surf. Sci. Catal. 7 (1981) 1462.

[29] A.L. Borer, R. Prins, J. Catal. 144 (1993) 439.

CHAPTER THREE

CO HYDROGENATION ON LANTHANA AND VANADIA DOUBLY PROMOTED Rh/SiO_2 CATALYSTS

[As published in Journal of Catalysis, 262, (2009), 119-126]

3.1 Introduction

Catalytic synthesis of ethanol and other higher alcohols from CO hydrogenation has been a subject of significant research since the 1980s. Higher alcohols synthesized from syngas derived from natural gas, coal, or biomass can be used as additives to gasoline or as an easily transportable source of hydrogen. Ethanol is especially desirable to produce selectively. Such produced ethanol would not only decrease the demand for imported crude oil but could also have a positive environmental impact [1].

Rh-based catalysts have been shown to have high activity for the synthesis of C_{2+} oxygenates due to the unique carbon monoxide adsorption behavior on Rh [2-6]. Extensive research efforts have been devoted to study the influence of supports and additives including La_2O_3 [2-6], SiO_2 [4, 5, 7-10], TiO_2 [3, 8-16], Al_2O_3 [8, 9, 11], ZrO_2 [2, 11, 17], CeO_2 [8, 11], MgO [8, 18], V_2O_3 [18-21], alkali metals [21-25], Fe [26], Mn [27-34], Ag [35] and Mo [36] on the catalytic activity of Rh for CO hydrogenation. SiO_2 has been frequently used as a support since most Rh-based catalysts supported on SiO_2 have shown moderate activity and good selectivity towards C_2 oxygenates during CO hydrogenation [37].

It is widely accepted that CO dissociation and hydrogenation to produce CH_x species is likely the first step for the synthesis of C_{2+} oxygenates from syngas on Rh-based catalysts. The CH_x species then undergoes three possible different reactions. One is to form C_2 oxygenates by CO insertion, the second is to produce CH_4 by hydrogenation, and the third is to undergo chain growth with another CH_x to produce C_{2+} hydrocarbons [37]. Many studies have suggested that C-O bond dissociation is the rate-limiting step for CO hydrogenation [16, 38], although it remains unclear whether C-O bond cleavage occurs through direct breaking of this bond in an adsorbed CO species or by a process involving hydrogen. In order to optimize the activity and selectivity of a catalyst for ethanol formation, the catalyst should have the ability to adsorb CO nondissociatively, to dissociate CO, to hydrogenate moderately, and to insert CO into a Rh-CH_x bond. A simple supported Rh catalyst does not seem to meet all these requirements optimally. Typical Rh catalysts for ethanol synthesis from syngas in recent studies all contain multiple components, such as Rh-Li-Mn-Fe [39] and Rh-Zr-Ir [40].

Lanthana and other rare earth oxides have been studied by many researchers for enhancing oxygenates synthesis from syngas and have shown interesting promotion/support effects on Rh for better ethanol formation [5, 17, 41-48]. However, their promotion mechanism remains unclear—it's unknown whether lanthana and other rare earth oxides enhance the formation of C_2-oxygenates by affecting the dispersion of Rh [44, 49], by facilitating CO dissociation or insertion [46, 47], or by stabilizing reaction intermediates [17]. The same is true for vanadia promoted Rh/SiO_2 [20, 50-55]. While Kip and co-workers suggested that V enhances reactivity and selectivity towards

ethanol by enhancing CO dissociation [55], other researchers have proposed that the function of V is to boost hydrogenation [53, 54, 56].

The objective of this study was to investigate the promoting mechanism of La and V, and more importantly, to explore the combined promotion effect of these two elements for CO hydrogenation on Rh/SiO_2. In this study, a series of La and/or V oxide promoted Rh/SiO_2 catalysts were prepared and characterized by TEM, CO chemisorption and FT-IR. Their catalytic activities were determined for CO hydrogenation in a fixed-bed reactor at 230°C and 1.8 atm.

3.2 Experimental

3.2.1 Catalyst preparation

$Rh(NO_3)_3$ hydrate (Rh ~36 wt%, Fluka), $La(NO_3)_3 \cdot 6H_2O$ (99.99%, Aldrich), $NH_4V_2O_3$ (99.5%, Alfa Aesar), and silica gel (99.95%, Alfa Aesar) were used in catalyst preparations. Silica gel was first ground and sieved to 30-50 mesh, washed using boiled distilled water for 3 times, and then calcined in air at 500°C for 4 hours before being used as a support (BET surface area after pretreatment was 251±2 m^2/g). Catalysts were prepared by sequential or co-impregnation to incipient wetness of silica gel with an aqueous solution of $Rh(NO_3)_3$ hydrate and aqueous solutions of precursors of the promoters (1 g silica gel / 2 ml solution), followed by drying at 90°C for 4 h, and then at 120°C overnight before being calcined in air at 500°C for 4 hours.

For the catalysts referred to as $Rh/M/SiO_2$ (M = La or V promoter), silica gel was first impregnated with the aqueous solution containing the nitrate of the promoter and then calcined in static air at 500°C for 4 h, followed by impregnation of the $Rh(NO_3)_3$ aqueous solution and calcination at 500°C for 4 h. $Rh\text{-}M/SiO_2$ represents a catalyst prepared by co-impregnation. Numbers in parentheses following the symbol for an element indicate the weight percent of that element based on the weight of the silica gel support. In the text, a singly promoted catalyst refers to a catalyst containing Rh and one promoter and a doubly promoted catalyst refers to one containing Rh and two promoters. Table 3.1 gives details about the catalyst compositions and preparations. The sequential impregnation method was chosen for V-containing catalysts in order to be consistent with the literature for comparison purposes [29, 54, 57]. For lanthana promoted Rh catalysts supported on silica, it has been reported that the sequence of impregnation has an effect on catalytic behavior [46]. Thus, for this study co-impregnation of the La additive with Rh was adopted since it is believed that well dispersed Rh particles form without being fully covered by La_2O_3 when that method is used [47].

Table 3.1 Preparation conditions and compositions of Rh-based catalysts[a].

Nomenclature	Composition (wt %)[b]	molar ratio of promoter/Rh	Metal loading method
$Rh(1.5)/SiO_2$	1.5		impregnation
$Rh(1.5)\text{-}La(2.6)/SiO_2$	1.5, 2.6	La/Rh = 1.3	co-impregnation
$Rh(1.5)/V(1.5)\ SiO_2$	1.5, 1.5	V/Rh = 2	sequential impregnation
$Rh(1.5)\text{-}La(2.6)/V(0.7)/\ SiO_2$	1.5, 2.6, 0.7	La/Rh = 1.3 V/Rh=1	co-sequential impregnation[c]
$Rh(1.5)\text{-}La(2.6)/V(1.5)/\ SiO_2$	1.5, 2.6, 1.5	La/Rh = 1.3 V/Rh=2	co-sequential impregnation
$Rh(1.5)\text{-}La(2.6)/V(2.2)/\ SiO_2$	1.5, 2.6, 2.2	La/Rh = 1.3 V/Rh=3	co-sequential impregnation
$Rh(1.5)\text{-}La(2.6)/V(3.7)/\ SiO_2$	1.5, 2.6, 3.7	La/Rh = 1.3 V/Rh=5	co-sequential impregnation
$Rh(1.5)\text{-}La(0.5)/V(3.7)/\ SiO_2$	1.5, 0.5, 3.7	La/Rh = 0.3 V/Rh=5	co-sequential impregnation
$Rh(1.5)\text{-}La(4)/V(1.5)/\ SiO_2$	1.5, 2.6, 1.5	La/Rh = 2 V/Rh=2	co-sequential impregnation
$Rh(1.5)\text{-}La(6)/V(1.5)/\ SiO_2$	1.5, 6, 1.5	La/Rh = 3 V/Rh=2	co-sequential impregnation

[a] All catalysts were calcined at 500°C after each impregnation step.
[b] wt% relative to the initial weight of the support material.
[c] First impregnation with an $NH_4V_2O_3$ solution, followed by calcination at 500°C; then co-impregnation with a Rh and La solution, followed again by calcination at 500°C.

3.2.2 Catalyst characterization

BET surface area was obtained using N_2 adsorption at -196^{o}C in a Micromeritics ASAP 2020. Prior to N_2 adsorption, the catalyst samples were degassed under a vacuum of 10^{-3} mm Hg for 4 h at 150^{o}C.

High resolution field emission microscopy images were obtained using a Hitachi 9500 electron microscope with 300 kv high magnification. A Scintag XDS 2000 θ/θ powder X-ray diffractometer (XRD) equipped with Cu Kα1/Kα2 (λ = 1.540592 Å and 1.544390 Å, respectively) radiation was employed for the collection of X-ray diffraction patterns with a step size of 0.03°.

The number of exposed rhodium surface atoms was determined by CO chemisorption using a Micromeritics ASAP 2010C. Catalyst samples of approximately 0.2 g were first evacuated at 110^{o}C for 30 min before being reduced at 500^{o}C in a hydrogen flow for 30 minutes, and then evacuated at 10^{-6} mm Hg and 500^{o}C for 120 min. After cooling under vacuum to 35^{o}C, the adsorption isotherm was recorded. The amount of chemisorbed CO was obtained by extrapolating the total adsorption isotherm to zero pressure, and the metal dispersion (Rh_s/Rh_{Tot}) was calculated subsequently assuming $CO/Rh_s=1$.

CO adsorption was also studied using a Nicolet 6700 FTIR spectrometer equipped with a DRIFT (diffuse reflectance infrared Fourier transform) cell with CaF_2 windows. The cell, whose windows were cooled by circulating water, could collect spectra over the temperature range 25-500^{o}C at atmospheric pressure. For a typical measurement, about 0.05 g sample was ground and placed in the sample holder. Prior to exposure to CO, the sample was reduced *in situ* at 500^{o}C in a flow of H_2 (20 mL/min) for 30 min and then purged with He (48 mL/min) at this temperature for 30 min. After cooling down to the desired temperature in the He flow, a background spectrum was taken. Then, 4 v/v % CO/He (total 50 mL/min) was introduced into the cell and the infrared spectra were taken at 4 cm^{-1} resolution and consisted of 128 interferograms to obtain a satisfactory signal-to-noise ratio.

3.2.3 Reaction

CO hydrogenation was performed in a fixed-bed differential reactor (316 stainless steel) with length ~300 mm and internal diameter ~5 mm. The catalyst (0.3 g) was diluted with inert α-alumina (3 g) to avoid channeling and hot spots. The catalyst and inert were loaded between quartz wool plugs and placed in the middle of the reactor with a thermocouple close to the catalyst bed. Prior to reaction, the catalyst was heated to 500^{o}C (heating rate ~6^{o}C /min) and reduced with hydrogen (flow rate = 30 mL/min) for 1 h. The catalyst was then cooled down to 230°C and the reaction started as gas flow was switched to a H_2-CO mixture (molar ratio of H_2/CO = 2, total flow rate = 45 mL/min) at 1.8 atm total pressure. A total pressure of 1.8 atm was used since this study is part of a more extended investigation using a variety of techniques including using SSITKA (steady-state isotopic transient kinetic analysis [58]) and equivalent reaction conditions are required for comparison of all the data. This pressure would not necessarily be the optimum for obtaining the maximum selectivity to oxygenates. Flow rates were controlled using Brooks 5840E series mass flow controllers and kept at a total flow rate of 45 mL/min. The products, including hydrocarbons and oxygenates, were analyzed on-line by an FID (flame ionization detector) in a gas chromatograph (Varian 3380 series) with a Restek RT-QPLOT column of I.D 0.53 mm and length 30 m. Carbon monoxide and other inorganic gases were analyzed by a TCD (thermal conductivity detector) after separation with a Restek HayeSep® Q column of I.D. 3.18 mm and length 1.83 m. The identification and calibration of gas products were accomplished using standard gases [alkanes (C_1-C_7), alkenes (C_2-C_7), and oxygenates (methanol, ethanol, 1-propanol, 1-butanol, acetaldehyde, and acetone)] as well as liquid samples (oxygenates). For all

measurements, the CO conversion was kept below 10%. The selectivity of a particular product was calculated based on carbon efficiency using the formula $n_iC_i / \sum n_iC_i$, where n_i and C_i are the carbon number and molar concentration of the *i*th product, respectively.

Arrhenius plots of the rates of CO conversion gave apparent activation energies of 25-27 kcal/mol for all the types of promoted catalysts; indicating no heat or mass transport limitations on the rate of reaction measurements.

3.3 Results and Discussion

3.3.1 Morphology of Rh-based catalysts

As-prepared Rh-based catalysts were small dark brownish granules of 30-50 mesh. The BET surface areas of all the Rh-based catalysts were measured to be ca. 250 m^2/g. No significant difference was observed in the surface areas for the catalysts prepared using different preparation methods, probably due to the fact that the concentrations of Rh and promoters were relatively low in all the catalysts prepared in this study.

X-ray diffraction (XRD) patterns (not shown) of these calcined or 500^oC reduced catalysts showed no crystalline phases, indicating that Rh, lanthana and vanadia were all highly dispersed. The XRD results were confirmed by TEM as shown in Fig. 3.1. The high resolution images of Rh(1.5)/SiO_2 [Fig. 3.1(a)] show evenly dispersed Rh clusters with particle sizes around 3 nm. However, for the La and V promoted catalyst Rh(1.5)-La(2.6)/V(1.5)/SiO_2, no clear image of Rh clusters could be identified, only some irregular-shaped patches in the range of 3-20 nm were distinguishable from the support,

as shown in Fig. 3.1(b). The singly promoted catalysts, Rh(1.5)-La(2.6)/SiO_2 and Rh(1.5)/V(1.5)/SiO_2, exhibited similar TEM images (not shown) as that of Rh(1.5)-La(2.6)/V(1.5)/SiO_2.

3.3.2 CO Chemisorption

Table 3.2 summarizes the results obtained from the volumetric CO chemisorption. La addition to Rh increases CO adsorption, which is in good agreement with the results reported by Bernal and Blanco [45]. On the contrary, the addition of V resulted in a decrease in both total and irreversible CO chemisorption, which is also consistent with the literature [57]. For the doubly promoted catalysts (La + V), the presence of V clearly diminished the CO chemisorption and especially the irreversible amount. It would appear, based on a comparison of the CO chemisorption results with these from TEM, that metal dispersion based on CO chemisorption for the V-promoted catalysts is probably under estimated.

(a)

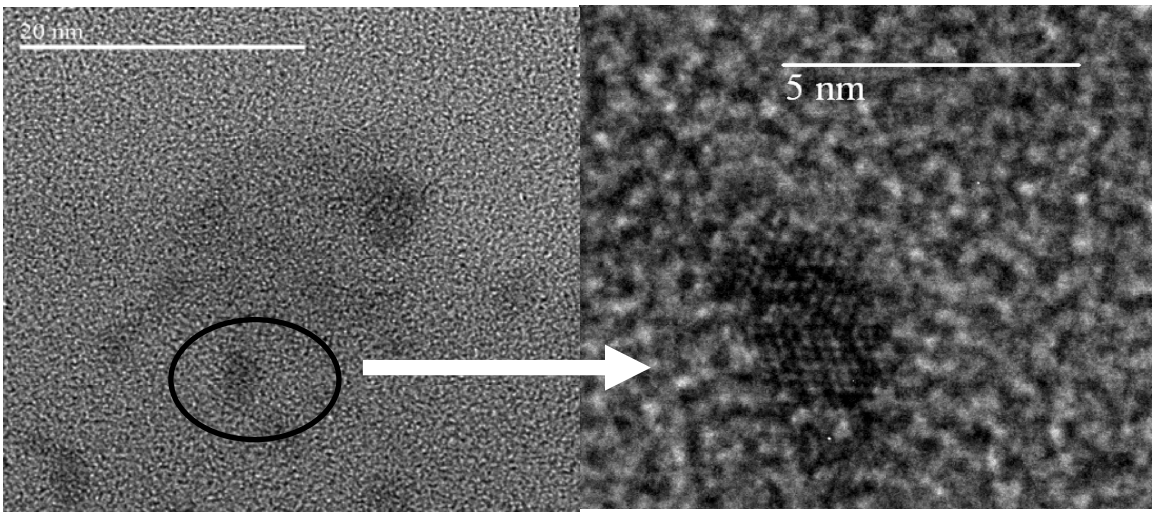

(b)

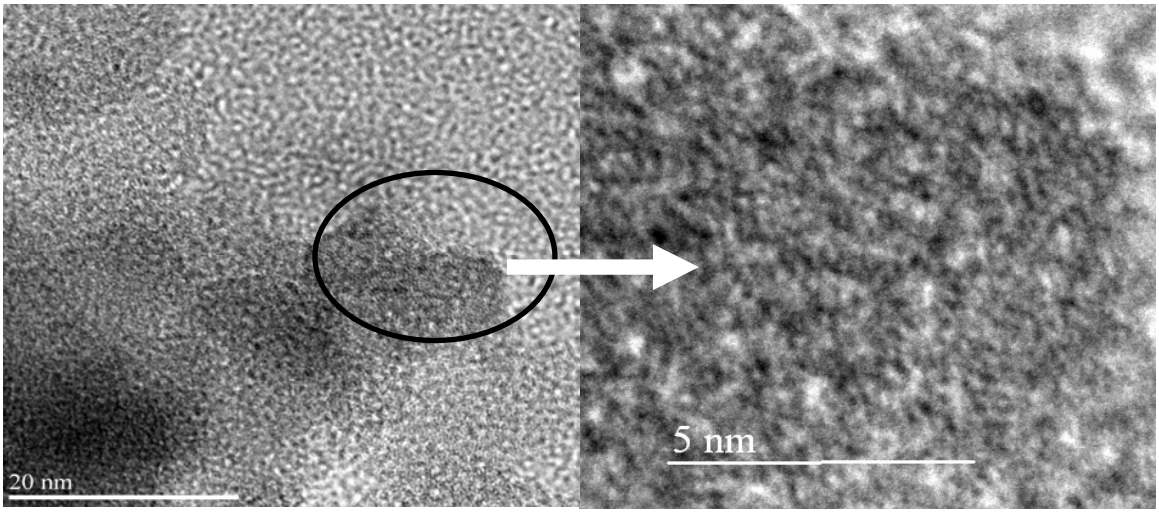

Figure 3.1 TEM micrographs of (a) Rh(1.5)/SiO_2 and (b) Rh(1.5)-a(2.6)/V(1.5)/SiO_2.

Table 3.2 CO Chemisorption on the reduced Rh-based catalysts.

Catalyst	CO-chemisorbed[a] (μmol/g cat.)		Metal Dispersion (%)[b]
	Total	Irrev.	
$Rh(1.5)/SiO_2$	48.1	42.9	37.2
$Rh(1.5)\text{-}La(2.6)/SiO_2$	83.2	76.5	65.4
$Rh(1.5)/V(1.5)/SiO_2$	29.6	6.9	22.9
$Rh(1.5)\text{-}La(2.6)/V(1.5)/SiO_2$	13.3	2.0	10.3

[a] Error = ±5% of the value measured.
[b] Based on total CO chemisorbed and an assumption of $CO/Rh_s=1$.

3.3.3 FTIR study

Infrared spectroscopy provides an alternate and powerful tool to study the interaction of CO with catalysts. Four representative Rh catalysts in this study were chosen for IR study – the bench mark non-promoted $Rh(1.5)/SiO_2$, 2 singly promoted catalysts $Rh(1.5)\text{-}La(2.6)/SiO_2$ and $Rh(1.5)/V(1.5)/SiO_2$, and a doubly promoted catalyst $Rh(1.5)\text{-}La(2.6)/V(1.5)/SiO_2$. A series of spectra acquired for these catalysts (after reduction at 500°C and desorption of H_2 followed by contact with CO at room temperature or 230°C, respectively for 30 minutes) is given in Fig. 3.2. In all the spectra, the bands centered around 2180 and 2125 cm^{-1} can be attributed to gaseous CO [59]. The IR spectrum of $Rh(1.5)/SiO_2$ interacting with CO at room temperature [Fig. 3.2(a)] exhibited a strong band at 2072 cm^{-1}, which can be attributed to linear adsorbed CO [CO(*l*)]; a doublet at 2092 and 2026 cm^{-1}, which can be assigned to the symmetric and asymmetric carbonyl stretching frequencies of gem-dicarbonyl $Rh(I)(CO)_2$; and a weak

broad peak at 1865 cm^{-1}, which is assigned to bridge-bonded CO [CO(*b*)] [60]. The formation of the dicarbonyl species could be an indication of highly dispersed Rh since it is widely accepted that the dicarbonyl species can only be formed on highly dispersed rhodium [61, 62]. The IR spectrum of CO adsorbed on the lanthana promoted catalyst looks identical to that of CO adsorbed on the non-promoted catalyst except that the peak of the bridge bonded CO shifted to a lower frequency, which is consistent with the literature and may be related to a tilted CO adsorption mode [CO(*t*)] [43]. The IR-spectra taken after exposing Rh(1.5)/V(1.5)/SiO_2 and Rh(1.5)-La(2.6)/V(1.5)/SiO_2 to CO [Fig. 3.2(c) and 3.2(d)] showed much lower intensities of CO(*l*) band and no CO(*b*) was observed. The suppression of CO absorption by the addition of vanadia to Rh/SiO_2 catalysts has previously been reported by several research groups [53, 57] and is also in agreement with the quantitative CO chemisorption results reported here. Two features related to CO adsorption on the doubly promoted Rh(1.5)-La(2.6)/V(1.5)/SiO_2 at room temperature are worthy noting here: first, as shown in Figure 3.2(d), the gem-dicarbonyl Rh(*I*)$(CO)_2$ dominates the IR spectrum; second, though the overall intensities of the adsorbed CO bands are lower than those of non-promoted and the lanthana promoted Rh/SiO_2, they are significantly greater than those of the vanadia promoted Rh/SiO_2. These features indicated high dispersion of Rh and moderate CO adsorption strength of the doubly promoted catalyst at room temperature.

For IR spectra recorded at the reaction temperature of 230^{o}C, the relative intensity of the dicarbonyl species decreased compared to the spectra recorded at room temperature for all the catalysts. The attenuation of the dicarbonyl species is likely due to

the reduction of $Rh^{I}(CO)_2$ to form CO_2 and $Rh_x^0(CO)$ species at high temperatures [63, 64]. For the non-promoted Rh(1.5)/SiO_2 and the lanthana promoted Rh(1.5)-La(2.6)/SiO_2, the intensities of the bridge-bonded CO(*b*) or CO(*t*) increased. However, at this temperature, there was still no CO(*b*) evident in the IR spectra for the V-containing catalysts. With regards to the adsorbed CO, that on Rh(1.5)-La(2.6)/SiO_2 had the highest intensity. Results may be attributed to the fact that lathana can interact directly with CO [43]. However, in the present study, exposing 2.6 wt% La_2O_3 supported on SiO_2 to CO did not produce any significant IR bands for adsorbed CO species at room temperature or 230^{o}C, suggesting that new sites available for CO adsorption might be at the Rh-LaO_x interface/surface. The IR spectrum of the vanadia promoted Rh catalyst, Rh(1.5)/V(1.5)/SiO_2, at 230^{o}C exhibited similar features to the spectrum recorded at room temperature except that the peaks were even weaker when compared to the other catalysts, indicating a likely stronger suppression of CO adsorption at higher temperature. One possible explanation is that at higher temperature, more Rh might be covered with vanadia. As shown in Figure 3.2(d), the IR spectrum taken at 230^{o}C of the doubly promoted catalyst exhibited weak gem-dicarbonyl Rh(*I*)$(CO)_2$ species besides CO(*l*) with moderate intensity, suggesting that high dispersion of Rh and moderate CO adsorption strength were conserved at high temperature for this catalyst. A more detailed discussion related to the IR study will be reported elsewhere [65].

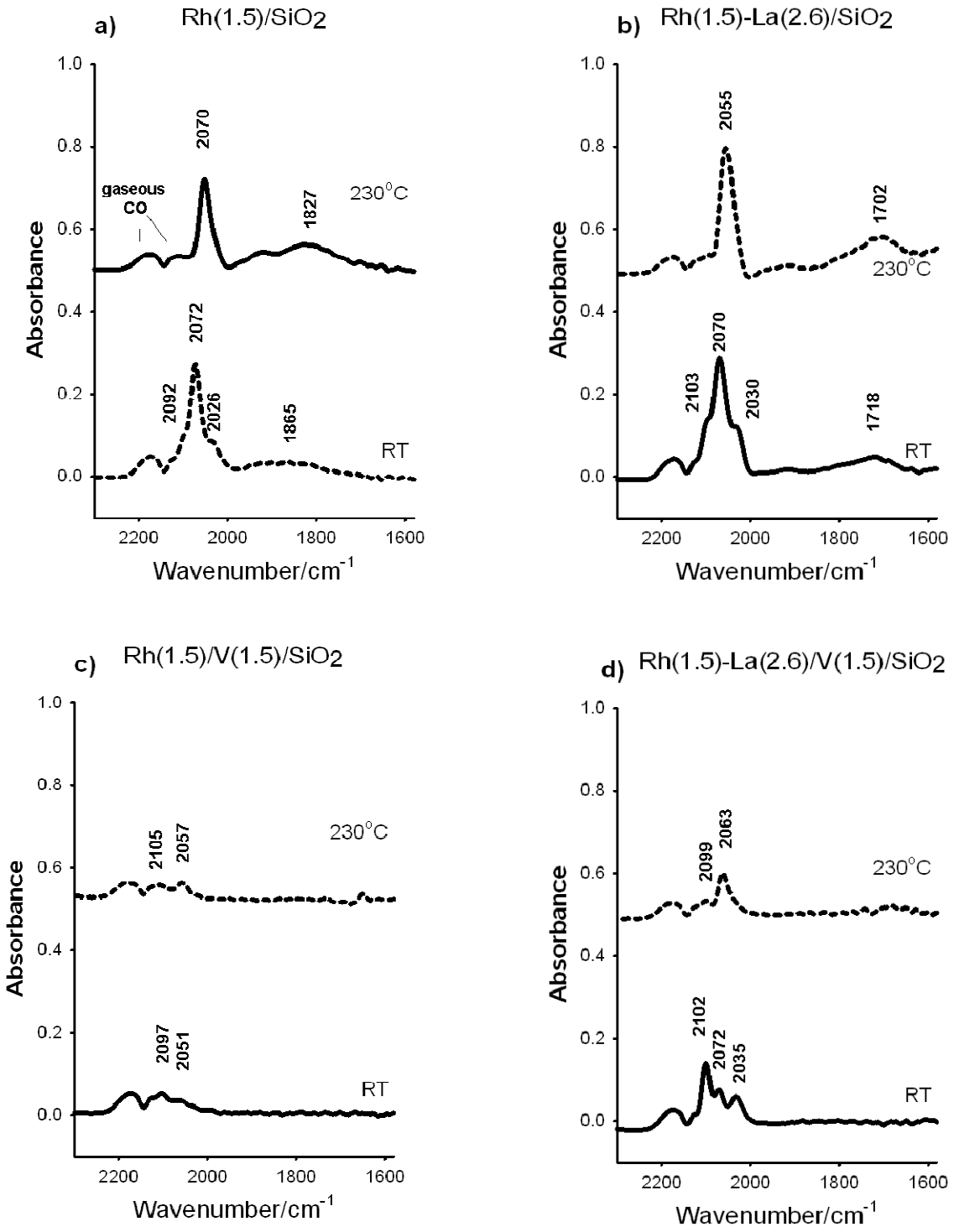

Figure 3.2 The infrared spectra of chemisorbed CO at room temperature and at 230 ^{o}C on (a) Rh(1.5)/SiO_2; (b) Rh(1.5)-La(2.6)/SiO_2; (c) Rh(1.5)/V(1.5)/SiO_2; (d) Rh(1.5)-La(2.6)/V(1.5)/SiO_2 after exposing the reduced catalysts to 4 v/v % CO/He (total 50 mL/min) for 30 minutes.

3.3.4 Catalytic activities

Table 3.3 compares the catalytic activities of the non-promoted and La and/or V promoted Rh/SiO_2 catalysts for CO hydrogenation at 230^oC. Negligible amounts of CO_2 were formed for all the catalysts under the reaction conditions used in this study, thus, all the reaction rates and selectivities were calculated without including CO_2. The results presented here confirm that both La and V affect the catalytic activity of Rh/SiO_2 for CO hydrogenation [41, 55]. It can be seen that all the promoted catalysts exhibited higher CO conversion rates than that of the non-promoted one. For the singly La promoted catalyst $Rh(1.5)\text{-}La(2.6)/SiO_2$, the selectivity towards the formation of ethanol was enhanced while the selectivity towards acetaldehyde decreased a little compared to non-promoted Rh/SiO_2. Methanol selectivity was also increased somewhat, but methane selectivity was less. Hydrocarbons still made up the majority of the total products although somewhat less than for the non-promoted catalyst. The higher total reactivity and higher C_2 oxygenate selectivity indicate that La may enhance both CO dissociation (assuming that C-O bond dissociation is the rate-limiting step for CO hydrogenation [16, 38]) and insertion by increasing CO adsorption and affecting CO interaction with the catalyst at the reaction temperature, as suggested by the IR study.

Compared to the La promoted catalyst, the V promoted Rh catalyst showed significant suppression of the formation of methane, an undesired low-value product, but the selectivity for ethanol was lower than that for the La promoted Rh/SiO_2 catalyst. The formation of higher hydrocarbon dominated with a selectivity of 66.8%. It has been proposed by Luo et al [56, 66] that vanadium ions of lower valence have a good capacity

for hydrogen storage, enhancing the hydrogenation ability. However, Kip et al. [57] studied ethylene-addition and found no significant difference in the amount of ethane formed on non-promoted and V_2O_3 promoted Rh/SiO_2, leading to a suggestion that the low activity of Rh/SiO_2 cannot be due simply to low hydrogenation activity. Judging from the low selectivity of CH_4 and the high fraction of olefins in the products in our study using $Rh(1.5)/V(1.5)/SiO_2$, our results indicate it is also unlikely that vanadium oxide boosts hydrogenation for the formation of hydrocarbons. On the other hand, the shift in selectivity from acetaldehyde to ethanol does suggest an increase in the hydrogenation function of the catalyst. This seeming contradiction may be due to different hydrogenation pathways for the formation of paraffins from olefins and alcohols from aldehydes. Based on the results of our CO chemisorption and IR studies, the addition of vanadium oxide suppresses CO adsorption, which may lead to increased H coverage on the Rh surface. It is possible that this also happens at reaction temperature and influences product selectivity. As suggested by Beutel et al. [53], it is more likely that increased capacity of hydrogen storage may assist CO dissociation by forming COH species easier first on the V promoted Rh catalyst, leading to increased formation of longer chain hydrocarbons and oxygenates. Certainly, if there were increased H coverage, it did not appear to have a positive effect on CH_4 synthesis.

Table 3.3: Catalytic activities of Rh-based catalysts [a, b].

Catalyst	SS* Rate (μmol/g/s)	SS Selectivity (%)[c]						$C_2^=/C_2$	$C_3^=/C_3$[f]
		CH_4	$C_{2+}HC$[d]	MeOH	Acetaldehyde	EtOH	Other C_{2+} oxy.[e]		
$Rh(1.5)/SiO_2$	0.03	48.1	28.7	1.2	6.5	15.6	-	1.8	12.0
$Rh(1.5)$-$La(2.6)/SiO_2$	0.09	35.3	32.0	3.2	5.8	23.6	-	1.2	3.3
$Rh(1.5)/V(1.5)/SiO_2$	0.09	12.5	66.8	5.0	2.1	12.5	1.3	4.8	10.3
$Rh(1.5)$-$La(2.6)/V(1.5)/SiO_2$	0.29	16.2	50.8	1.8	5.4	20.8	4.9	3.3	12.1

[a] Catalyst: 0.3 g; Inert: α-alumina 3 g; Pretreatment: 500°C in H_2; Reaction conditions: T = 230°C, P = 1.8 atm, flow rate = 45 mL/min (H_2/CO =2); Data taken at 15 h TOS after steady state reached.
[b] Error = ±5% of all the values measured except for $Rh(1.5)/SiO_2$ which was ±10% due to low activity.
[c] Carbon selectivity = $n_iC_i / \sum n_iC_i$.
[d] Hydrocarbons with 2 or more carbons.
[e] Oxygenates with 2 or more carbons, not indicating acetaldehyde and ethanol.
[f] $C_n^=/C_n$ is the ratio of C_n olefin selectivity to C_n paraffin selectivity (n = 2, 3).
* Steady-state.

As shown in Table 3.3, compared to Rh/SiO_2 promoted only by La or by V, the doubly promoted catalyst $Rh(1.5)\text{-}La(2.6)/V(1.5)/SiO_2$ combined the positive promoting effects of both La and V, resulting in the highest CO hydrogenation rate (about 9 times higher than Rh/SiO_2), high ethanol and other C_{2+} oxygenates selectivities, and low selectivities for methane and methanol. These results may be related to the intimate contact of Rh with both V and La, resulting in modified CO and H_2 adsorption as suggested by CO chemisorption and IR studies, which leads to faster CO dissociation, insertion and hydrogenation.

Table 3.4 presents the effects on CO hydrogenation of La/Rh and V/Rh ratios in the doubly promoted Rh/SiO_2 catalysts. It can be concluded that a V/Rh ratio ranging from 1-5 had little impact on the total activity for CO hydrogenation. However, as V/Rh changed from 1 to 2, both total oxygenate and ethanol selectivities increased while those for acetaldehyde and methane decreased. This suggests that the main effect of V was to enhance chain growth, probably by accelerating CO dissociation and hydrogenation. When the La/Rh ratio was increased from 0.3 to 3, methane selectivity appeared to increase while the activity shows a peak at 1.3. La appears to affect V-Rh effects but excess La shows negative results. Since varying the La/Rh and V/Rh ratios showed different effects, it is safe to conclude that the better performance of the doubly promoted (La+V) catalyst is not because of a simple additive effect but rather a synergistic one. Use of just more of each promoter by itself is not able to produce the enhanced catalytic performance.

Table 3.4 Effect of V/Rh and La/Rh ratio on catalytic activities of doubly promoted Rh catalysts [a, b].

Catalyst	La/Rh Molar Ratio	V/Rh Molar Ratio	SS Rate (μmol/g/s)	SS Selectivity (%)[c]					
				CH_4	$C_{2+}HC$[d]	MeOH	Acetaldehyde	EtOH	Other C_{2+} oxy.[e]
Rh(1.5)-La(2.6)/V(0.75)/SiO_2	1.3	1	0.27	19.1	50.3	1.9	9.3	16.7	1.3
Rh(1.5)-La(2.6)/V(1.5)/SiO_2	1.3	2	0.29	16.2	50.8	1.8	5.4	20.8	4.9
Rh(1.5)-La(2.6)/V(2.2)/SiO_2	1.3	3	0.32	14.0	53.2	2.8	5.5	20.5	4.0
Rh(1.5)-La(2.6)/V(3.7)/SiO_2	1.3	5	0.29	14.8	52.2	2.7	5.2	21.1	4.0
Rh(1.5)-La(0.5)/V(1.5)/SiO_2	0.3	2	0.17	10.5	60.6	4.6	3.8	17.8	2.8
Rh(1.5)-La(4)/V(1.5)/SiO_2	2	2	0.19	16.6	47.3	2.3	8.9	22.2	2.7
Rh(1.5)-La(6)/V(1.5)/SiO_2	3	2	0.17	21.8	42.4	1.4	11.5	18.3	4.6

[a] Catalyst: 0.3 g; Inert : α-alumina 3 g; Pretreatment 500 °C; Reaction conditions: T = 230 °C, P = 1.8 atm, flow rate = 45 cc/min (H_2/CO =2); data taken at 15 h after steady state reached.
[b] Error = ±5% of the value measured.
[c] Carbon selectivity = $n_iC_i / \sum n_iC_i$
[d] Hydrocarbons with 2 or more carbons
[e] Oxygenates with 2 or more carbons, not including acetaldehyde or ethanol.

Figure 3.3 shows the time-on-stream (TOS) behavior of CO conversion on $Rh(1.5)/SiO_2$, the singly promoted catalysts $Rh(1.5)\text{-}La(2.6)/SiO_2$ and $Rh(1.5)/V(1.5)/SiO_2$, and one of the doubly promoted catalysts $Rh(1.5)\text{-}La(2.6)/V(1.5)/SiO_2$. The activity of the non-promoted $Rh(1.5)/SiO_2$ was relatively constant while the activities of $Rh(1.5)\text{-}La(2.6)/SiO_2$ and $Rh(1.5)\text{-}La(2.6)/V(1.5)/SiO_2$ decreased slightly during the first eight hours and then remained steady. In contrast, the CO hydrogenation activity on $Rh(1.5)/V(1.5)/SiO_2$ exhibited an induction period lasting for 8 hours before a steady-state was reached. Not many previous studies have been reported regarding the activation and deactivation behaviors of Rh-based catalysts for CO hydrogenation. Several research groups have observed performance versus TOS for non-promoted and promoted Rh/SiO_2 catalysts [55, 67-69]. It has been suggested that deactivation during the initial stages of reaction may be due to the inhibiting effect of CO since strongly adsorbed CO on Rh sites may be less likely to be hydrogenated [68, 69]. The re-structuring of the Rh surface during the reaction may also be a cause for the deactivation.

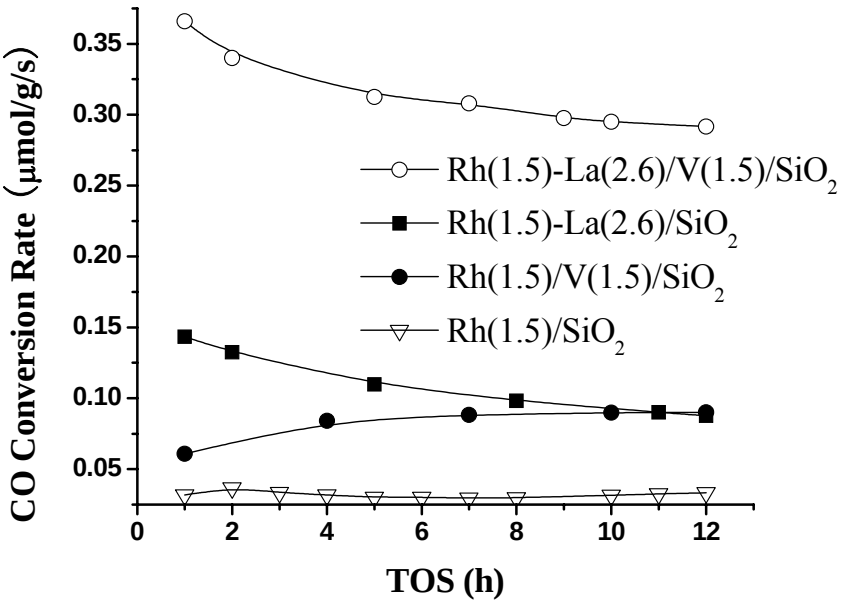

Figure 3.3 CO conversion rate vs TOS for $Rh(1.5)/SiO_2$, $Rh(1.5)\text{-}La(2.6)/SiO_2$ and $Rh(1.5)\text{-}La(2.6)/V(1.5)/SiO_2$,

Figure 3.4 compares the selectivities during CO hydrogenation with TOS on these four catalysts. While not all the selectivities changed much with TOS, there were still several interesting results. The selectivity for acetaldehyde for the non-promoted and La promoted catalysts showed an opposite trend from ethanol. This is consistent with what Chuang et al. [37] proposed, namely that the ethanol selectivity improves by suppressing acetaldehyde production through hydrogenation since acetaldehyde is an intermediate to ethanol. However, no such trend was seen for the V-promoted and doubly promoted catalysts. Finally, the selectivities for $Rh(1.5)\text{-}La(2.6)\text{-}V(1.5)/SiO_2$ did not change with TOS as much as the singly promoted catalysts $Rh(1.5)\text{-}La(2.6)/SiO_2$ and $Rh(1.5)/V(1.5)/SiO_2$, providing additional evidence for a synergistic effect of La and V.

(a) $Rh(1.5)/SiO_2$

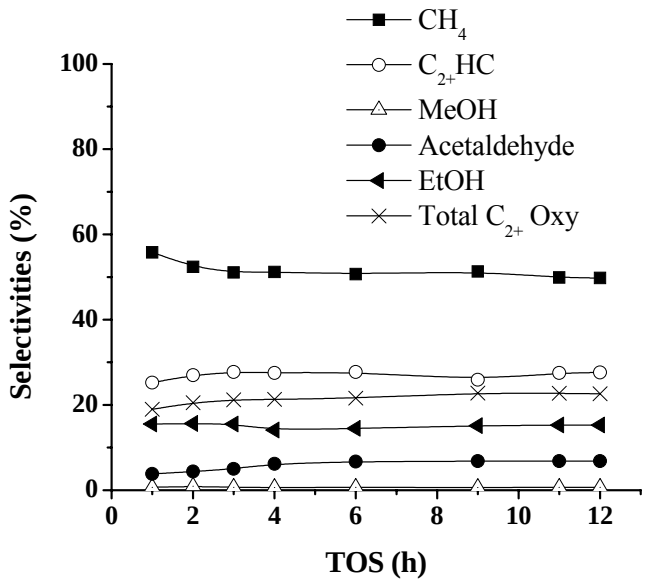

(b) $Rh(1.5)\text{-}La(2.6)/SiO_2$

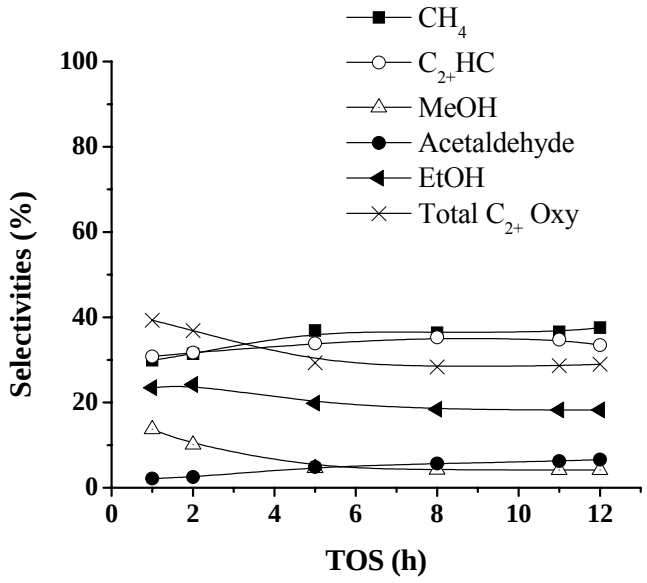

(c) Rh(1.5)/V(1.5)/SiO_2

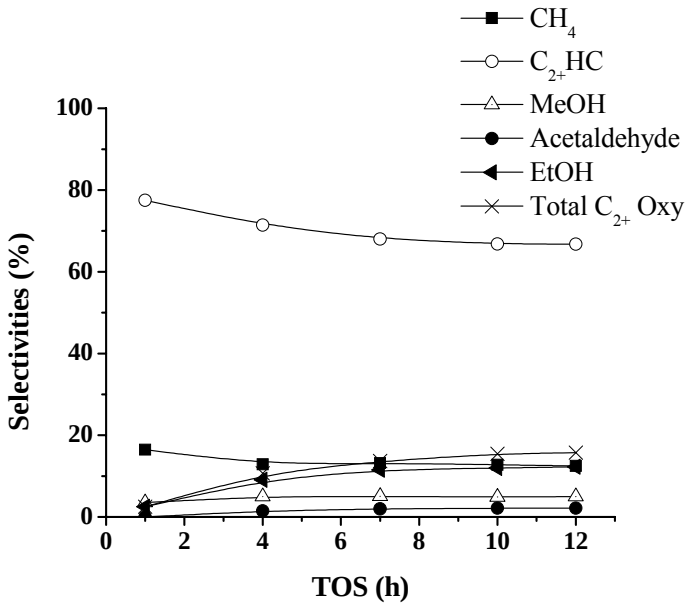

(d) Rh(1.5)-La(2.6)/V(1.5)/SiO_2

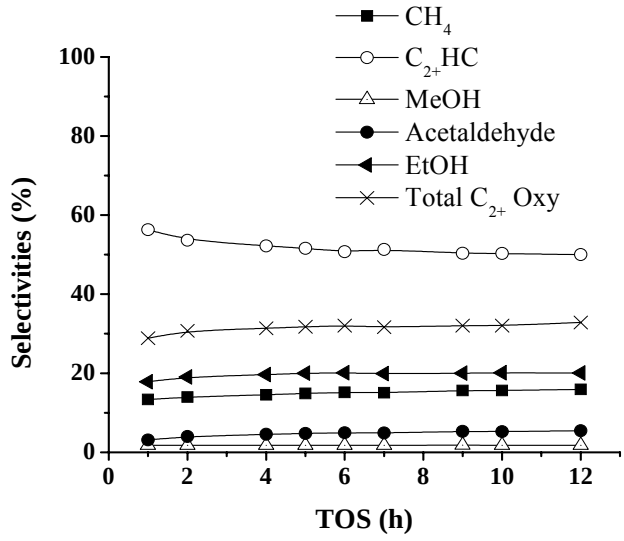

Figure 3.4 Product selectivities vs. TOS for (a) Rh(1.5)/SiO_2, (b) Rh(1.5)-La(2.6)/SiO_2, (c) Rh(1.5)-V(1.5)/SiO_2 and (d) Rh(1.5)-La(2.6)/V(1.5)/SiO_2.

3.4 Conclusions

A series of La and/or V promoted Rh/SiO_2 catalysts was prepared using the incipient wetness impregnation method. Powder X-ray diffraction and TEM results suggested that that Rh, lanthana and vanadia were all highly dispersed in the promoted Rh/SiO_2 catalysts, with no Rh particles distinguishable in TEM images. CO chemisorption and FT-IR studies indicated significantly different CO adsorption behaviors of the different catalysts. V promotion decreased CO adsorption while La promotion showed the opposite effect. Compared to the singly promoted catalysts Rh-La/SiO_2 and $Rh/V/SiO_2$, the doubly promoted Rh-$La/V/SiO_2$ catalysts exhibited higher activity and better selectivity towards ethanol formation. The catalytic performance of the Rh-$La/V/SiO_2$ catalyst was not affected significantly by increasing the V content beyond V/Rh=2; however, La promotion greater than La/Rh=2 resulted in less desirable catalytic properties. The high performance of the Rh-$La/V/SiO_2$ catalysts appears to be due to a synergistic promoting effect of lanthana and vanadia, modifying both chemisorption and catalytic properties.

3.5 Acknowledgments

We acknowledge the financial support from the U. S. Department of Energy (Award No 68 DE-PS26-06NT42801). We thank Amar Kumbhar from the EM Lab at Clemson

University for his help in TEM measurements. We also thank Drs. Kaewta Suwannakarn and Nattaporn Lohitharn for discussions about GC analysis. Walter Torres acknowledges a leave of absence from Universidad del Valle, Colombia.

3.6 References

[1] G.A. Mills, Fuel 73 (1994) 1243.

[2] M. Ichikawa, J. Chem. Soc., Chem. Commun. 13 (1978) 566.

[3] M. Ichikawa, Bull. Chem. Soc. Jpn. 51 (1978) 2273.

[4] R.P. Underwood, A.T. Bell, Appl. Catal. 21 (1986) 157.

[5] R.P. Underwood, A.T. Bell, Appl. Catal. 34 (1987) 289.

[6] G. Van der Lee, B. Schuller, H. Post, T.L.F. Favre, V. Ponec, J. Catal. 98 (1986) 522.

[7] H. Arakawa, K. Takeuchi, T. Matsuzaki, Y. Sugi, Chem. Lett. 9 (1984) 1607.

[8] J.R. Katzer, A.W. Sleight, P. Gajardo, J.B. Michel, E.F. Gleason, S. McMillan, Faraday Discuss. Chem. Soc. 72 (1981) 121.

[9] T. Ioannides, X. Verykios, J. Catal. 140 (1993) 353.

[10] T. Ioannides, A.M. Efstathiou, Z.L. Zhang, X.E. Verykios, J. Catal. 156 (1995) 265.

[11] P. Gajardo, E.F. Gleason, J.R. Katzer, A.W. Sleight, Stu. Surf. Sci. Catal. 7 (1981) 1462.

[12] T. Ioannides, X.E. Verykios, J. Catal. 145 (1994) 479.

[13] T. Ioannides, X.E. Verykios, M. Tsapatsis, C. Economou, J. Catal. 145 (1994) 491.

[14] Z.L. Zhang, A. Kladi, X.E. Verykios, J. Phys. Chem. 98 (1994) 6804.

[15] Z.L. Zhang, A. Kladi, X.E. Verykios, J. Mol. Catal. 89 (1994) 229.

[16] Z.L. Zhang, A. Kladi, X.E. Verykios, J. Catal. 156 (1995) 37.

[17] C. Mazzocchia, P. Gronchi, A. Kaddouri, E. Tempesti, L. Zanderighi, A. Kiennemann, J. Mol. Catal. A: Chem. 165 (2001) 219.

[18] G. Van der Lee, V. Ponec, J. Catal. 99 (1986) 511.

[19] P. Gronchi, E. Tempesti, C. Mazzocchia, Appl. Catal., A 120 (1994) 115.

[20] J. Kowalski, G.V.D. Lee, V. Ponec, Appl. Catal. 19 (1985) 423.

[21] B.J. Kip, E.G.F. Hermans, R. Prins, Appl. Catal. 35 (1987) 141.

[22] T. Hanaoka, H. Arakawa, T. Matsuzaki, Y. Sugi, K. Kanno, Y. Abe, Catal. Today 58 (2000) 271.

[23] S. Kagami, S. Naito, Y. Kikuzono, K. Tamaru, J. Chem. Soc., Chem. Commun. 6 (1983) 256.

[24] H. Orita, S. Naito, K. Tamaru, Chem. Lett. 8 (1983) 1161.

[25] S.C. Chuang, J.G. Goodwin, Jr., I. Wender, J. Catal. 95 (1985) 435.

[26] R. Burch, M.J. Hayes, J. Catal. 165 (1997) 249.

[27] M. Ojeda, M.L. Granados, S. Rojas, P. Terreros, F.J. Garcia-Garcia, J.L.G. Fierro, Appl. Catal., A 261 (2004) 47.

[28] P.-Z. Lin, D.-B. Liang, H.-Y. Luo, C.-H. Xu, H.-W. Zhou, S.-Y. Huang, L.-W. Lin, Appl. Catal., A 131 (1995) 207.

[29] S. Ishiguro, S. Ito, K. Kunimori, Catal. Today 45 (1998) 197.

[30] K.P. De Jong, J.H.E. Glezer, H.P.C.E. Kuipers, A. Knoester, C.A. Emeis, J. Catal. 124 (1990) 520.

[31] T. Beutel, H. Knozinger, H. Trevino, Z.C. Zhang, W.M.H. Sachtler, C. Dossi, R. Psaro, R. Ugo, J. Chem. Soc., Faraday Trans. 90 (1994) 1335.

[32] H. Trevino, G.D. Lei, W.M.H. Sachtler, J. Catal. 154 (1995) 245.

[33] H. Trevino, W.M.H. Sachtler, Catal. Lett. 27 (1994) 251.

[34] H. Trevino, T. Hyeon, W.M.H. Sachtler, J. Catal. 170 (1997) 236.

[35] S.S.C. Chuang, S.I. Pien, J. Catal. 138 (1992) 536.

[36] D.I. Kondarides, Z.L. Zhang, X.E. Verykios, J. Catal. 176 (1998) 536.

[37] S.S.C. Chuang, R.W. Stevens, Jr., R. Khatri, Top. Catal. 32 (2005) 225.

[38] I.A. Fisher, A.T. Bell, J. Catal. 162 (1996) 54.

[39] H.Y. Luo, P.Z. Lin, S.B. Xie, H.W. Zhou, C.H. Xu, S.Y. Huang, L.W. Lin, D.B. Liang, P.L. Yin, Q. Xin, J. Mol. Catal. A: Chem. 122 (1997) 115.

[40] H. Luo, H. Zhou, 2002, US Patent 6 500 781 (2002), to BASF Aktiengesellschaft.

[41] P. Gronchi, S. Marengo, C. Mazzocchia, E. Tempesti, R. DelRosso, React. Kinet. Catal. Lett. 60 (1997) 79.

[42] R.P. Underwood, A.T. Bell, J. Catal. 111 (1988) 325.

[43] R.P. Underwood, A.T. Bell, J. Catal. 109 (1988) 61.

[44] R. Kieffer, A. Kiennemann, M. Rodriguez, S. Bernal, J.M. Rodriguezizquierdo, Appl. Catal. 42 (1988) 77.

[45] S. Bernal, G. Blanco, J.J. Calvino, M.A. Cauqui, J.M. Rodriguez-Izquierdo, J. Alloys Comp. 250 (1997) 461.

[46] A.L. Borer, R. Prins, Stud. Surf. Sci. Catal. 75 (1993) 765.

[47] A.L. Borer, R. Prins, J. Catal. 144 (1993) 439.

[48] Y.H. Du, D.A. Chen, K.R. Tsai, Appl. Catal. 35 (1987) 77.

[49] M. Ferrandon, T. Krause, Appl. Catal., A 311 (2006) 135.

[50] S.-I. Ito, C. Chibana, K. Nagashima, S. Kameoka, K. Tomishige, K. Kunimori, Appl. Catal., A 236 (2002) 113.

[51] S.-I. Ito, S. Ishiguro, K. Kunimori, Catal. Today 44 (1998) 145.

[52] S.-I. Ito, S. Ishiguro, K. Nagashima, K. Kunimori, Catal. Lett. 55 (1998) 197.

[53] T. Beutel, O.S. Alekseev, Y.A. Ryndin, V.A. Likholobov, H. Knoezinger, J. Catal. 169 (1997) 132.

[54] T. Beutel, V. Siborov, B. Tesche, H. Knoezinger, J. Catal. 167 (1997) 379

[55] B.J. Kip, P.A.T. Smeets, J. Van Grondelle, R. Prins, Appl. Catal. 33 (1987) 181.

[56] H.Y. Luo, H.W. Zhou, L.W. Lin, D.B. Liang, C. Li, D. Fu, Q. Xin, J. Catal. 145 (1994) 232.

[57] B.J. Kip, P.A.T. Smeets, J.H.M.C. Van Wolput, H.W. Zandbergen, J. Van Grondelle, R. Prins, Appl. Catal. 33 (1987) 157.

[58] N. Lohitharn, J.G. Goodwin, Jr. Catal. 257 (2008) 142.

[59] J. Bak, S. Clausen, Appl. Spectrosc. 53 (1999) 697.

[60] A.C. Yang, C.W. Garland, J. Phys. Chem 61 (1957) 1504.

[61] P. Basu, D. Panayotov, J.T. Yates, J. Phys. Chem. 91 (1987) 3133.

[62] P. Basu, D. Panayotov, J.T. Yates, J. Am. Chem. Soc. 110 (1988) 2074.

[63] F. Solymosi, M. Pasztor, J. Phys. Chem. 89 (1985) 4789.

[64] F. Solymosi, M. Pasztor, J. Phys. Chem. 90 (1986) 5312.

[65] X. Mo, J. Gao, J.G. Goodwin, Jr., Catal. Today (2008) submitted.

[66] H.Y. Luo, W. Zhang, H.W. Zhou, S.Y. Huang, P.Z. Lin, Y.J. Ding, L.W. Lin, Appl. Catal., A: General 214 (2001) 161.

[67] M.W. Mcquire, C.H. Rochester, J.A. Anderson, J. Chem. Soc., Faraday Trans. 87 (1991) 1921.

[68] K. Gilhooley, S.D. Jackson, S. Rigby, Appl. Catal. 21 (1986) 349.

[69] K. Gilhooley, S.D. Jackson, S. Rigby, J. Chem. Soc., Faraday Trans. 82 (1986) 431.

CHAPTER FOUR

La, V, AND Fe PROMOTION OF Rh/SiO_2 FOR CO HYDROGENATION: DETAILED ANALYSIS OF KINETICS AND MECHANISM

[As published in Journal of Catalysis, 268, (2009), 142-149]

4.1 Introduction

The hydrogenation of CO to form hydrocarbon and oxygenated products has been investigated by a host of researchers since the 1920s, but it was not until the 1980s that the ability of Rh-based catalysts to selectively produce C_2 oxygenates was pursued [1-4]. It has been suggested that the high performance of Rh-based catalysts for the formation of ethanol and other C_{2+} oxygenates is due to the unique carbon monoxide adsorption behavior on Rh surfaces [1, 2]. Since ethanol is a major fuel additive, a promising fuel alternative and a means to store hydrogen in a liquid form for use in hydrogen fuel cells, Rh catalyzed CO hydrogenation has attracted much attention in the last thirty years. Extensive research efforts have been devoted to study the influence of promoters on Rh-based catalyst characteristics and much detailed information can be found in several recent reviews [2-4].

In our previous studies [5-7], the effects of La, V and Fe promotion of Rh/SiO_2 for CO hydrogenation have been investigated. It was found that the addition of La, V or Fe all increased the activity of Rh/SiO_2 to different extents, and the selectivites varied substantially with the addition of the different promoter(s). For instance, the addition of

La resulted in a higher selectivity to ethanol, whereas the addition of V suppressed the formation of methane [6]. The addition of Fe, on the other hand, decreased the formation of higher hydrocarbons [7]. It was also determined that the combination of two or three different promoters resulted in significantly different catalytic activities. The La-V doubly promoted Rh/SiO_2 catalyst exhibited the highest activity and a moderate selectivity towards ethanol and other C_{2+} oxygenates [5]. On the other hand, the La-V-Fe triply promoted Rh/SiO_2 catalyst showed the highest selectivity for ethanol for the reaction conditions utilized and a moderate activity [7]. It was also found that the addition of La enhanced CO chemisorption while V and Fe partially suppressed CO adsorption [7]. The addition of V or Fe also modified the H_2-TPD characteristics of Rh/SiO_2. It was proposed that the good performance of the multiply promoted catalyst was due to a synergistic promoting effect of the combined addition of different promoters through intimate contact with Rh.

The purpose of this study was to further probe the promoting mechanisms of these additives by investigating the effects of partial pressure of H_2 (in the range of 0.4-2.4 atm) and CO (in the range of 0.1-0.8 atm) on CO hydrogenation on the Rh-based catalysts. Moreover, the kinetic analysis was extended to determine the effects of different promoters on the mechanistic pathway for the formation of products. Methane formation was one focus for the mechanic pathway study in this investigation for the following reasons: (i) CO hydrogenation consists of a complex net of reaction pathways to form hydrocarbons and oxygenates. To derive a complete mechanism including the formation of every possible product is out of the scope of this study since our primary interest was

to examine the promoting effect of different promoters. A study focused on CH_4, an important but undesirable product but with fewer required steps in the CO hydrogenation network, is more tractable. (ii) Even though the CO hydrogenation network is complicated, it has been generally accepted that the first step in the synthesis of hydrocarbons and possibly C_{2+} oxygenates is the formation of CH_x (x = 0 – 3) species, which has also been suggested by many researchers to be the rate-limiting step on different catalysts [2, 8-12]. Thus, a mechanistic study of CH_4 (formed the hydrogenation of the CH_x species) should shed some light on the effects of promoters of interest on the formation of C_{2+} oxygenates (formed mainly perhaps insertion of CO into a metal-CH_x bond) and higher hydrocarbons (formed by mainly CH_x chain growth). Because of the high value and versatile applications of ethanol compared to hydrocarbon products, the formation mechanism for ethanol was also studied in this research, being likely somewhat related to that for the formation of methane.

4.2 Experimental

4.2.1 Catalyst preparation

Catalysts were prepared by sequential or co-impregnation as described in detail in our earlier study [5]. $Rh(NO_3)_3$ hydrate (Rh ~36 wt%, Fluka), $La(NO_3)_3{\cdot}6H_2O$ (99.99%, Aldrich) NH_4VO_3 (99.5%, Alfa Aesar) and $Fe(NO_3)_3{\cdot}9H_2O$ (98.0%, Alfa Aesar) were used as purchased. Silica gel (99.95%, Alfa Aesar) was first ground and sieved to 30-50 mesh, washed with boiled distilled water for 3 times, followed by calcination in air at 500

^{o}C for 4 h before being used as a support (BET surface area after pretreatment was 250±2 m^2/g). An aqueous solution of $Rh(NO_3)_3$ hydrate and/or precursors of the promoters (2 ml solution/1 g silica gel) was added dropwise to the silica gel until incipient wetness. The aqueous solution of NH_4VO_3 was prepared at elevated temperature (~80^{o}C) because of its low solubility at room temperature prior to mixing with other solutions; all the other aqueous solutions were prepared at room temperature. The catalyst precursor was dried at 90^{o}C for 4 h and then at 120^{o}C overnight before being calcined in air at 500^{o}C for 4 h.

4.2.2 Reaction

CO hydrogenation was conducted in a fixed-bed differential reactor (316 stainless steel) with length ~300 mm and internal diameter ~5 mm. A catalyst (0.3g) and an inert (α-Al_2O_3, 3g) were loaded between quartz wool plugs, placed in the middle of the reactor with a thermocouple close to the catalyst bed. Ultrahigh-purity H_2 and CO (99.999%, National Welders) used in this work were purified by molecular sieve traps (Alltech) to remove H_2O, and CO was further purified using a CO purifier (Swagelok) to remove CO_2 and carbonyls. Prior to reaction, the catalyst was reduced in-situ in hydrogen (flow rate = 30 mL/min, heating rate = 5^{o}C/min), holding at 500^{o}C for 1 h. The catalyst was then cooled down to the reaction temperature and the reaction started as gas flow was switched to H_2/CO (H_2 flow rate = 30 mL/min, CO flow rate = 15 mL/min) for the initial reaction study. Brooks 5840E series mass flow controllers were used to control flow rates. The kinetics study was carried out after reaction steady state reached (in less than 15 hr). In all cases, conversion was below 5% in order to assure differential conditions.

Runs were repeated to determine repeatability and error (in Table 1 and 2). The apparent activation energies of CO conversion and different product formations were given by Arrhenius plots over the temperature range from 210 to 270^{o}C. In order to derive the apparent order of CO in the power rate law, H_2 partial pressure was kept at 1.2 atm (H_2 flow rate = 30 mL/min) and CO partial pressure varied from 0.1 to 0.8 atm. For example, for a CO partial pressure of 0.8 atm, the CO flow rate was set to 20 mL/min while H_2 flow rate was remained at 30 mL/min, and the total pressure was adjusted to 2.0 atm. For the apparent order of H_2, CO partial pressure was kept at 0.6 atm (CO flow rate = 15 mL/min) and H_2 partial pressure varied from 0.4 to 2.4 atm. We also carried out another series of experiments using He as a diluting agent for CO or H_2 to keep total pressure constant at 1.8 atm. The almost identical kinetic results (within 10% experimental error) obtained this way with what was obtained over a wider total pressure range indicated the validity of the kinetic study carried out by varying total pressure and the flow rate of one reactant but keeping the partial pressure and the flow rate of the other reactant constant. Due to the limitation of the experimental setup (e.g. the range of the CO MFC was much smaller than the H_2 MFC), more reliable data points were able to be obtained by varying total pressure instead of using a diluting agent, results reported in this paper were based on the data obtained by varying total pressure. The reaction rate did not change by varying space velocities or particle sizes, suggesting no existence of external and internal mass transfer, respectively. The activation energies of CO hydrogenation from Arrhenius plots was found to be ca. 25 kcal/mol, the expected value, and confirmed the absence of heat or mass transport limitations on the rate of reaction measurements.

The products, including hydrocarbons and oxygenates, were analyzed on-line by an FID (flame ionization detector) in a gas chromatograph (Varian 3380 series) with a Restek RT-QPLOT column. CO and other inorganic gases were analyzed by a TCD (thermal conductivity detector) after separation with a Restek HayeSep® Q column. The analysis details can be found in our previous paper [5]. The selectivity of a particular product was calculated based on carbon efficiency using the formula $n_iC_i / \sum n_iC_i$, where n_i and C_i are the carbon number and molar concentration of the *i*th product, respectively.

4.3 Results

4.3.1 Catalytic activities of Rh-based catalysts for CO hydrogenation

Table 4.1 shows preparation sequence, composition, atomic ratio of promoter/Rh, steady-state rate, and selectivities for different products of the catalysts at 230°C and a flow rate of 45 mL/min (H_2/CO=2), which are consistent with our previous studies [5-7]. All the reaction rates and selectivities were calculated without including CO_2 since negligible amounts below GC detection of CO_2 were formed for all the catalysts under the reaction conditions used in this study. Addition of promoters modified both rate and selectivities. La, V and Fe all enhanced activity and La and Fe boosted ethanol selectivity, while V suppressed methane selectivity. The La and V doubly promoted catalyst showed the highest activity. The triply promoted catalyst RhLaFeV was the best catalyst for ethanol (EtOH) formation at these reaction conditions because of the high activity and ethanol selectivity.

Table 4.1 Composition and Catalytic activities of SiO_2-supported Rh-based catalysts.

Nomenclature	Composition (wt %) and impregnation sequence [a]	molar ratio of promoter/Rh	SS* Rate [b] (μmol/g/s)	Selectivity (%) [b]					
				CH_4	$C_{2+}HC$[d]	MeOH	Acetal-dehyde	EtOH	Other C_{2+} oxy [e]
Rh	Rh(1.5)		0.03	48.1	28.7	1.2	6.5	15.6	-
RhLa	Rh(1.5)-La(2.6)	La/Rh = 1.3	0.07	38.8	27.4	4.1	8.3	21.5	0.1
RhV	Rh(1.5)/V(1.5)	V/Rh = 2	0.09	12.6	64.1	6.0	1.5	13.6	1.5
RhFe	Rh(1.5)-Fe(0.8)	Fe/Rh = 1	0.11	55.3	13.7	9.5	2.2	19.4	-
RhLaV	Rh(1.5)-La(2.6)/V(1.5)	La/Rh = 1.3 V/Rh = 2	0.23	15.8	51.2	2.7	6.1	22.3	1.8
RhLaFeV	Rh(1.5)-Fe(0.8)-La(2.6)/V(1.5)	La/Rh = 1.33 V/Rh = 2 Fe/Rh = 1	0.21	19.4	33.6	5.6	3.5	34.4	3.5

* Steady state. SS rate = μmol CO conversed/gcat.*s.

[a] For the catalysts referred to as Rh/M (M = La , V or Fe promoter), silica gel was first impregnated with the aqueous solution containing the precursor of M and then impregnated by $Rh(NO_3)_3$ aqueous solution and calcination at 500°C for 4 h. On the other hand, Rh-M refers to a catalyst prepared by co-impregnation. Numbers in parentheses following the symbol for an element indicate the weight percent of that element based on the weight of the silica gel support.

[b] Catalyst: 0.3 g; Inert : α-alumina 3 g; Pretreatment 500 °C; Reaction conditions: T = 230 °C, P = 1.8 atm, flow rate = 45mL/min (H_2/CO =2), data taken at 15 h after steady state reached; Experimental error: ±5%.

[c] Molar selectivity = $n_iC_i / \sum n_iC_i$.

[d] Hydrocarbons with 2 or more carbons.

[e] Other oxygenates besides acetaldehyde and ethanol with 2 or more carbons.

4.3.2 Influence of the partial pressure

The variations in steady-state reaction rate selectivities to CH_4, C_2H_n, C_3H_n and EtOH obtained using the Rh-based catalysts at different H_2 or CO partial pressures are shown in Fig. 4.1 and 4.2. Methanol and acetaldehyde are not included here because the selectivities were too low to study the trends.

As presented in Fig. 4.1 (a), when H_2 partial pressure was increased from 0.4 to 2.4 atm with the partial pressure of CO held at 0.6 atm, the steady-state rate rose steadily for all the catalysts. The CO conversion rate on the doubly promoted RhLaV catalyst increased nearly 5 times, more significantly than all the other catalysts. However, with the addition of Fe as the third promoter, this increase was somewhat lower. In Fig. 4.1(b), compared to the non-promoted catalyst Rh for which the selectivity for CH_4 increased significantly with H_2 partial pressure; addition of any of the promoters caused a lower increase. It is obvious that V-containing catalysts exhibit much lower CH_4 selectivity compared to other catalysts even at higher H_2 partial pressure. The catalysts with by far the lowest CH_4 selectivities were RhV<RhLaV<RhLaFeV. Both C_2H_n and C_3H_n selectivities decreased with increasing H_2 partial pressure, with the promoters significantly affecting the absolute C_2H_n and C_3H_n selectivities as shown in Fig. 4.1(c) and 4.1(d). As shown in Fig. 4.1(e), the selectivity for EtOH increased somewhat with increasing H_2 partial pressure, except for the Fe singly promoted catalyst. For that catalyst, EtOH selectivity actually decreased a little with increasing H_2 partial pressure.

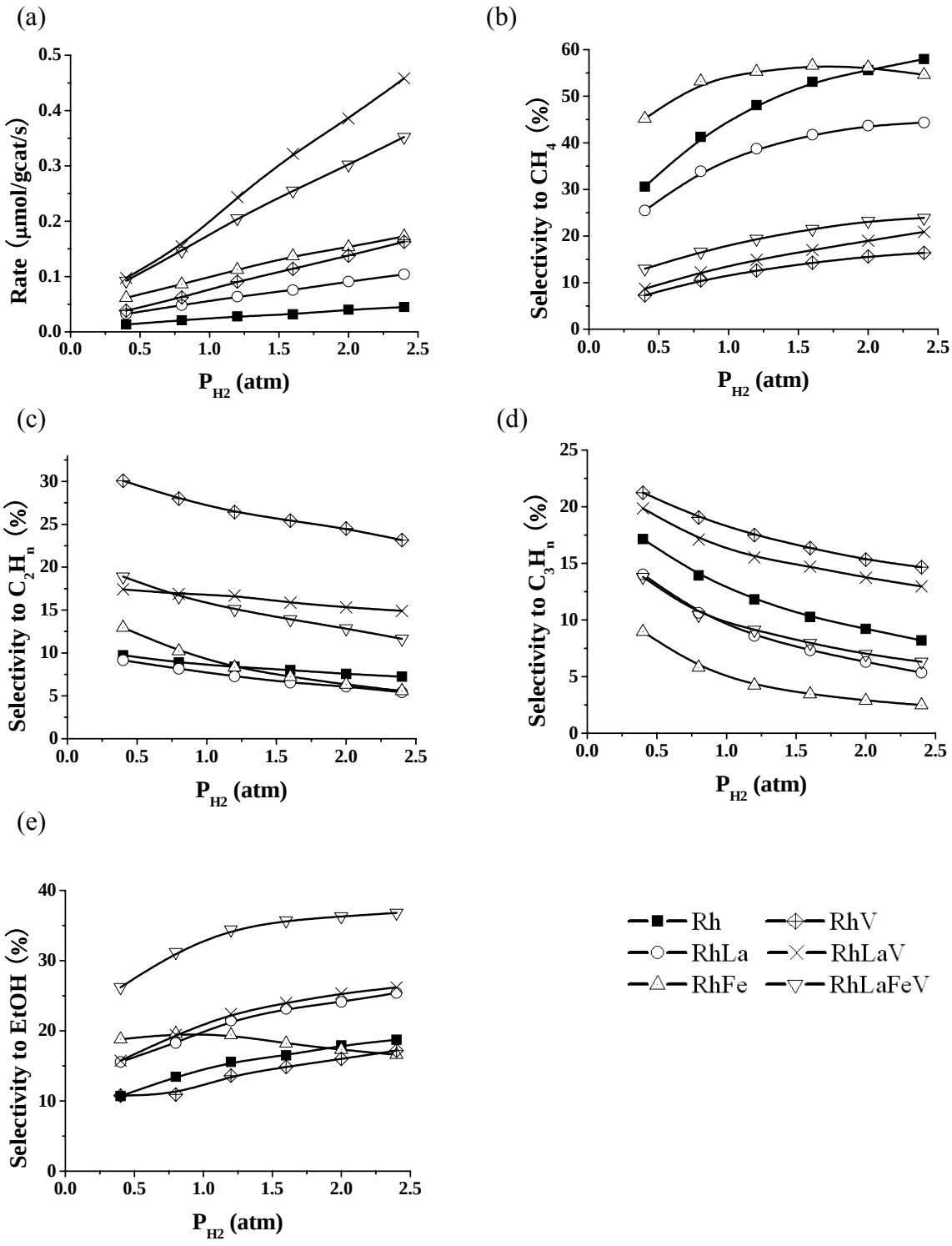

Figure 4.1 The effect of H_2 partial pressure on (a) CO conversion rate, (b) selectivity to CH_4, (c) selectivity to C_2H_n, (d) selectivity to C_3H_n, (e) selectivity to EtOH at 230 °C.

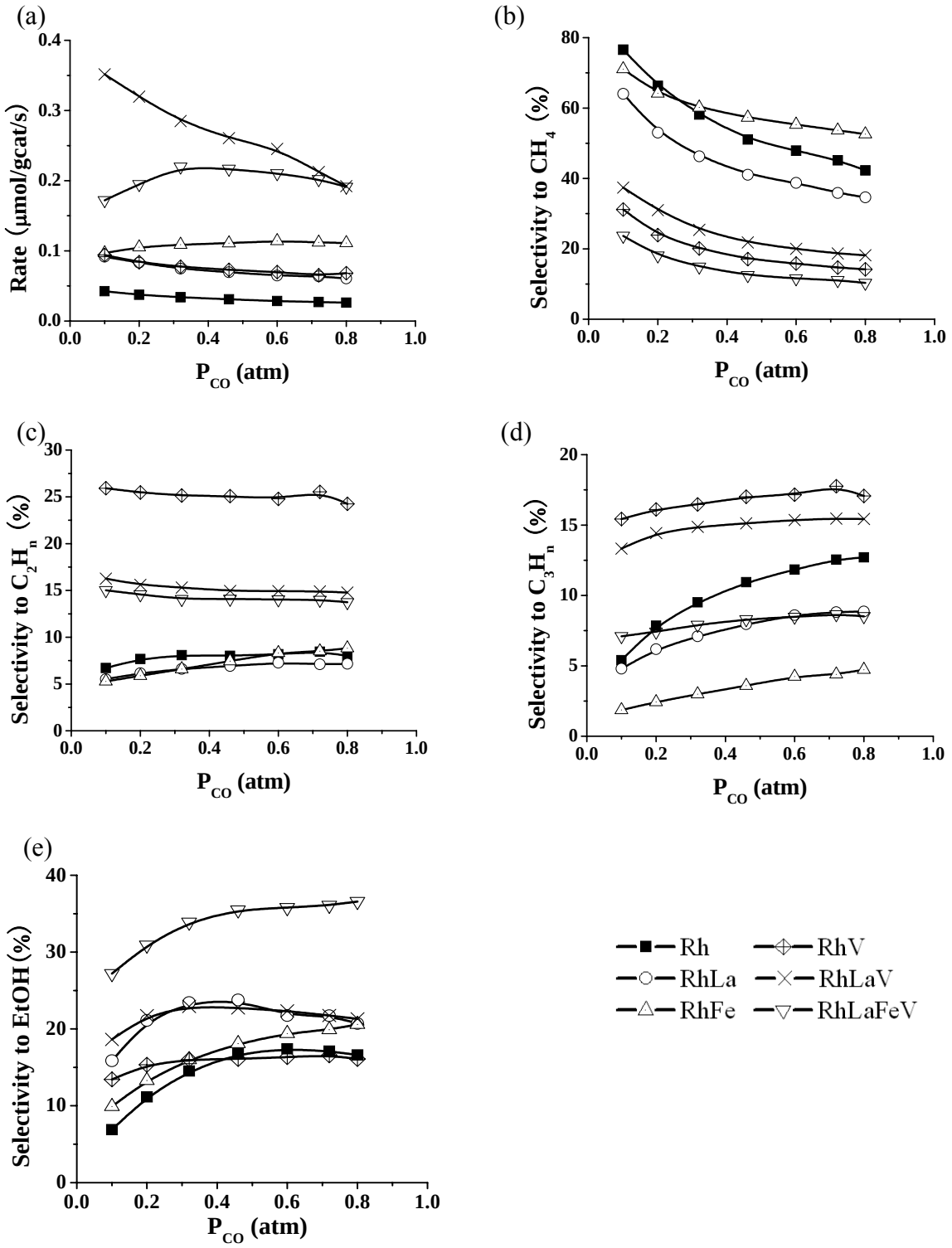

Figure 4.2 The effect of CO partial pressure on (a) CO conversion rate, (b) selectivity to CH_4, (c) selectivity to C_2H_n, (d) selectivity to C_3H_n, (e) selectivity to EtOH at 230 °C.

Fig 4.2 presents the steady-state rate and selectivities for CH_4, C_2H_n, C_3H_n and EtOH with the CO partial pressure varying from 0.1 to 0.8 atm and H_2 partial pressure held at 1.2 atm. In Fig. 4.2(a), it can be seen that the total CO conversion rate was only slightly affected by increasing CO partial pressure for all the catalysts except the La-V doubly promoted catalyst. The selectivity to CH_4 decreased with CO partial pressure for all the catalysts, as shown in Fig. 4.2(b). Different from the effect of P_{H2}, the CO partial pressure did not affect C_2H_n selectivities for any significant degree as shown in Fig. 4.2(c). In Fig. 4.2(d), it can be seen that, while the C_3H_n selectivity for the nonpromoted Rh catalyst significantly increased with increasing CO partial pressure, those for all the promoted catalysts did not. The selectivity for EtOH increased somewhat with increasing CO partial pressure for the nonpromoted, Fe, and LaFeV promoted catalysts as shown in Fig. 4.2(e). The other catalysts showed only small increases.

4.3.3 Power-law expression

The power-law rate parameters in the form of $r = Ae^{-E_a/RT}P_{H_2}^{x}P_{CO}^{y}$ for the synthesis of CH_4, C_2H_n, C_3H_n, EtOH and total CO conversion are summarized in Tables 4.2 and 4.3. Since the formations of different products from CO hydrogenation follow somewhat different pathways, it is more meaningful to examine the power-law rate parameters for each individual product rather than the rate parameters for the overall reaction of CO. The low standard deviations for the activation energy and reaction order measurements along with their correlation coefficients (>0.97) indicate that these parameters represent the data well. Results in the literature for kinetic parameters of CO hydrogenation on Rh

catalysts vary significantly due to differences in pressure, temperature and conversion [10, 13, 14].

As can be seen in Table 4.2, the x and y values varied for the different promoters, with all the results between -0.2 to 1.4 for the reaction order of H_2 and between -0.8 to 0.6 for that of CO. Our results in Table 4.3 for activation energies are consistent with the published data [13, 14]. It can be seen that, in general, the activation energies were higher for the La promoted catalysts but lower for the Fe promoted ones compared to the nonpromoted catalyst. Thus, based on the results shown in Table 4.2 and 4.3, it is quite obvious that the effects of the addition of different promoters were quite different.

Table 4.2 Reaction orders [a, b, c, d] for the synthesis of CH_4, C_2H_n, C_3H_n, EtOH and total CO conversion at 230°C

Catalysts	CO Conversion		CH_4 Formation		C_2H_n Formation		C_3H_n Formation		EtOH Formation	
	x	y	x	y	x	y	x	y	x	y
Rh	0.55	-0.26	1.03	-0.67	0.61	-0.35	0.07	0.11	1.02	-0.13
RhLa	0.65	-0.49	0.97	-0.79	0.47	-0.41	0.15	-0.22	0.93	-0.54
RhFe	0.58	0.03	0.69	-0.11	0.11	0.35	-0.14	0.53	0.51	0.30
RhV	0.84	-0.31	1.35	-0.71	0.88	-0.41	0.61	-0.26	1.09	-0.22
RhLaV	0.88	-0.65	1.37	-0.74	0.8	-0.4	0.65	-0.32	1.17	-0.45
RhLaFeV	0.75	-0.21	1.10	-0.55	0.49	-0.25	0.32	-0.16	0.94	-0.16

[a] Catalyst: 0.3 g; inert: α-alumina 3 g; pretreatment: 500°C in H_2; data taken at 15 h TOS after steady state reached.

[b] The rate parameters for each catalyst are determined by fitting a power-law rate expression of the form $r = Ae^{-E_a/RT} P_{H_2}^{x} P_{CO}^{y}$

[c] Error = ±10% for all the values measured.

[d] To determine x, P_{CO}=0.6 atm was used and P_{H2} was varied from 0.4 to 2.4 atm; to determine y, P_{H2}=1.2 atm was used and P_{CO} was varied from 0.46 to 0.8 atm.

Table 4.3 Activation energy [a, b, c, d] for the synthesis of CH_4, C_2H_n, C_3H_n, EtOH and total CO conversion

Catalysts	CO Conversion	CH_4 Formation	C_2H_n Formation	C_3H_n Formation	EtOH Formation
Rh	25.6	29.2	29.6	24.3	18.3
RhLa	27.4	31.6	30.2	30	24.2
RhFe	21.5	23.9	22.6	23	15.7
RhV	26.9	30.9	28.5	28.5	17.6
RhLaV	27.4	30.5	28.4	29.5	21.3
RhLaFeV	25.3	28.2	27.6	27.4	21.5

[a] Catalyst: 0.3 g; Inert: α-alumina 3 g; Pretreatment: 500°C in H_2; Data taken at 15 h TOS after steady state reached.

[b] At constant flow rate = 45 mL/min (H_2/CO =2), P = 1.8 atm, the activation energy for each catalyst is determined by $\ln r = \ln A - \frac{E_a}{RT}$ while temperature varied from 210 to 270°C.

[c] Error = ±10% for all the values measured.

[d] The unit of activation energy is kcal/mol.

4.4 Discussion

4.4.1 Effects of promoters on kinetics

It is widely accepted that H_2 and CO adsorption on a catalyst surface are two key factors in the CO hydrogenation process. In Fig. 4.1(b), (c) and (d), the selectivity for CH_4 increases slightly and the selectivities for higher hydrocarbons decrease with increasing H_2 partial pressure. This is understandable because the increased hydrogen coverage on a Rh-based catalyst surface would definitely increase the hydrogenation of CH_x species, leading to more methane. On the other hand, increased H_2 partial pressure may also decrease CO adsorption and dissociation, resulting in less chain growth. It can be seen in Fig. 4.1(e) that EtOH showed a different trend from C_2H_n or C_3H_n on all the catalysts, indicating that the formation of ethanol involves a different pathway compared to the formation of higher hydrocarbons. On a catalyst surface, an increase in CO adsorption may result in a decrease in H_2 adsorption, as a result of which CH_4 selectivity would decrease. Thus, as seen in Fig. 4.2 (b), increasing CO partial pressure resulted in a decrease in CH_4 selectivity for all catalysts. There was also an increase in EtOH selectivity for all the catalysts (Fig. 4.2 (e)).

As evidenced by IR, chemisorption and CO-TPD [7, 15-18], CO adsorption is enhanced by La addition, especially when small amounts of La are added. As a result, adding La increases the activity compared to non-promoted Rh/SiO_2 as seen in Figs. 4.1 (a) and 4.2 (a). In Table 4.2, the reaction orders of CO for La promoted catalysts were

more negative compared to those for the non-promoted catalyst, almost certainly due to the promotion of CO adsorption by La addition as found in our previous work [5], leading to a greater decrease in reaction rate with increasing partial pressure of CO. However, judging from the fact that the hydrogen reaction orders for all the products on RhLa did not change much compared to those for Rh, the main function of the addition of La appears not to be an enhancement of hydrogenation as suggested by Borer and Prins [18]. In what seems contradictory, La addition increases the activity of Rh/SiO_2 by increasing CO adsorption but this also causes the rate to have a higher negative order in CO partial pressure.

Addition of V also increased the activity as shown in Fig. 4.1(a) and 4.2(a). This is understandable because, even though CO adsorption is partially suppressed by V addition [5], the activity of adsorbed CO may actually increase at the catalytic surface [6]. There are also some interesting differences in the orders of reaction between RhLa and RhV. Contrary to the case for RhLa, hydrogen reaction orders for all species on RhV were larger than those on Rh while that for CO was almost the same, showing higher dependency on hydrogen. This result is consistent with the TPD results from our previous study, which showed reduced H_2 desorption around the reaction temperature with the addition of V [7]. Several research groups have proposed that the addition of V boosts hydrogenation [19-22]. The seeming discrepancy between these results and the ones here may be due to one or more of the following reasons: (i) the conditions for catalyst preparation and pretreatment are different, and it is well know that these conditions strongly affect the interactions between V and Rh [23-25] leading to different

catalytic behavior; (ii) even if V boosts H_2 desorption at higher temperature as claimed by some researchers [19], it is questionable whether these strongly bonded H atoms would be available for the reaction under normal reaction conditions.

The activity of RhLaFeV did not change as much as RhLaV with H_2 partial pressure in Fig. 4.1(a). The sharper decrease in C_2H_n selectivity with increasing H_2 partial pressure observed on Fe promoted catalysts in Fig. 4.1(c) may be due to an improved hydrogenation ability which leads to more methanol and methane. Burch and Petch [26] have suggested that Fe may act as a reservoir for spillover H_2 on the surface of Rh catalysts. Also, since the presence of Fe increases the availability of hydrogen (or the efficiency with which hydrogen is utilized) and at the same time suppresses CO adsorption [7], the dependence on CO partial pressure for RhFe is different from RhLa or RhV as shown in Fig. 4.2(a) and in Table 4.2. In addition, the enhanced hydrogen adsorption could interfere with CO adsorption, which might account for the hindering effect on EtOH selectivity with increasing H_2 partial pressure for RhFe, as shown in Fig. 4.1(e).

4.4.2 Mechanistic study

(i) Methane formation

The mechanism for the formation of methane will now be addressed, which may shed some light on how the different promoters affect CO hydrogenation. However, even for methane formation, there are disagreements in the literature about whether C-O bond cleavage occurs in CO hydrogenation via direct dissociation (carbide models [8, 9, 11,

27-31]) or via a hydrogen-assisted process [10, 12, 32-43]. There has been an increasing focus more recently on the hydrogen-assisted mechanism because several authors have provided strong evidence supporting this mechanism, especially for Rh-based catalysts [10, 32-39, 41-43]. Based on isotopic analysis comparing hydrogen to deuterium, Mori et al. [41, 43] suggested that the rate-limiting step for CO hydrogenation is the dissociation of H_nCO, where n=1, 2 or 3. Based on BOC-MP calculations, Shustorovich and Bell [42] supported the hypothesis that the dissociation of H_nCO is more favorable than the direct dissociation of CO on Pd and Pt. Later, Bell and co-workers suggested that both CO and CO_2 hydrogenation go through hydrogen assisted dissociation to form methane on Rh [10, 39].

By comparing various proposed mechanism with the power-law parameters in Table 4.2, most could be ruled out with the exception of that of Bell and co-workers. Because of its similarity that mechanism but with more detail regarding hydrogen-assisted CO dissociation for gas methane formation, the model of Holmen and co-workers [34] was chosen to describe the mechanism for CO hydrogenation under our reaction conditions, even though it was originally written for CO hydrogenation on Co. As shown in Fig. 4.3, the sequence begins with the adsorption of CO and dissociation of H_2. Then the adsorbed CO is hydrogenated to produce CH_xO species, which subsequently dissociate to form adsorbed CH_3 and O species.

In order to determine the rate-limiting steps for the methane formation for our promoted Rh catalysts, a Langmuir-Hinshelwood approach was used with the mechanism given in Fig. 4.3 to derive rate expressions for different possible rate-limiting steps,

which can be compared with power-law parameters to verify the mechanism and to better understand the effects of the promoters on the reaction. In Fig. 4.3, Step (7), (8) and (9) are believed to go to equilibrium too quickly to be considered as rate-limiting steps [34]. Since adsorbed CO occupies most of the surface sites on Rh [44, 45] and CO conversion is very low (<5%), the intermediates to produce other products should not occupy a significant part of the active sites and therefore are left out of the adsorption term (the denominator) of the derived rate expressions.

$$\frac{1}{2}H_2 + S \longleftrightarrow H - S \quad (1)$$

$$CO + S \longleftrightarrow CO - S \quad (2)$$

$$CO - S + H - S \longleftrightarrow CHO - S + S \quad (3)$$

$$CHO - S + H - S \longleftrightarrow CH_2O - S + S \quad (4)$$

$$CH_2O - S + H - S \longleftrightarrow CH_3O - S + S \quad (5)$$

$$CH_3O - S + S \longleftrightarrow CH_3 - S + O - S \quad (6)$$

$$O - S + H - S \longleftrightarrow HO - S + S \quad (7)$$

$$HO - S + H - S \longleftrightarrow H_2O + 2S \quad (8)$$

$$CH_3 - S + H - S \longleftrightarrow CH_4 + 2S \quad (9)$$

Figure 4.3 Proposed mechanism for CH_4 formation.

The rate expressions derived assuming one of the steps from Steps (1)-(6) in Fig. 4.3 as the rate-limiting step are shown in Table 4.4, where k_i is the kinetic parameter. K_i is an equilibrium constant for the ith step in Fig. 4.3. The concentration of vacant active sites [S] is determined from a balance of the total concentration of the active sites [S_0] which is assumed to be constant. [S_0] is equal to [S] plus the sum of all sites occupied by reactants and products. In Table 4.4, the ranges of possible reaction orders x and y in an equivalent power law rate expression based on the derived mechanistic rate expression are given assuming that step to be rate-limiting. Comparing the ranges of possible reaction orders with the experimental power-law results for CH_4 formation in Table 4.2, Step 1, 2 or 3 as the rate limiting step cannot fit the experimental data because all the apparent orders for H_2 for the different catalysts were larger than 0.5. For Rh and RhLa, the apparent order for H_2 partial pressure was approximately equal to 1 (Table 2). It is generally agreed that the H_2 desorption activation energy is relatively low and most of the active sites are occupied by CO on Rh and RhLa [9, 27, 33-35]. Thus, the H_2 terms in the denominator are reported to be statistically insignificant and can be neglected in the mechanistic rate expression. As a result, Step (4) (resulting H_2 exponent ~1) is more likely to be the rate limiting step than either Step (5) or (6) (resulting H_2 exponent ~1.5).

For the Fe singly promoted Rh/SiO_2 catalyst, it is to be expected that x (0.7 as shown in Table 4.2) is a little bit different from the La promoted or nonpromoted catalysts because the concentration of hydrogen on the surface should no longer be ignored since the addition of Fe leads to a significant suppression of CO adsorption, although CO adsorption still occupies most of the active sites on surface as a result of

weakening H_2 adsorption as determined by Egawa et al. using HREELS and TPD methods [46]. Since Steps (1), (2), and (3) have already been ruled out for all the catalysts, the rate-limiting step should be Step (4), (5) or (6). Also, it is not practical to compare these three possibilities as for RhLa or Rh because H_2 terms in the denominator can no longer be ignored compared to CO terms.

The H_2 power law parameters for CH_4 formation are much larger than 1.0 for RhV (1.35) and RhLaV (1.37), thus, the rate limiting step for these two catalysts may be either Step (5) or (6). This is suggested by other data since the V addition hinders CO adsorption but increases desorption/reactivity of adsorbed CO species [6], which, thus, may result in a change in the rate-limiting step. However, for RhLaFeV, step 4 could also be the rate limiting step even though x=1.1 and is only slightly >1. Thus, x=1.1 can be considered to be within experimental and Langmuir-Hinshelwood error of x=1.0.

It is difficult to distinguish different possible rate expressions or figure out the values of the equilibrium constants by our present work due to the complexity of the mechanism and the assumptions required using the Langmuir-Hinshelwood approach. Nevertheless, a sound conclusion can be drawn here is that the addition of different promoters resulted in different rate limiting steps, which can be ascribed to the modified CO/H_2 adsorption, reactivity of adsorbed species on Rh/SiO_2 promoted by different promoters.

Table 4.4: Rate-limiting step assumed and the resulted rate expression in various possibilities for CH_4 formation

Possible rate-limiting step for CH_4 from Fig. 3	Rate Expressions	x [a]	y [a]
1	$\frac{k_1[S_0]P_{H_2}^{1/2}}{\left[1+K_2P_{CO}\right]}$	0.5	-1<y<0
2	$\frac{k_2[S_0]P_{CO}}{\left[1+K_1(P_{H_2})^{1/2}\right]}$	-0.5<x<0	1
3	$\frac{k_3K_2K_1\left[S_0\right]^2P_{H_2}^{1/2}P_{CO}}{\left[1+K_1(P_{H_2})^{1/2}+K_2P_{CO}\right]^2}$	-0.5<x< 0.5	-1<y<1
4	$\frac{k_4K_3K_2K_1^2\left[S_0\right]^2P_{H_2}P_{CO}}{\left[1+K_1(P_{H_2})^{1/2}+K_2P_{CO}+K_3K_2K_1P_{H_2}^{1/2}P_{CO}\right]^2}$	0<x<1	-1<y<1
5	$\frac{k_5K_4K_3K_2K_1^3\left[S_0\right]^2P_{H_2}^{3/2}P_{CO}}{\left[1+K_1(P_{H_2})^{1/2}+K_2P_{CO}+K_3K_2K_1P_{H_2}^{1/2}P_{CO}+K_4K_3K_2K_1^2P_{H_2}P_{CO}\right]^2}$	0.5<x<1.5	-1<y<1
6	$\frac{k_6K_5K_4K_3K_2K_1^3\left[S_0\right]^2P_{H_2}^{3/2}P_{CO}}{\left[\begin{array}{l}1+K_1(P_{H_2})^{1/2}+K_2P_{CO}+K_3K_2K_1P_{H_2}^{1/2}P_{CO}+K_4K_3K_2K_1^2P_{H_2}P_{CO}+\\ K_5K_4K_3K_2K_1^3P_{H_2}^{3/2}P_{CO}\end{array}\right]^2}$	-1.5<x<1.5	-1<y<1

[a] x, y would be the orders of reaction of H_2 and CO in the equivalent power-law rate expression $r = Ae^{-E_a/RT}P_{H_2}^{x}P_{CO}^{y}$

Table 4.5: Rate-limiting step assumed and the resulted rate expression in various possibilities for EtOH formation

Possible rate-limiting step for EtOH from Fig. 4	Rate Expression	x [a]	y [a]
9`	$\frac{k_{10}K_9K_8K_6K_5K_4^2K_3^2K_2^2K_1^7\left[S_0\right]^2 P_{H_2O}^{-1}P_{H_2}^{7/2}P_{CO}^2}{\left[1+K_1(P_{H_2})^{1/2}+K_2P_{CO}+K_3K_2K_1P_{H_2}^{1/2}P_{CO}+K_4K_3K_2K_1^2P_{H_2}P_{CO}+K_5K_4K_3K_2K_1^3P_{H_2}^{3/2}P_{CO}+K_9K_8K_6K_5K_4K_3K_2K_1^5P_{H_2}^{5/2}P_{CO}P_{H_2O}\right]^2}$	-1.5<x<3.5	0<y<2
10`	$\frac{k_{11}K_{10}K_9K_8K_6K_5K_4^2K_3^2K_2^2K_1^8\left[S_0\right]^2 P_{H_2O}^{-1}P_{H_2}^{4}P_{CO}^2}{\left[1+K_1(P_{H_2})^{1/2}+K_2P_{CO}+K_3K_2K_1P_{H_2}^{1/2}P_{CO}+K_4K_3K_2K_1^2P_{H_2}P_{CO}+K_5K_4K_3K_2K_1^3P_{H_2}^{3/2}P_{CO}+K_9K_8K_6K_5K_4K_3K_2K_1^5P_{H_2}^{5/2}P_{CO}P_{H_2O}+K_{10}K_9K_8K_6K_5K_4^2K_3^2K_2^2K_1^7\left[S_0\right]^2 P_{H_2O}^{-1}P_{H_2}^{7/2}P_{CO}^2\right]^2}$	-3<x<4	-2<y< 2

[a] x, y would be the orders of reaction of H_2 and CO in the equivalent power-law rate expression $r = Ae^{-E_a/RT}P_{H_2}^{x}P_{CO}^{y}$

(ii) Ethanol formation

Since ethanol synthesis is one of the key issues of CO hydrogenation, extensive efforts have been focused on the mechanism of ethanol formation. However, since the insertion step may occur through different reaction routes-insertion of CH_xO into a metal-CH_x bond (x=0, 1, 2 or 3), there are few detailed results in the literature regarding the ethanol synthesis mechanism on Rh. A scheme, however, is proposed in Fig. 4.4 based on methane formation mechanism. Moreover, this mechanism of ethanol formation is similar to the mechanism Holmen and co-workers [34] proposed for Co catalysts by comparing the activation energies for possible insertion steps by microkinetic modeling.

$$\frac{1}{2}H_2 + S \longleftrightarrow H - S \quad (1)$$

$$CO + S \longleftrightarrow CO - S \quad (2)$$

$$CO - S + H - S \longleftrightarrow CHO - S + S \quad (3)$$

$$CHO - S + H - S \longleftrightarrow CH_2O - S + S \quad (4)$$

$$CH_2O - S + H - S \longleftrightarrow CH_3O - S + S \quad (5)$$

$$CH_3O - S + S \longleftrightarrow CH_3 - S + O - S \quad (6)$$

$$O - S + H - S \longleftrightarrow HO - S + S \quad (7)$$

$$HO - S + H - S \longleftrightarrow H_2O + 2S \quad (8)$$

$$CH_3 - S + CH_2O - S \longleftrightarrow CH_3CH_2O - S + S \quad (9)$$

$$CH_3CH_2O - S + H - S \longleftrightarrow CH_3CH_2OH + 2S \quad (10)$$

Figure 4.4 Proposed mechanism for EtOH formation.

In Table 4.2, it can be seen that the even though the reaction order for H_2 partial pressure did not change much between methane and ethanol formation, the reaction order for CO partial pressure changed significantly. Thus, it can be concluded that there are different rate-limiting steps for ethanol and methane formation. Since (1) the rate expressions for rate limiting step of steps (1)-(6) were already evaluated in determining the rate limiting step for methane formation and (2) since the rate limiting step for ethanol and methane appear to be different, it is unlikely that adsorption of CO or H_2 (step (1) and (2)) or the synthesis of CH_3 species (step (3) – (6)) provide the rate limiting step for ethanol. Thus, most likely, the rate-limiting step for ethanol formation is step (9`) or (10`); steps (7) and (8) being earlier ruled out as for fast. Table 4.5 shows these two possibilities and the ranges of apparent reaction orders x and y based on the derived Langmuir-Hinshelwood mechanistic rate expressions. Since most of the reaction orders for CO partial pressure are negative in Table 4.2, the rate limiting step in ethanol formation mechanism should be Step (10`) for all the catalysts except perhaps RhFe. However, it is difficult to distinguish between Step (9`) and (10`) for RhFe because the reaction order for CO partial pressure on RhFe is higher than others (around 0.30).

4.5 Conclusions

A series of Rh-based catalysts with single or combined promoters among La, V and Fe were prepared by sequential or co-impregnation method. A kinetics study of CO

hydrogenation on these catalysts was conducted to understand the mechanism and the role of promoters.

All the catalysts except RhFe and RhLaFeV showed the same trends in CO conversion and selectivities to different products with increasing CO or H_2 partial pressure. The influence of partial pressure to activity is more obvious for RhLaV than other catalysts, which appears to due to a synergistic promoting effect of La and V. For the Fe promoted catalysts, the CO conversion rate increases with CO partial pressure, which may because Fe serves like a reservoir to hydrogen on the catalyst surface.

The parameters obtained from power law were used to fit the rate expressions derived based on different limiting steps to understand the reaction mechanism and the effects of different promoters. The fact that coefficient x is positive and the coefficient y is negative indicates promotion by hydrogen and inhibition by carbon monoxide. By comparing the power law parameters with the Langmuir-Hinshelwood rate expression, $CHO-S+H-S \longleftrightarrow CH_2O+S$ is more likely to be the rate limiting step for the methane formation on Rh and RhLa. The rate limiting step for the methane formation on RhV and RhLaV is $CH_2O-S+H-S \longleftrightarrow CH_3O-S+S$ or $CH_3O-S+S \longleftrightarrow CH_3-S+O-S$. For ethanol synthesis, $C_2H_5O-S+H-S \longleftrightarrow C_2H_5OH+2S$ is the possible rate limiting step for all the catalysts except RhFe. However, it is unclear that whether $CH_3-S+CH_2O-S \longleftrightarrow C_2H_5O-S+S$ or $C_2H_5O-S+H-S \longleftrightarrow C_2H_5OH+2S$ is the rate limiting step for ethanol synthesis on RhFe.

4.6 Acknowledgments

We acknowledge financial support from the U. S. Department of Energy (Award No 68 DE-PS26-06NT42801).

4.7 References

[1] J.P. Hindermann, G.J. Hutchings, A. Kiennemann, Catal. Rev. Sci. Eng. 35 (1993) 1.

[2] S.S.C. Chuang, R.W. Stevens, Jr., R. Khatri, Top. Catal. 32 (2005) 225.

[3] J.J. Spivey, A. Egbebi, Chem. Soc. Rev. 36 (2007) 1514.

[4] V. Subramani, S.K. Gangwal, Energy Fuels 22 (2008) 814.

[5] J. Gao, X. Mo, A.C. Chien, W. Torres, J.G. Goodwin, Jr., J. Catal. 262 (2009) 119.

[6] X. Mo, J. Gao, J.G. Goodwin, Jr., Catal. Today 147 (2009) 139.

[7] X. Mo, J. Gao, N. Umnajkaseam, J.G. Goodwin, Jr., J. Catal. 267 (2009) 167.

[8] B. Sarup, B.W. Wojciechowski, Can. J. Chem. Eng. 67 (1989) 620.

[9] B. Sarup, B.W. Wojciechowski, Can. J. Chem. Eng. 67 (1989) 62.

[10] I.A. Fisher, A.T. Bell, J. Catal. 162 (1996) 54.

[11] J.M.H. Lo, T. Ziegler, J. Phy. Chem., C 111 (2007) 11012.

[12] O.R. Inderwildi, S.J. Jenkins, D.A. King, J. Phy. Chem., C 112 (2008) 1305.

[13] R.P. Underwood, A.T. Bell, Appl.Catal. 21 (1986) 157.

[14] P. Gronchi, S. Marengo, C. Mazzocchia, E. Tempesti, R. DelRosso, React. Kinet. Catal. Lett. 60 (1997) 79.

[15] R.P. Underwood, A.T. Bell, J. Catal. 111 (1988) 325.

[16] R.P. Underwood, A.T. Bell, J. Catal. 109 (1988) 61.

[17] A.L. Borer, R. Prins, Stud. Surf. Sci. Catal. 75 (1993) 765.

[18] A.L. Borer, R. Prins, J. Catal. 144 (1993) 439.

[19] H.Y. Luo, H.W. Zhou, L.W. Lin, D.B. Liang, C. Li, D. Fu, Q. Xin, J. Catal. 145 (1994) 232.

[20] T. Koerts, R.A. Vansanten, J. Catal. 134 (1992) 13.

[21] T. Beutel, O.S. Alekseev, Y.A. Ryndin, V.A. Likholobov, H. Knoezinger, J. Catal. 169 (1997) 132.

[22] H.Y. Luo, W. Zhang, H.W. Zhou, S.Y. Huang, P.Z. Lin, Y.J. Ding, L.W. Lin, Appl. Catal., A 214 (2001) 161.

[23] S. Ishiguro, S. Ito, K. Kunimori, Catal. Today 45 (1998) 197.

[24] T. Beutel, V. Siborov, B. Tesche, H. Knoezinger, J. Catal. 167 (1997) 379

[25] S.-i. Ito, C. Chibana, K. Nagashima, S. Kameoka, K. Tomishige, K. Kunimori, Appl. Catal., A 236 (2002) 113.

[26] R. Burch, M.I. Petch, Appl Catal., A 88 (1992) 39.

[27] I.C. Yates, C.N. Satterfield, Energy & Fuels 5 (1991) 168.

[28] G.P. van der Laan, A.A.C.M. Beenackers, Appl. Catal., A 193 (2000) 39.

[29] C.S. Kellner, A.T. Bell, J. Catal. 70 (1981) 418.

[30] C.G. Takoudis, Ind. Eng. Chem. Prod. Res. Dev. 23 (1984) 149.

[31] D.B. Dadyburjor, J. Catal. 82 (1983) 489.

[32] Y.I.P. N. V. Pavlenko, Theor. Exp. Chem. 33 (1997) 254.

[33] N.V.P.a.G.D.Z. A. I. Tripol'skii, Theor. Exp. Chem. 33 (1997) 165.

[34] S. Storsaeter, D. Chen, A. Holmen, Surf. Sci. 600 (2006) 2051.

[35] C. Mazzocchia, P. Gronchi, A. Kaddouri, E. Tempesti, L. Zanderighi, A. Kiennemann, J. Mol. Catal., A 165 (2001) 219.

[36] B.H. Davis, Fuel Process Tech. 71 (2001) 157.

[37] C.F. Huo, Y.W. Li, J.G. Wang, H.J. Jiao, J. Phy. Chem. C 112 (2008) 14108.

[38] M.A. Vannice, J. Catal. 37 (1975) 449.

[39] K.J. Williams, A.B. Boffa, M. Salmeron, A.T. Bell, G.A. Somorjai, Catal. Lett. 9 (1991) 415.

[40] G.A. Huff, C.N. Satterfield, Ind. Eng. Chem. Process Des. Dev. 23 (1984) 696.

[41] Y. Mori, T. Mori, T. Hattori, Y. Murakami, Appl. Catal. 66 (1990) 59.

[42] E. Shustorovich, A.T. Bell, J. Catal. 113 (1988) 341.

[43] Y. Mori, T. Mori, T. Hattori, Y. Murakami, Appl. Catal. 55 (1989) 225.

[44] Y. Kim, H.C. Peebles, J.M. White, Surf. Sci. 114 (1982) 363.

[45] L.J. Richter, B.A. Gurney, W. Ho, J. Chem. Phys. 86 (1987) 477.

[46] C. Egawa, S. Endo, H. Iwai, S. Oki, Surf. Sci. 474 (2001) 14.

CHAPTER FIVE

THE EFFECT OF STRONG METAL-OXIDE INTERACTIONS IN PROMOTED RH/SIO2 ON CO HYDROGENATION: ANALYSIS AT THE SITE LEVEL USING SSITKA

5.1 Introduction

In order to decrease the demand for crude oil and lessen the environmental impact, Rh-based catalysts have been extensively studied in the CO hydrogenation reaction because their high selectivity towards ethanol [1-6]. There have been many discussions on the influences of supports and promoters for the synthesis of ethanol and other alcohols from CO hydrogenation. However, in recent literature, silica supports are more favorable than others for ethanol production by increasing Rh dispersion and the concentration of Rh^{+} on catalyst surface, which might be helpful for oxygenate formation [7, 8]. V is an important promoter for ethanol production on Rh/SiO_2 [9-15]. In our previous studies [16-18], it was found that the addition of V increased activity three times more than non promoted Rh/SiO_2, and also suppressed methane formation significantly [18]. Many factors including both reaction and pretreatment conditions have been shown to influence the activity and selectivities of V promoted Rh/SiO_2. There is little agreement in discussions about how V modifies catalyst behavior of Rh/SiO_2. While Kip and co-workers suggested that V enhances reactivity and selectivity towards ethanol by enhancing CO dissociation [15], other researchers have proposed that the function of V is to boost hydrogenation [13, 14, 19, 20]. It was also found that V suppressed CO

adsorption [16] and also modified the H_2-TPD characteristics of Rh/SiO_2 [18]. It was suggested in our earlier IR study that the higher catalytic activity of the V singly-promoted Rh/SiO2 catalyst may be ascribed to an increased desorption rate/reactivity of the adsorbed CO species since the addition of V appeared to reduce the total number of reaction sites [16].

It was found that the activity and selectivity of the catalysts with group 8 metals supported on transition metal oxides, is strongly dependent on the pretreatment conditions [21-23]. In 1978, Tauster and coworkers first proposed that strong metal-support interactions were a reason for this behavior [21, 23]. After that, there are numerous studies regarding the influence of the strong metal-oxide interaction (SMOI) effect [8, 24-46]. Usually, catalytic activities and CO or H_2 adsorption are more or less suppressed by SMOI effect. However, the interpretations regarding the reasons for the SMOI effect are much less agreeable. Several theories have been proposed to explain SMOI including formation of alloys [23, 25, 27, 34, 40], the electronic influence of the promoter or support oxide [8, 24, 28, 41] and a covering of the metal particles by the promoter or support oxide after reduction at high temperature [13, 15, 30, 33, 42-45, 47, 48].

SMOI effect has been found on Rh/SiO_2 promoted by group 8 transition metal oxides since the end of 1980s but less widely studied compared to other transition metals [13, 14, 49-53]. For V promoted Rh/SiO_2, Kip et al [15, 54] found that Rh helped V reduction while V hampered Rh reduction by TPR experiments, which is consistent with our previous results [18], indicating an intimate contact between Rh and V. With FTIR

spectroscopy, Beutel et al [13] also found SMOI effect on V promoted Rh/SiO_2. Moreover, both high temperature reduction and high temperature calcination were proved to induce SMOI effects leading to a partial coverage of the Rh metal surface by V oxide. By studying CO_2 reforming of methane over V promoted Rh/SiO_2, Sigl et al. [55] suggested a formation of a partial VO_x overlayer on Rh surface when calcination temperature was higher than 500 °C. It was proposed that new sites were created at Rh-VO_x interfacial region that are considered to be relatively active for CO_2 reforming.

Steady-state isotopic transient kinetic analysis (SSITKA) is a powerful tool to analyze surface reaction. It may be the most accurate kinetic technique for characterizing surface reaction parameters under reaction conditions [56]. However, there is few detailed SSITKA study on V promoted Rh-based catalysts for CO hydrogenation. It was reported by Koerts and Santen [20] that vanadium promotion decreased the desorption rate of ethanol, enhanced the hydrogenation rate to ethanol, and increased the surface concentration of oxygenated intermediates in isotopic labeling experiments. However, a long delay in ethanol production was also mentioned in their paper, which is contradict to what Burch and Petch [57] found in their transient experiments for non-promoted and Fe, Li, Mn-promoted Rh/SiO_2 by switching CO/H_2 to hydrogen or helium.

The focus of this study is to investigate the modification of Rh/SiO_2 by V on the active sites for CO hydrogenation for a better understanding of SMOI of Rh and VO_x. In this work, non-promoted and V promoted Rh/SiO_2 were prepared by the impregnation method and their catalytic activities were tested for CO hydrogenation at 230 °C and 1.8 atm, after being reduced at different temperatures. The SMOI effects on the V promoted

catalysts were further examined by H_2 chemisorption and SSITKA. Even though H_2 chemisorption was carried out at room temperature and SSITKA was under methanation conditions to simplify the mass spectrometry (MS) analysis, it is valuable to shed some light on the change of the surface status by SMOI effects.

5.2 Experimental

5.2.1 Catalyst preparation

Since the catalysts used in this study were the same as those used in our studies reported earlier, a detailed description of catalyst preparation can be referred to our earlier paper [16]. As support, silica gel (99.95%, Alfa Aesar) was used, obtained by first grounding and sieving to 30-50 mesh, washing with boiled distilled water for 3 times, and subsequent calcination in air at 500^{o}C for 4 h. This resulted in SiO_2 with a high surface area (BET surface area after pretreatment was 250±2 m^2/g). The catalysts were calcined at 500^{o}C to remove nitrogen. It was reported by Beutel et al. that the SMOI effects could be induced when T_{cal} is higher than 973K [13]. Thus, a 500^{o}C calcination was also designed to eliminate the influence of calcination temperature. $Rh(NO_3)_3$ hydrate (Rh ~36 wt%, Fluka) and NH_4VO_3 (99.5%, Alfa Aesar) were used as purchased. Catalysts were prepared by incipient wetting this support with an aqueous solution of $Rh(NO_3)_3$ hydrate or NH_4VO_3 (2 mL solution/1 g silica gel), subsequently drying at 90^{o}C for 4 h and then at 120^{o}C overnight. To remove nitrogenous residues from the precursors, the catalysts were calcined in air at 500^{o}C for 4 h. Rh weight content was always around

1.5% and V was 1.5% if added. The notation of Rh/SiO_2 will be used for silica supported Rh catalyst, while $Rh/V/SiO_2$ will represent silica supported Rh catalyst promoted with V by sequential impregnation.

5.2.2 H_2 chemisorption

The number of exposed rhodium surface atoms was determined by H_2 chemisorption using a Micromeritics ASAP 2010C. Catalyst samples of approximately 0.2 g were first evacuated at 110°C for 30 min before being reduced at certain temperature in a hydrogen flow for 30 minutes, and then evacuated at 10^{-6} mm Hg and reduction temperature for 120 min. After cooling under vacuum to 35°C, the adsorption isotherm was recorded. The amount of chemisorbed H_2 was obtained by extrapolating the total adsorption isotherm to zero pressure, and the metal dispersion was calculated subsequently assuming $H/Rh_s=1$.

5.2.3 Reaction

CO hydrogenation was carried out in a fixed-bed differential reactor (316 stainless steel) with length ~300 mm and internal diameter ~5 mm. 0.3g catalyst and 3g inert were loaded between quartz wool plugs and placed in the middle of the reactor with a thermocouple close to the catalyst bed. In this work, molecular sieve traps (Alltech) were used to remove H_2O and CO, and a CO purifier (Swagelok) was applied to remove CO_2 and carbonyls. Prior to reaction, the catalyst was reduced in-situ with hydrogen (flow rate = 30 mL/min) at a specific reduction temperature for 1 h. According to our

study, the activity of Rh/SiO_2 reduced at 700°C dropped significantly compared to that reduced at 600°C, which probably indicated a pronouncing sintering. Thus, the effect of reduction temperature was studied only in the range of 300-600°C of in this work. Also, a same temperature ramping rate of 5°C/min was used for both of the catalysts. After reduction, the catalyst was then cooled down to reaction temperature and reaction started as gas flow was switched to H_2/CO (H_2 flow rate = 30 mL/min, CO flow rate = 15 mL/min) for initial reaction study. Brooks 5840E series mass flow controllers were used to control flow rates. The activation energies of CO hydrogenation between 210 and 280^{o}C from Arrhenius plots was found out to be around 25 kcal/mol, which indicated that the reaction was under kinetic control.

The reaction products, including C_1-C_7 hydrocarbons and oxygenates, were separated chromatographically using a Restek RT-QPLOT column (30m, 0.53mm ID) and detected by an FID (flame ionization detector) in a gas chromatograph (Varian 3800 series). CO and other inorganic gases were analyzed by a TCD (thermal conductivity detector) after separation with a Restek HayeSep® Q column. The analysis details can be found in our previous paper [16]. The selectivity of a particular product was calculated as $S_i=n_iC_i / \sum n_iC_i$, where n_i and C_i are the carbon number and molar concentration of the *i*th product, respectively. The activity is expressed as A=μmol CO/gcat.*s, where numerator denotes the amount of CO converted into products.

5.2.4 SSITKA

Isotopic analysis was carried out in a steady state isotopic transient kinetic analysis (SSITKA) system as described elsewhere [58]. Figure 5.1 shows the reaction system setup for SSITKA. Isotopic transient measurements were carried out by switching from two feed streams with same flow rate but containing different isotopic labeling of reactant species (^{12}CO (5%Ar) vs ^{13}CO) after reactions reached steady state. The effluent gas was analyzed on-line by GC as described for the standard reaction and a Pfeiffer mass spectrometer (MS) with a high speed acquisition system. Back-pressure regulators on both reactant streams were used to maintain the same pressure on both feed stream, thus, switching of the feed streams could result in minimum disturbing of reaction conditions. The gas lines used in the system were designed to be as short as possible to minimize gas holdup in the system. Moreover, the 5% Ar in ^{12}CO flow is used as an inert tracer to determine the holdup time. The reaction conditions were the same as the standard reaction except the temperature and flow rates. For SSITKA, reaction temperature was switched to 280 ^{o}C and the H_2 flow rate was 20 times as high as CO flow rate (total flow rate = 60 mL/min, H_2: He: CO=20: 19: 1) to maximize methane production.

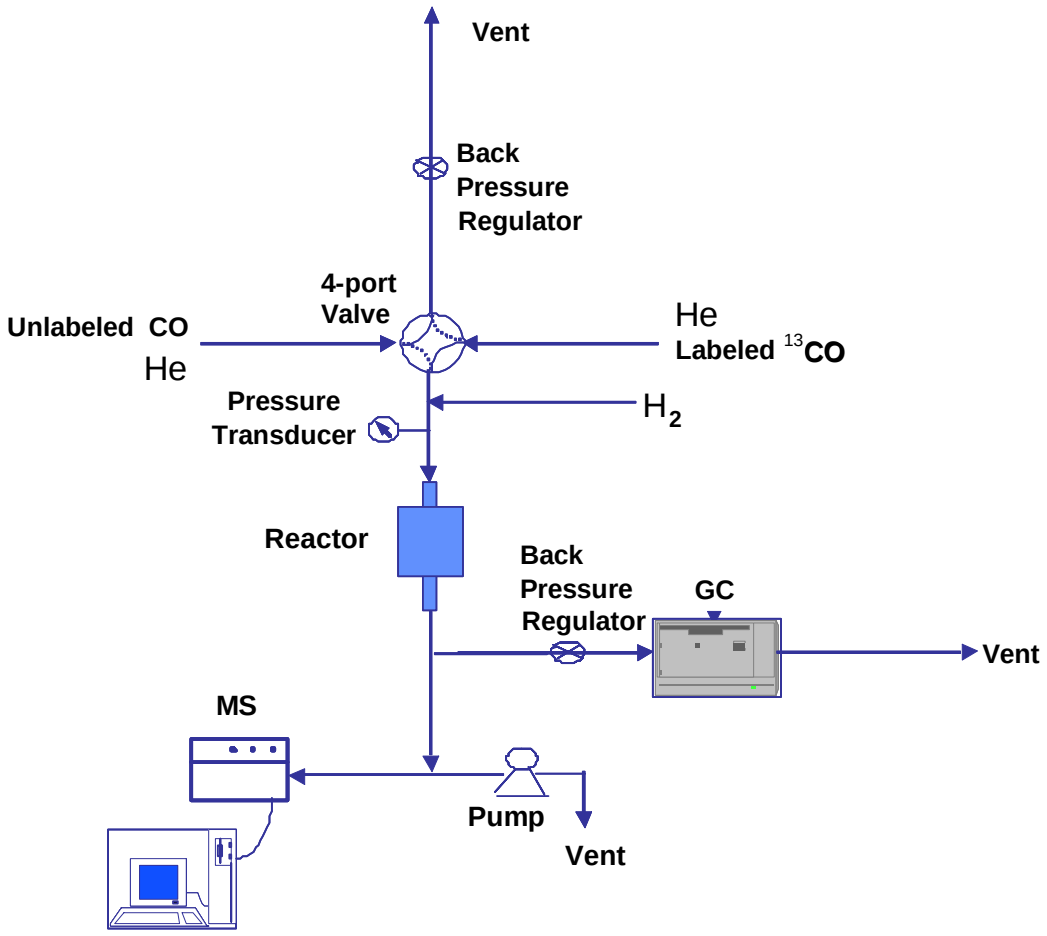

Figure 5.1 The reaction system set up for SSITKA at methanation condition.

5.3 Results

5.3.1 H_2 Chemisorption

Table 5.1: Determination of accessible surface Rh dispersion and H_2 chemisorbed [a].

Catalyst	Reduction Temperature (°C)	H_2-chemisorbed (μmol/gcat.)		Metal Dispersion (%)	
		Total	Irrev.	Total	Irrev.
Rh/SiO_2	600	31.1	15.0	48.1	23.1
	300	31.7	13.2	49.0	20.4
$Rh/V/SiO_2$	600	0.25	-	0.39	-
	500	0.35	-	0.54	-
	400	0.57	0.17	0.88	0.26
	300	1.18	0.19	1.83	0.29

[a] Catalyst: 0.2 g. Metal dispersion is based on total H_2 chemisorbed and an assumption of H/Rh_s=1. Experimental error: ±10%.

Table 5.1 shows the influence of reduction temperature on H_2 chemisorption at 35 °C. The amounts of total H_2 chemisorbed and irreversible H_2 chemisorbed are both provided. The metal dispersion was calculated by assuming an adsorbed H atom to surface Rh atom stoichiometry of 1:1. It is widely accepted that the concentration of accessible surface Rh atoms is determined more accurate by H_2 adsorption than CO adsorption, because the stoichiometry of CO chemisorption is uncertain-CO can adsorb simultaneously as a gem-dicarbonyl, a linear carbonyl and a bridge carbonyl [5, 17]. However, even this H_2 chemisorption technique is not without its difficulties and uncertainties. The chemisorption cannot present the reaction condition since it was taken at room temperature to avoid the spillover of H_2 to support at high temperature. But still, it can shed some light on how SMOI effects influence the catalyst behaviors. As can be seen in Table 5.1, the reduction temperature did not influence the H_2 chemisorption results on Rh/SiO_2, indicating no sintering effect under reduction temperature 300-600 °C.

For $Rh/V/SiO_2$, , the amount of H_2 chemisorption was decreased significantly by the addition of V, which is similar to CO chemisorption [16]. It is probably due to a covering of Rh particle by V on catalyst surface. It is also obvious that the amount of H_2 adsorption increased with decreasing reduction temperature, suggesting that the interaction of VO_x with Rh become more significant with higher reduction temperature. It is probably because a partial VO_x overlayer on the Rh surface was formed by SMOI effects [55]. At higher reduction temperature, this overlayer results in lower chemisorption by reducing the amount of accessible Rh atoms. However, since the catalysts cannot be seen through TEM because of the relatively low loading of Rh, there is also possibility that the growth of Rh particle size with increasing reduction temperature may also result in the decrease of H_2 chemisorption. The reason to rule out this possibility will be discussed in the following SSITKA section.

5.3.2 Reaction study

Table 5.2 shows the catalytic activities and selectivities of Rh/SiO_2 and $Rh/V/SiO_2$ reduced at different temperatures. For Rh/SiO_2, when reduction temperature increased from 300 to 600 °C, activities were similar within experimental error, which excludes the possibility of sintering an the reduction temperature increased. With respects to the selectivities, molar ratios of olefin to paraffin for C_2 or C_3 hydrocarbons were also almost the same. This suggests reduction temperature did not influence the hydrogenation ability of Rh/SiO_2. The oxygenate selectivities were essentially independent of the reduction temperature. Interestingly, there was less C_{2+} hydrocarbon

production while more methane produced as Rh/SiO_2 reduced at higher reduction temperature. In recent years, the interaction between Rh and SiO_2 was also reported to influence the catalyst activity [59, 60]. Hayashi et al. [60] proposed that this interaction caused the existence of $Rh^{\delta+}$ and thus, modified the selectivities. In our work, the SMOI effects between Rh and SiO_2 probably changed the properties of the active sites with reduction temperature increasing from 300 to 600°C. As a result, activity was consistent but C_{2+} hydrocarbon was more likely to form than methane when reduced at higher temperature. However, the effect of reduction temperature on V promoted catalyst for CO hydrogenation is significantly different from that on Rh/SiO_2. The activity decreased dramatically with the increasing reduction temperature. The SMOI effects to product distribution is also changed in V promoted catalyst which exhibits a tendency of decreasing methane and constant C_{2+} hydrocarbons with higher reduction temperature. The production of methanol increased while the selectivities of all the other oxygenates were not affected much by increasing reduction temperature. It is possible that methane and methanol are formed by the same kind of intermediates on the surface, thus, the increase of methanol formation is in coincidence with a decrease of methane production. In our previous paper [61], mechanism of CO hydrogenation on Rh-based catalyst were discussed based on literature review and kinetic study. It was believed that on Rh-based catalysts, methane was formed by hydrogen first interact with adsorbed CO to form CH_xO species, and then split to CH_x species to be further hydrogenated to methane. SMOI effects between V and Rh may hinder the ability of active sites to split CH_xO species to CH_x species, as a result, more CH_xO species form methanol by direct

hydrogenation. SMOI effects did not correlate with hydrogenation ability of $Rh/V/SiO_2$ for other C_{2+} hydrocarbon because the molar ratios of olefin to paraffin for C_2 or C_3 were almost constant with different reduction temperature. Our findings that activity was suppressed by SMOI effects are in agreement with those of Hayek group [26]. They investigated the catalytic activity of Rh/VO_x and observed that activity decreased steadily when reduction temperature increased from 200 to 600 °C. It may be due to V covering free metal surface area, which forms a partial VO_x overlayer on the Rh surface and as a result decreases the amount of active sites [14, 55]. Also, it could in part due to the formation of stable bulk alloy phases [26]. Rupprechter et al. suggested that in the most active state the structure of the Rh particles should be highly disordered, and with higher temperature reduction the particles were more likely to exhibit rounded profiles [62].

Table 5.2: Catalytic activities of Rh/SiO_2 and $Rh/V/SiO_2$ reduced at different temperatures [a]

Catalyst	Reduction Temperature (°C)	SS Rate [*] (μmol/gcat/s)	Selectivity (%) [b]						$C_{2=}/C_2$ [e]	$C_{3=}/C_3$ [e]
			CH_4	$C_{2+}HC$ [c]	MeOH	Acetaldehyde	EtOH	Other C_{2+} oxy [d]		
$Rh(1.5)/SiO_2$	300	0.03	34.3	46.4	-	4.1	15.2		2.0	2.6
	400	0.03	35.2	43.7	-	3.3	17.9	-	1.8	2.7
	500	0.03	48.1	28.7	1.2	6.5	15.6	-	1.9	2.6
	600	0.04	55.4	19.6	-	4.9	20.1	-	1.8	2.5
$Rh(1.5)/V(1.5)/SiO_2$	300	0.63	20.0	58.0	2.6	3.9	14.2	1.3	2.6	11.7
	400	0.45	18.2	56.9	2.9	4.0	16.5	1.4	3.1	12.1
	500	0.10	12.4	60.5	6.5	3.1	15.8	1.7	3.2	10.1
	600	0.05	11.4	59.5	11.7	2.1	15.4	-	3.3	8.4

[*] Steady state.
[a] Catalyst: 0.3 g, Inert : α-alumina 3 g; reaction at 230 °C; P = 1.8 atm, flow rate = 45mL/min (H_2/CO =2), data taken at 15 h after steady state reached. Experimental error: ±10%.
[b] Molar selectivity = $n_iC_i / \sum n_iC_i$.
[c] Hydrocarbons with 2 or more carbons.
[d] Other oxygenates with 2 or more carbons.
[e] Molar ratio of C_n olefin / C_n paraffin.

5.3.3 SSITKA Study

Table 5.3: The effect of reduction temperature on surface kinetic parameters for Rh/V/SiO2 [a]

Reduction Temperature (°C)	Rate (μmol/gcat/s)	CH_4 selectivity (%)	τ_{CO} (s)	TOF_{CO} (s^{-1}) [b]	N_{CO} (μmol/gcat) [c]	τ_{CH4} (s)	TOF_{CH4} (s^{-1}) [b]	N_{CH4} (μmol/gcat) [c]
300	0.048	90.2	4.98	0.20	9.04	5.77	0.17	0.25
400	0.039	93.6	3.90	0.26	7.11	4.50	0.22	0.17
500	0.029	84.8	2.42	0.41	4.42	2.69	0.37	0.07
600	0.022	79.1	0.62	1.61	1.13	0.63	1.59	0.01

[a] Catalyst: 0.3 g, Inert : α-alumina 3 g; reaction at 280 °C; P = 1.8 atm, flow rate = 60 mL/min (H_2: He: CO=20: 19: 1). Experimental error: ±10%.
[b] $TOF_i = 1/\tau_i$.
[c] N_i =Rate * $Selectivity_i$ % * τ_i.

The SSITKA experiments show that there is a significant difference in overall activity and active surface intermediates (N) with different reduction temperature for $Rh/V/SiO_2$. The results are summarized in Table 5.3. The experiments have been carried out under methanation e.g. higher temperature than those of standard reaction conditions and a large excess of H_2. The purpose of the increase in the temperature and H_2 partial pressure was to obtain CH_4 as the primary product in order to simplify the mass spectrometric (MS) analysis. In our study on $Rh/V/SiO_2$, the selectivity to methane varies between 80% and 95%. Even though the SSITKA results were carried out at methanation conditions, it is a valuable tool to understand how SMOI effects modify catalyst surface and provide a theory to explain the reason for SMOI effects. An example of a normalized transient of $^{12}CH_4$ comparing to Ar obtained by switching from ^{12}CO to

^{13}CO is given in Figure 5.2. The difference in area under normalized transit curves of a particular species and the inert tracer (Ar) gives the average surface residence time (τ_i). Turnover frequency (TOF) can be related to average surface residence time by TOF = $1/\tau_i$. The concentration of active surface intermediates (N_i) can be calculated by $N_i = Rate_i * \tau_i$ [56].

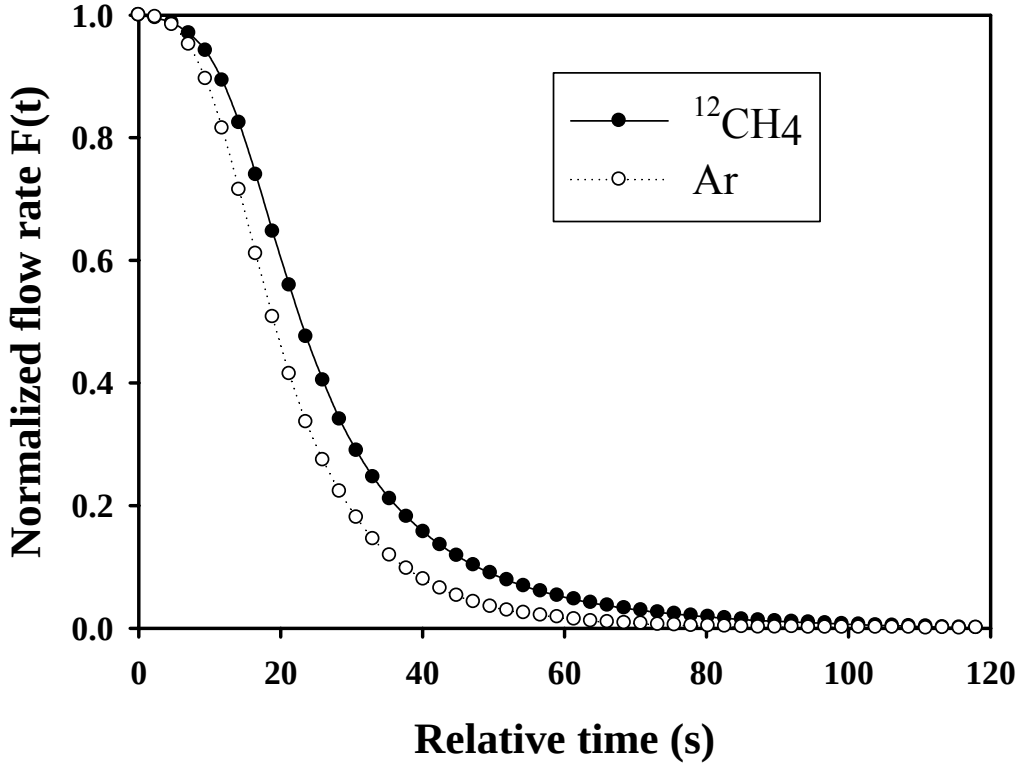

Figure 5.2 Typical normalized transit response of $^{12}CH_4$ and Ar for $Rh/V/SiO_2$.

Table 5.3 shows that same as reaction study, even in methanation reaction condition, the activity decreased when reduction temperature increased. The higher

reduction temperature also leaded to shorter residence time and higher turnover frequency. It is obvious that the linear decrease in activity was accompanied by a similar decrease in the surface concentration of active intermediates leads to methane (N_{CH4} in Table 5.3). The surface concentration of reversibly adsorbed CO (N_{CO}) (i.e., CO that adsorbed and desorbed on surface) in Table 5.3 also decreased with reduction temperature, which suggests that the significantly declines in activity was not due to carbon deposition on the active sites. Consistent with chemisorption results, it proves that SMOI effects can reduce the concentration of active sites by modifying catalyst surface. In our previous IR paper [17], it was reported that different from other promoters, the addition of V suppressed CO adsorption, but significantly enhanced the mobility and/or reactivity of these adsorbed CO species judging from the CO(*l*) depleting rate in a He or H_2/He flow on the V singly-promoted catalyst. This is probably due to the SMOI effects on the catalyst surface. The SSITKA results in Table 5.2 also suggest that, with the increasing of SMOI effects at higher reduction temperature, both residence time and concentration of intermediates decrease. The increase in turn over frequencies with increasing reduction temperature indicates that properties of active sites changed, instead of just simple particle size growing due to sintering, which explained that the real reason for our chemisorption results. Instead, there may be new sites created at the interfacial region of Rh and VO_x by SMOI effects, and the activity of these sites for CO hydrogenation would be relatively high.

5.4 Conclusions

This study explored SMOI effects induced by high temperature reduction for $Rh/V/SiO_2$. Compared to Rh/SiO_2, the SMOI effects showed significant influence to CO hydrogenation reaction on $Rh/V/SiO_2$. By SSITKA, the surface kinetic parameters were determined to understand the surface modification of catalyst surface by SMOI effects.

It was suggested that the activity of Rh/SiO_2 did not change when reduction temperature increased from 300 to 600 °C, indicating there is no sintering effect. H_2 chemisorption indicated that H_2 adsorption at room temperature decreased with increasing reduction temperature for $Rh/V/SiO_2$, suggesting that the concentration of active sites on the catalyst surface was reduced. In reaction study, most of the product distribution on Rh/SiO_2 was held constant with rising reduction temperature except the hydrocarbon chain growth was somewhat improved. For $Rh/V/SiO_2$, the activity decreased when reduction temperature increased because of SMOI effects. Also, more CH_x or CH_xO (x = 1, 2 or 3) species on the surface were oxygenated to methanol instead of going through hydrogenation process to produce methane. However, C_{2+} oxygenate and C_{2+} hydrocarbon selectivities were not influenced by SMOI effects. As indicated by SSITKA, the residence time were decreased by SMOI effects which were induced by high reduction temperature. By determining the concentration of surface intermediates for $Rh/V/SiO_2$ with different reduction temperature pretreatment with SSITKA, it was found out that SMOI effects decreased the concentration of active intermediates, which correlate directly with activity.

5.5 Acknowledgments

We acknowledge financial support from the U. S. Department of Energy (Award No 68 DE-PS26-06NT42801).

5.6 References

[1] M. Ichikawa, J. Chem. Soc., Chem. Commun. 13 (1978) 566.

[2] M. Ichikawa, Bull. Chem. Soc. Jpn. 51 (1978) 2273.

[3] J.J. Spivey, A.A. Egbebi, Chem. Soc. Rev. 36 (2007) 1514.

[4] R.P. Underwood, A.T. Bell, Appl. Catal. 21 (1986) 157.

[5] R.P. Underwood, A.T. Bell, Appl. Catal. 34 (1987) 289.

[6] G. Van der Lee, B. Schuller, H. Post, T.L.F. Favre, V. Ponec, J. Catal. 98 (1986) 522.

[7] W.M. Chen, Y.J. Ding, D.H. Jiang, Z.D. Pan, H.Y. Luo, Catal. Lett. 104 (2005) 177.

[8] T. Ioannides, X. Verykios, J. Catal. 140 (1993) 353.

[9] J. Kowalski, G.V.D. Lee, V. Ponec, Appl. Catal. 19 (1985) 423.

[10] S.-I. Ito, C. Chibana, K. Nagashima, S. Kameoka, K. Tomishige, K. Kunimori, Appl. Catal., A 236 (2002) 113.

[11] S.-I. Ito, S. Ishiguro, K. Kunimori, Catal. Today 44 (1998) 145.

[12] S.-I. Ito, S. Ishiguro, K. Nagashima, K. Kunimori, Catal. Lett. 55 (1998) 197.

[13] T. Beutel, O.S. Alekseev, Y.A. Ryndin, V.A. Likholobov, H. Knoezinger, J. Catal. 169 (1997) 132.

[14] T. Beutel, V. Siborov, B. Tesche, H. Knoezinger, J. Catal. 167 (1997) 379

[15] B.J. Kip, P.A.T. Smeets, J. Van Grondelle, R. Prins, Appl. Catal. 33 (1987) 181.

[16] J. Gao, X. Mo, A.C. Chien, W. Torres, J.G. Goodwin, Jr., J. Catal. 262 (2009) 119.

[17] X. Mo, J. Gao, J.G. Goodwin, Jr., Catal. Today 147 (2009) 139.

[18] X. Mo, J. Gao, N. Umnajkaseam, J.G. Goodwin, Jr., J. Catal. 267 (2009) 167.

[19] H.Y. Luo, H.W. Zhou, L.W. Lin, D.B. Liang, C. Li, D. Fu, Q. Xin, J. Catal. 145 (1994) 232.

[20] T. Koerts, R.A. Vansanten, J. Catal. 134 (1992) 13.

[21] S.J. Tauster, S.C. Fung, J. Catal. 55 (1978) 29.

[22] P. Gallezot, A. Alarcondiaz, J.A. Dalmon, A.J. Renouprez, B. Imelik, J. Catal. 39 (1975) 334.

[23] S.J. Tauster, S.C. Fung, R.L. Garten, J. Am. Chem. Soc. 100 (1978) 170.

[24] J.A. Horsley, J. Am. Chem. Soc. 101 (1979) 2870.

[25] S. Penner, B. Jenewein, D. Wang, R. Schlogl, K. Hayek, Appl. Catal., A 308 (2006) 31.

[26] B. Jenewein, S. Penner, K. Hayek, Appl. Catal., A 308 (2006) 43.

[27] S. Penner, B. Jenewein, D. Wang, R. Schlogl, K. Hayek, Phys. Chem. Chem. Phys. 8 (2006) 1223.

[28] D.C. Koningsberger, J.H.A. Martens, R. Prins, D.R. Short, D.E. Sayers, J. Phys. Chem. 90 (1986) 3047.

[29] P. Meriaudeau, O.H. Ellestad, M. Dufaux, C. Naccache, J. Catal. 75 (1982) 243.

[30] H.R. Sadeghi, V.E. Henrich, J. Catal. 87 (1984) 279.

[31] U. Diebold, Surf. Sci. Rep. 48 (2003) 53.

[32] A.D.C. Faro, C. Kemball, J. Chem. Soc., Faraday Trans. 91 (1995) 741.

[33] C. Linsmeier, H. Knozinger, E. Taglauer, Nucl. Instrum. Meth. B 118 (1996) 533.

[34] M. Zimowska, J.B. Wagner, J. Dziedzic, J. Camra, B. Borzeccka-Prokop, M. Najbar, Chem. Phys. Lett. 417 (2006) 137.

[35] H. Orita, S. Naito, K. Tamaru, J. Chem. Soc. Chem. Commun. (1983) 993.

[36] K. Kunimori, H. Abe, T. Uchijima, Chem. Lett. (1983) 1619.

[37] T. Uchijima, Catal. Today 28 (1996) 105.

[38] J.P. Belzunegui, J. Sanz, J.M. Guil, J. Phys. Chem. B 109 (2005) 19390.

[39] R. Brown, C. Kemball, J. Chem. Soc., Faraday Trans. 92 (1996) 281.

[40] L. Brewer, Science 161 (1968) 115.

[41] B. Viswanathan, K. Tanaka, I. Toyoshima, Langmuir 2 (1986) 113.

[42] D.E. Resasco, G.L. Haller, J. Catal. 82 (1983) 279.

[43] B.H. Chen, J.M. White, J. Phys. Chem. 87 (1983) 1327.

[44] J. Santos, J. Phillips, J.A. Dumesic, J. Catal. 81 (1983) 147.

[45] A.B. Boffa, A.T. Bell, G.A. Somorjai, J. Catal. 139 (1993) 602.

[46] A. Boffa, C. Lin, A.T. Bell, G.A. Somorjai, J. Catal 149 (1994) 149.

[47] A.B. Boffa, A.T. Bell, G.A. Somorjai, J Catal 139 (1993) 602.

[48] J.A. Cairns, J.E.E. Baglin, G.J. Clark, J.F. Ziegler, J. Catal. 83 (1983) 301.

[49] Z. Hu, T. Wakasugi, A. Maeda, K. Kunimori, T. Uchijima, J. Catal. 127 (1991) 276.

[50] Y.G. Yin, T. Wakasugi, H. Shindo, S. Ito, K. Kunimori, T. Uchijima, Catal. Lett. 9 (1991) 43.

[51] Z. Hu, H. Nakamura, K. Kunimori, Y. Yokoyama, H. Asano, M. Soma, T. Uchijima, J. Catal. 119 (1989) 33.

[52] G. Vanderlee, A.G.T.M. Bastein, J. Vandenboogert, B. Schuller, H.Y. Luo, V. Ponec, J. Chem. Soc., Faraday Trans. 83 (1987) 2103.

[53] A.G.T.M. Bastein, W.J. Vanderboogert, G. Vanderlee, H. Luo, B. Schuller, V. Ponec, Appl. Catal. 29 (1987) 243.

[54] B.J. Kip, P.A.T. Smeets, J.H.M.C. Van Wolput, H.W. Zandbergen, J. Van Grondelle, R. Prins, Appl. Catal. 33 (1987) 157.

[55] M. Sigl, M.C.J. Bradford, H. Knozinger, M.A. Vannice, Top. Catal. 8 (1999) 211.

[56] S.L. Shannon, J.G. Goodwin, Chem. Rev. 95 (1995) 677.

[57] R. Burch, M.I. Petch, Appl. Catal., A 88 (1992) 39.

[58] N. Lohitharn, J. Goodwin, G., Jr., J. Catal. 257 (2008) 142

[59] N.P. Socolova, Colloid Surf. A 239 (2004) 125.

[60] H. Hayashi, M. Kishida, K. Wakabayashi, Catal. Surv. Jpn. 6 (2002) 9.

[61] J. Gao, X. Mo, J.G. Goodwin, Jr., J. Catal. 268 (2009) 142.

[62] G. Rupprechter, K. Hayek, H. Hofmeister, J. Catal. 173 (1998) 409.

CHAPTER SIX

RELATIONSHIPS BETWEEN OXYGENATE AND HYDROCARBON FORMATION DURING CO HYDROGENATION ON Rh/SiO_2: USE OF MULTIPRODUCT SSITKA

6.1 Introduction

Ethanol (EtOH) synthesized from syngas derived from natural gas [1], coal [2] or biomass [3] can be used as an additive to gasoline or as an easily transportable and storable source of hydrogen. Compared to gasoline alone, the use of ethanol with gasoline offers several advantages such less pollution and more efficient combustion due to its chemical properties. The incentive for incorporating ethanol in liquid fuels also lies in the general acceptance of new gasoline regulations with more restrictions. Accordingly, much recent research and development in syngas conversion has dealt with ethanol synthesis.

Rh-based catalysts have been found to be the most efficient catalysts for the synthesis of C_{2+} oxygenates due to the unique carbon monoxide adsorption behavior on Rh [4-7]. Understanding the mechanism of CO hydrogenation is essential for better catalyst design that could lead to commercialization of a selective ethanol synthesis process. Even though Fischer-Tropsch synthesis (FTS) has been widely studied since 1923 [8], there is still controversy in the literature about the mechanism for CO hydrogenation due to its complexity. For instance, one controversy is whether C-O bond

cleavage occurs during CO hydrogenation via direct dissociation (carbide mechanism) [9-15] or via a hydrogen-assisted process [16-32]. Recently, Choi and Liu [32] focused on EtOH synthesis from CO and H_2 on Rh (111) using density functional theory (DFT) and found that the optimal reaction pathway for the formation of methanol (MeOH) goes through H insertion into adsorbed –CO species, while the formation of CH_4 favors H assisted CO dissociation through the bond rupture of -CH_3O species into –CH_3 and –O. However, to the contrary, in another recent work, Mei et al. [33] still preferred the carbide model to explain using a DFT approach the mechanism for CO hydrogenation on a quasi-(111) surface facet on a 1 nm in diameter Rh_{50} cluster.

Steady-state isotopic transient kinetic analysis (SSITKA) is a powerful tool to evaluate concentration of intermediates, site activity, site heterogeneity and surface reaction mechanism [34]. This technique was developed first by Biloen [35], Bennett [36], and Happel [37] in late 1970s and early 1980s. SSITKA involves a switch from an unlabeled reactant to an isotopically labeled one at steady state of the reaction, the detection of the resulting isotopic transients in the products by mass spectroscopy (MS), and an analysis of these transients to determine surface reaction kinetic parameters. Because of its wide applicability and relatively low cost, SSITKA has now been used by a significant number of researchers. For CO hydrogenation, SSITKA has been employed to better probe the surface reaction parameters on various catalysts including are based on Fe [38-42], Pd [43-46], Co [40, 41, 47-49], Ni [50, 51], Ru [52-54] and Rh [55-63]. However, for Rh-based catalysts, there are few detailed studies reported on different product formation at the site level.

The objective of this study was to better understand the mechanism of formation of different products on Rh/SiO_2 at the site level by the application of SSITKA. For this study, 1.5 wt% Rh/SiO_2 was prepared and used as the catalyst for two reasons:

(i) Low amounts of Rh (i.e., 1.5 wt%) supported on SiO_2 produce highly dispersed Rh that is representative of the Rh clusters used in theoretical modeling work;

(ii) Rh-based catalysts supported on SiO_2 have shown reasonable selectivities for both hydrocarbons and oxygenates during CO hydrogenation [64-66].

6.2 Experimental

6.2.1 Catalyst preparation

Since the Rh/SiO_2 catalyst used in this study was the same as that used in a previous study, a detailed description of catalyst preparation can be found in an earlier paper [67]. Silica gel (99.95%, Alfa Aesar) was first grounded and sieved to 30-50 mesh, washed with boiled distilled water for 3 times, and subsequently calcined in air at 500 ^{o}C for 4 h before being used as the support. $Rh(NO_3)_3$ hydrate (Rh ~36 wt%, Fluka) was used as purchased. An aqueous solution of $Rh(NO_3)_3$ hydrate was added dropwise to the silica gel until incipient wetness. The catalyst precursor was dried at 90^{o}C for 4 h and then at 120^{o}C overnight before being calcined in air at 500^{o}C for 4 h to remove

nitrogenous residues from the precursors. Rh content was kept at 1.5 wt% based on the support weight.

6.2.2 CO hydrogenation

The reaction system setup is shown in Figure 6.1. CO hydrogenation was carried out in a fixed-bed differential reactor (316 stainless steel) with length ~300 mm and internal diameter ~5 mm. Catalyst and inert (α-Al_2O_3) were mixed and loaded between quartz wool plugs placed in the middle of the reactor with a thermocouple close to the catalyst bed.

Molecular sieve traps (Alltech) were used to remove H_2O, and a CO purifier (Swagelok) was applied to the flow from the CO cylinder to remove CO_2 and any carbonyls. A Varian 3380 GC equipped with an FID (flame ionization detector) and a TCD (thermal conductivity detector) was used to analyze the reaction rate and product distribution. A Restek RT-QPLOT column (30m, 0.53mm ID) connecting with the FID was capable of separating C_1-C_7 hydrocarbons and oxygenates, while another Restek packed column (80/100, 6ft) connecting with the TCD was used to separate CO and other inorganic gases.

Prior to reaction, the catalyst was reduced at 500°C (ramped to temperature at 5°C/min) under 30 mL/min hydrogen for 1 h. After reduction, the reaction was carried out at 250°C and a pressure of 1.8 atm. The total flow rate of the reaction mixture was

kept constant at 30 mL/min with 9 mL/min of 95% CO + 5% Ar, 18 mL/min of H_2 and 3 mL/min of He to obtain a H_2:CO ratio of 2:1, which is favorable for EtOH production [68]. The reaction conversion was always kept at less than 5% to avoid mass or heat transfer effects. Even though the selectivities for oxygenates, especially for EtOH may not be as great as those at more optimum conditions (e.g., lower reaction temperature), these reaction conditions were chosen to maximize yields of C_1-C_2 products, especially the C_2 oxygenates, so that they could be detected by MS. The apparent activation energy (25-28 kcal/mol) and the good linearity of Arrhenius Plots indicated that there were no mass or heat transfer limitations under the reaction conditions used.

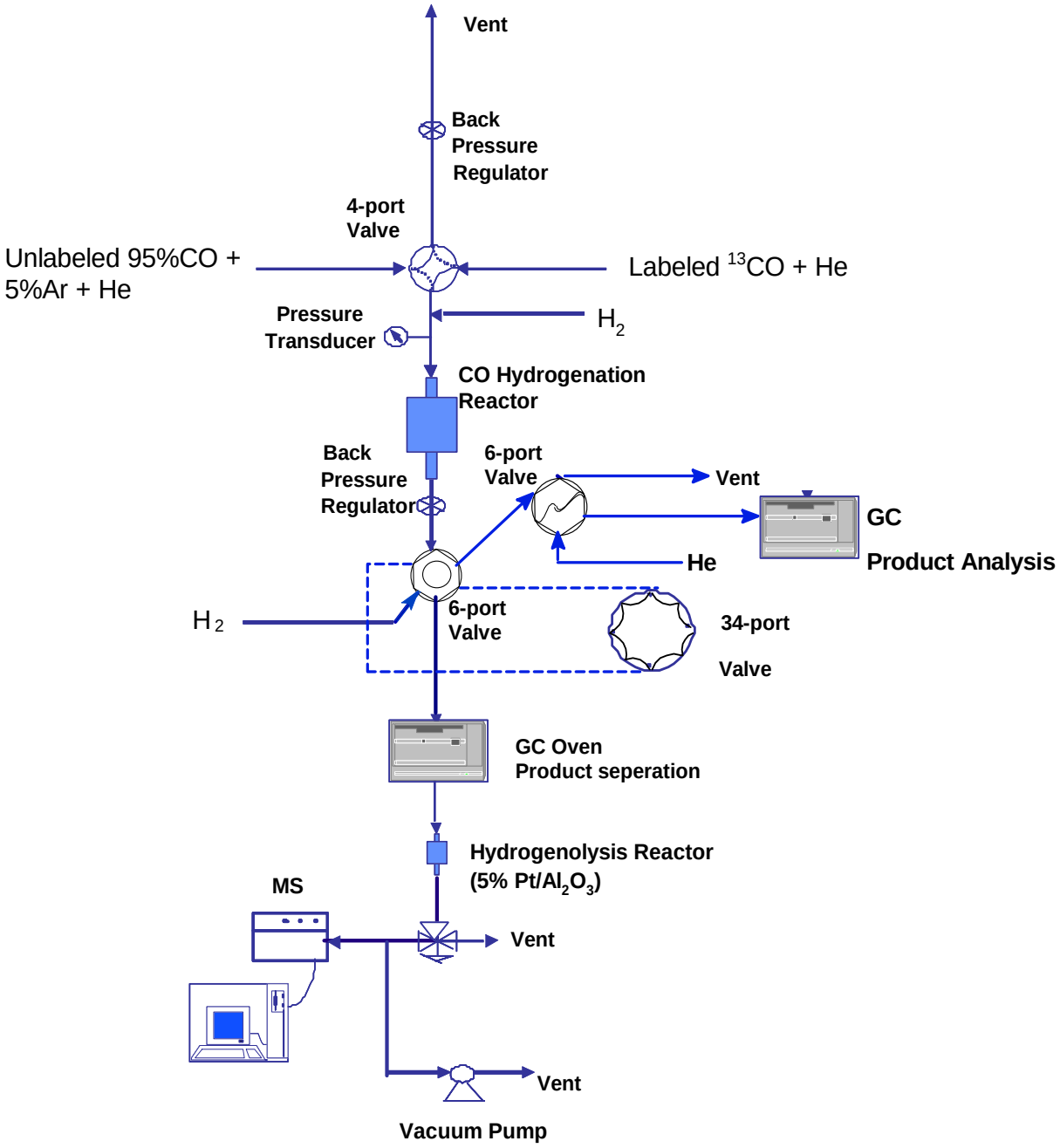

Figure 6.1 The system setup for multiproduct SSITKA.

6.2.3 SSITKA

An isotopic switch was carried out after reaction steady-state was reached (after 15 hours). A switch between 95% ^{12}CO + 5% Ar and ^{13}CO was made using a Valco 2-position valve with an electric actuator without disturbing any other reaction conditions. The 5% Ar in the ^{12}CO flow was used as an inert tracer to determine the gas phase holdup time. Two back pressure regulators in the system were used to minimize pressure disturbance while switching. A Valco 34-port valve was employed to collect 16 samples during the 10 minute period of the isotopic transients after switching. The collected effluent samples were injected separately into another Restek RT-QPLOT column in the GC with 30 mL/min H_2 as the carrier gas. The products were separated by the column and then fed into a hydrogenolysis/hydrogenation reactor (containing 5 g of 5% Pt/Al_2O_3) with the source of H_2 being the carrier gas. This reactor was maintained at 400°C in order to convert hydrocarbons and oxygenates totally to methane. The resulting product CH_4 was subsequently fed into an MS (Pfeiffer Vacuum) for analysis. The MS was equipped with a high speed data-acquisition system interfaced to a computer using Balzers Quadstar 422 v 6.0 software. The isotopic concentration measured by the MS was able to be used with the time for the collection of each sample in the 34-port valve and the identity of the compound separated by the GC sent to the hydrogenolysis reactor to construct the isotopic transients for the various products. An example of the normalized transients for ^{12}C in CH_4, C_2H_n, MeOH, AcH and EtOH obtained by

switching from ^{12}CO to ^{13}CO is given in Figure 6.2. It would be meaningful to study C_2H_4 and C_2H_6 separately, but in our SSITKA study, C_2H_6 was the predominant C_2 hydrocarbon formed (> 90% based on GC analysis). Thus, the amount of C_2H_4 was too small for isotopic tracing analysis.

Surface kinetic parameters, including the average surface residence times and surface concentrations of intermediates for CH_4, C_2H_n, MeOH, AcH and EtOH were determined from the isotopic transient curves using SSITKA data analysis software. The difference in area under the normalized transient curves of a particular species (i) and the inert tracer (Ar) gives the average surface reaction residence time (τ_i). The concentration of active surface intermediates for a particular product can be calculated by $N_i = Rate_i * \tau_i$ [34, 69].

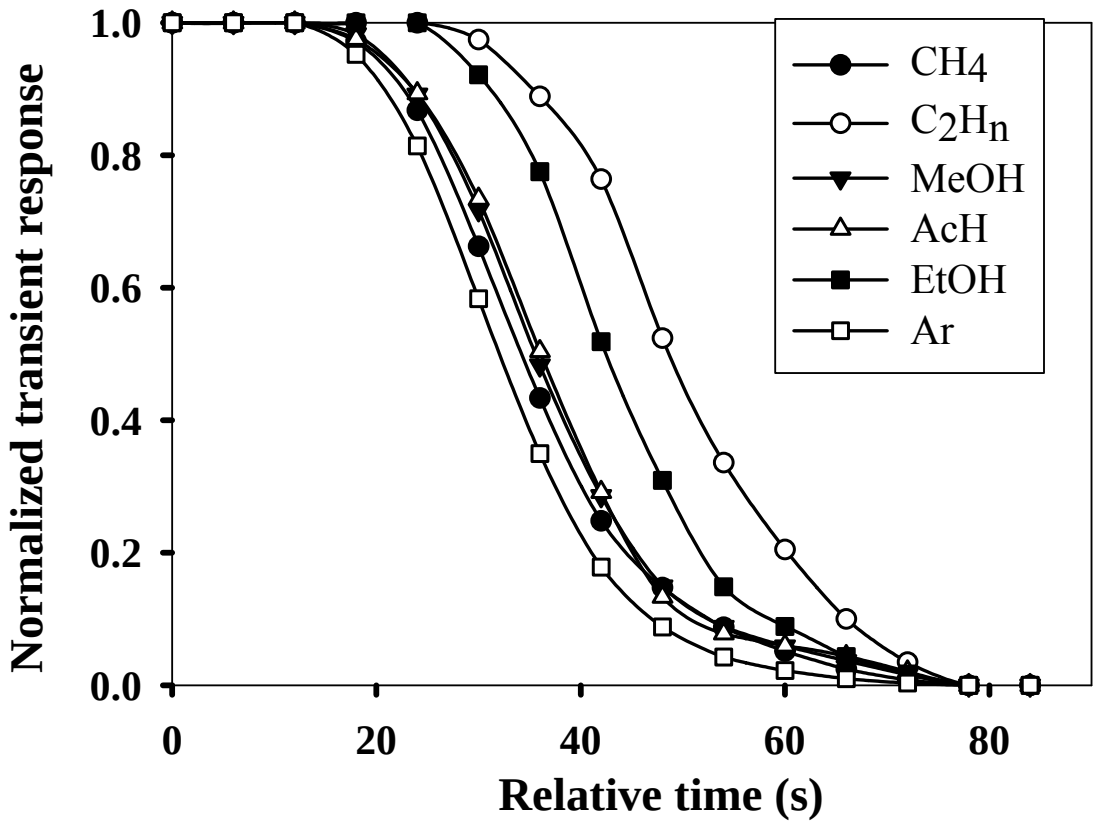

Figure 6.2 Typical normalized transient responses for ^{12}C in CH_4, C_2H_n, MeOH, AcH, EtOH, and for Ar during reaction on Rh/SiO_2.

6.3 Results

Table 6.1 shows the surface kinetic parameters for different products on varying amounts of the Rh/SiO_2 catalyst. The % CO conversions were all under differential

conditions (< 5%) and the selectivities for different products were constant regardless of the amount of catalyst being used. However, the average surface reaction residence times of MeOH and AcH (acetaldehyde) changed with the amount of the catalyst being used, while the residence times for all the other products were not affected. This was due to the ease of readsorption of these products and the resulting chromatographic effect [45]. To clarify, Figure 6.3 shows how the average surface reaction residence times for MeOH and AcH change with the amount of Rh/SiO_2 catalyst used in our study. When the catalyst amount changed from 0.2 to 1.0 g, the average surface reaction residence times for MeOH and AcH formation increased linearly, from 2.7 to 4.2 s and from 2.6 to 4.0 s, respectively. Thus, contrary for other products, readsorption of MeOH and AcH on Rh/SiO_2 could not be ignored and had to be addressed before the surface reaction residence times could be evaluated. This was accomplished by extrapolating the residence times determined for different amounts of catalyst to 0 g of catalyst, i.e., an infinitely thin bed [46]. By extrapolating the trend line to 0 g catalyst, the surface residence times for MeOH and AcH formation on the surface were determined to both be approximately 2.3 s.

Table 6.1: The surface reaction kinetic parameters for CO hydrogenation on the nonpromoted Rh/SiO_2 catalyst. [a]

0.2 g Rh/SiO_2 [i]					
Product [h]	Rate [b] (μmol of C/g/s)	%HC Selectivity [c]	τ_i [d] (s)	$TOF_{ITK,\,i}$ [e] (s^{-1})	N_i [f] (μmol of C/g)
CH_4	0.076	64.0	2.7	0.37	0.20
C_2H_n [g]	0.011	9.7	14.9	0.07	0.17
MeOH	0.001	0.5	2.7	0.37	0.00
AcH	0.005	4.2	2.6	0.38	0.01
EtOH	0.006	5.1	10.3	0.10	0.06
0.6 g Rh/SiO_2 [j]					
Product [h]	Rate [b] (μmol of C/g/s)	%HC Selectivity [c]	τ_i [d] (s)	$TOF_{ITK,\,i}$ [e] (s^{-1})	N_i [f] (μmol of C/g)
CH_4	0.069	64.0	2.8	0.35	0.20
C_2H_n [g]	0.011	9.8	14.8	0.07	0.16
MeOH	0.001	0.5	3.6	0.28	0.00
AcH	0.005	4.7	3.6	0.28	0.02
EtOH	0.005	5.0	10.3	0.10	0.06
1.0 g Rh/SiO_2 [k]					
Product [h]	Rate [b] (μmol of C/g/s)	%HC Selectivity [c]	τ_i [d] (s)	$TOF_{ITK,\,i}$ [e] (s^{-1})	N_i [f] (μmol of C/g)
CH_4	0.073	70.0	3.1	0.32	0.22
C_2H_n [g]	0.009	8.9	13.6	0.07	0.13
MeOH	0.001	0.6	4.2	0.24	0.00
AcH	0.003	3.2	4.0	0.25	0.01
EtOH	0.005	4.5	10.6	0.09	0.05

[a] Reaction was carried out at 250 °C; P = 1.8 atm, flow rate = 30 mL/min (H_2:He:CO = 6:1:3). The measurements reported were done after 15 h of reaction when steady state was reached.
[b] Steady-state rate.
[c] Molar selectivity = $n_iC_i / \sum n_iC_i$.
[d] Surface residence time of intermediates.
[e] $TOF_{ITK,\,i} = 1/\tau_i$.
[f] $N_i = Rate_i * \tau_i$.
[g] Hydrocarbons with 2 carbons.
[h] Experimental errors of all the results for CH_4 and C_2H_n are ±5%; experimental errors of all the results for MeOH and AcH are ±12%; Experimental errors of all the results for EtOH are ±8%.
[i] 0.2 g catalyst was used with 2.8 g α-Al_2O_3 dilution.
[j] 0.6 g catalyst was used with 2.4 g α-Al_2O_3 dilution.
[k] 1.0 g catalyst was used with 2 g α-Al_2O_3 dilution.

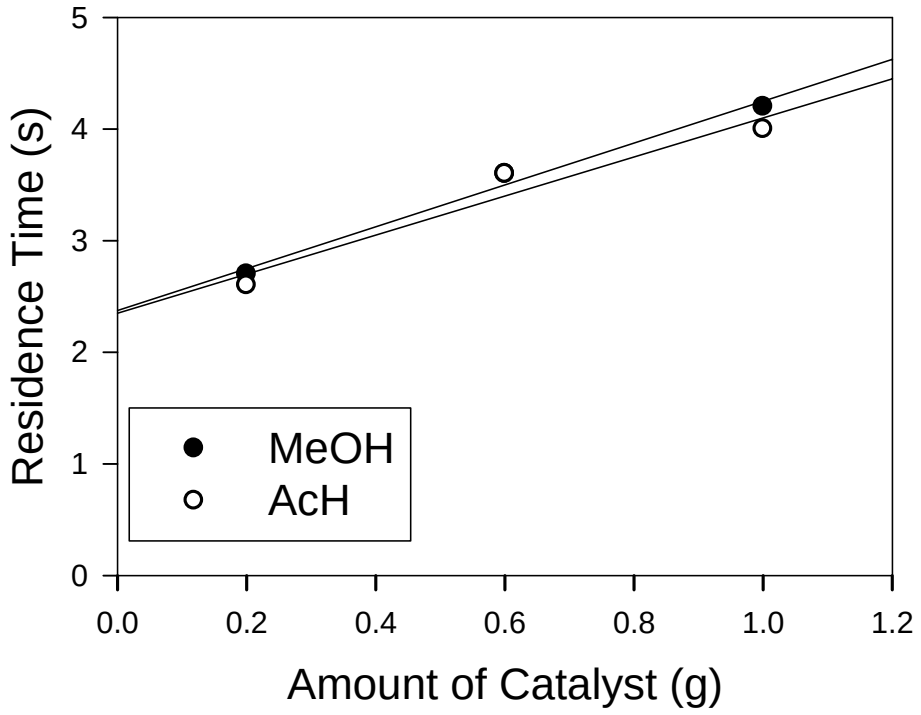

Figure 6.3 The change of surface residence times for MeOH and AcH formation with different amounts of Rh/SiO_2 catalyst.

With respect to the surface reaction residence time for each individual product, the residence time for C_2H_n was the longest among all the C_1-C_2 hydrocarbon and oxygenate products. The surface reaction residence time for MeOH was somewhat shorter than that for CH_4 but the selectivity to CH_4 was more than 100 times than that for MeOH. The concentration of intermediates for EtOH was larger than that for AcH, but the turnover frequency (TOF_{ITK}) of sites based on SSITKA ($TOF_{ITK,i} = 1/ \tau_i$) for AcH formation was higher than that for EtOH formation. It is interesting to note that the

residence time for MeOH was about the same as AcH while the selectivity for AcH was around an order of magnitude greater than that for MeOH.

6.4 Discussion

6.4.1 Relationship between selectivity and surface reaction residence time

One advantage of SSITKA is that it can provide the surface reaction residence time and the concentration of active intermediates on the surface without having to know the details of the reaction mechanism. However, with these parameters, a proposed mechanism should be able to be after disproved or substantiated. Before analysis and discussion of the detailed mechanism of CO hydrogenation on Rh/SiO_2 based on the SSITKA, it is useful to present some basic definitions and parameter relationships.

In terms of measured rate of reaction,

$$R_i = \frac{1}{\tau_i} N_i$$

where R_i represents the reaction rate to produce the specific product *i* and N_i represents the amount of active intermediates (in terms of carbon atoms) on the surface that leads to product *i* [69]. In the case of SSITKA of CO hydrogenation, these parameters can be determined for any reactant or product molecules containing carbon (since carbon is isotopically traced). N_i is closely related to the number of active sites on the catalyst

surface at any time used for product *i* formation [69]. Residence time of a product, τ_i (the average surface reaction residence time to form *i*), is equal to the sum of all the reaction residence times for the intermediates leading to that particular product *i*.

If two products share any intermediates (and hence also the same type of sites), the ratio between their selectivities (S_i) should be related to the inverse of the τ_i's. For example, if

$$\tau_1 > \tau_2,$$

then it must be that

$$N_1 < N_2$$

due to the probability that more active intermediates will form product 2 due to its faster formation rate (smaller τ_i) than will form product 1. Thus, since both $N_1 < N_2$ and $(1/\tau_1) < (1/\tau_2)$,

$$(1/\tau_1) \times N_1 < (1/\tau_2) \times N_2.$$

And, by definition,

$$R_1 < R_2.$$

Thus,

$$S_1 < S_2.$$

So, in summary, if two products share any carbon-containing intermediates, if $\tau_1 > \tau_2$, then $S_1 < S_2$. If not, they do not share any intermediates in their many formation routes, unless somehow secondary reaction could decrease the amount of product 2 detected.

6.4.2 Relationship between CH_4 and MeOH formation.

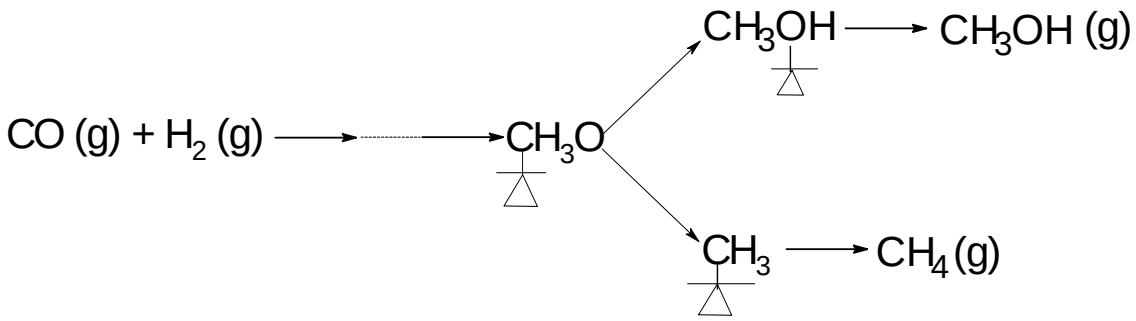

Figure 6.4 Recently proposed pathways of MeOH and CH_4 formation during CO hydrogenation (based on reference [18, 32]).

Comparing our results with the mechanism shown in Figure 6.4, which is essentially that used by Choi and Liu [32] and Holmen's group [18], the following points can be made:

a) According to this mechanism, if the surface reaction residence time for CH_4 is larger than that for MeOH, the selectivity to MeOH should be larger than CH_4 since they are formed on the same type of site and share at least some intermediates in their

formation. However, in our results for Rh/SiO_2, the selectivity to CH_4 was nearly 120 times larger than that for MeOH, but the surface reaction residence time for CH_4 was slightly longer than that for MeOH (2.7 vs. 2.3 s).

b) The $–CH_3OH$ or/and $–CH_3$ species on the surface may also take part in other product formations. For instance, if there is a large amount of $–CH_3$ species that also take part in C_{2+} hydrocarbon or oxygenate formation, then the selectivity to CH_4 should be even lower than expected. However, this is not the case since S_{CH4} is more than 100 times larger than S_{MeOH}. It was proposed by Takeuchi at al. [69] that EtOH could be formed from MeOH homologation in CO hydrogenation, which could explain low MeOH selectivity and the high selectivity ratio. But there was no dimethyl ether detected in the system to prove the further reaction of MeOH (MeOH homologation or condensation/coupling) on the surface.

c) If the formation routes of MeOH and CH_4 share at least one common intermediate on the same kind of active sites, it is impossible to explain based on SSITKA data the big difference between selectivities to MeOH and to CH_4 with no such difference between their formation residence times.

Thus, even though the reaction mechanism on Rh(111) and other metals has been proposed based on theoretical calculation, the modeling work assumed that the same reaction sites were used to produce CH_4 and MeOH. If there were only one kind of reaction sites on Rh/SiO_2, all carbon-containing products would share at least one common intermediate, adsorbed CO. This appears not to be true for CH_4 and MeOH formation on Rh/SiO_2. Thus, it is probable that there is more than one kind of sites on the

catalyst surface. The SSITKA results suggest that most of the active sites for MeOH and CH_4 formation are different and indicate that there are many more sites producing CH_4 than sites producing MeOH. As shown in Table 6.1, the number of intermediates (N_i) on the Rh/SiO_2 catalyst used for CH_4 formation was around 20 mol/g cat while for MeOH it was less than 0.01 mol/g cat. Thus, the selectivity to CH_4 was much larger than that for MeOH even through the intrinsic rates of formation (inverse residence times) were similar.

In short, the assumption of a single type of site would appear to be the most fundamental cause for the failure of the mechanism shown in Figure 6.4 to apply to CO hydrogenation on supported Rh or possibly Rh clusters with different crystalline faces, as gleamed from for the formation of CH_4 and MeOH. Different from perhaps Rh(111), it is reasonable that there would be more than one kind of Rh sites on the Rh/SiO_2 catalyst surface. As a matter of fact, while Yates et al. [71] detected only one single hydrogen desorption peak for Rh(111) with TPD, in our previous study [72] two hydrogen desorption peaks were detected for Rh/SiO_2, which is similar to the results of Bertucco and Bennett [73] results for a 10% Rh/SiO_2 catalyst. It is well known that besides increasing the dispersion of Rh, a support may interact with Rh due to SMOI, affecting the morphology of the Rh clusters, the oxidation state and stability of reaction intermediates [64, 73-78]. Thus, it may be reasonable that Rh/SiO_2 would show different behavior from Rh(111) in CO hydrogenation. However, Choi and Liu [32] had no experimental selectivity data for comparison when they did their modeling work on Rh(111).

We, thus, cannot rule out that CH_4 and MeOH may be able to be made on the same sites on Rh(111). Our conclusions are based and applied only to the system we studied, Rh/SiO_2. However, our results do serve as a caution to using the assumption that CH_4 and MeOH share intermediates, no matter how attractive such a possibility is, for heterogeneous catalyst surfaces.

6.4.3 Relationship between the formation of C_2 products and C_1 products

Due to the complexity in the chain growth step, there are few detailed studies in the literature regarding the mechanism of C_2 product synthesis, especially for C_2 oxygenates.

Table 6.1 shows that the selectivity to MeOH was significantly lower than that for any of the C_2 products (AcH, EtOH or C_2H_n) and that the surface reaction residence time for MeOH formation was much shorter. If MeOH and any C_2 products (hydrocarbons and oxygenates) shared an intermediate ($–CH_xO$), C_2 product selectivity should have been lower than that for MeOH since all of the C_2 products had longer surface reaction residence times than MeOH. Thus, it is unlikely for any of the C_2 products to have shared an intermediate with MeOH on Rh/SiO_2.

On the other hand, the selectivity to CH_4 was higher than that for any of the C_2 products and the surface reaction residence time for CH_4 was shorter. Thus, the

possibility that all C_2 products share intermediates on the same active sites with CH_4 is possible and cannot be excluded.

6.4.4 Relationship of AcH and C_2H_n formation

It is interesting to note that, the surface reaction residence time for C_2H_n synthesis was longer than that for any other C_1-C_2 product while the selectivity for C_2H_n was not the lowest, which suggests that the mechanism for C_2H_n synthesis is perhaps more complex than the mechanisms for the other products discussed earlier. Figure 6.5 shows two popular mechanisms recently proposed for C_2H_n formation. One is related to AcH formation as an integral part to forming C_2 hydrocarbons [18], as shown in possibility 6.5(a); the other one has AcH and C_2H_n sharing a common $–CH_x$ intermediate, with different chain growth steps to produce AcH or C_2H_n, as shown in possibility 6.5(b) [33].

Following the same logical reasoning applied earlier, possibility 6.5(a) is not valid for Rh/SiO_2 because τ_{C2Hn} was significant longer than τ_{AcH} (14.4 vs. 4.1 s) but S_{C2Hn} was larger than S_{AcH} (9.5 vs. 4.1%). Possibility 6.5(b) is more likely to be true on Rh/SiO_2. The fact that S_{AcH} was lower than expected could be explained by the further reaction of the intermediates to form other products (e.g., $–C_2H_xO$ may be an intermediates for both AcH, EtOH and C_3H_xO formation). However, there have been few studies on the mechanism of C_{2+} hydrocarbon and oxygenate synthesis on Rh-based catalysts so far, and the SSITKA results are not sufficient yet to elucidate the mechanism further.

(a)

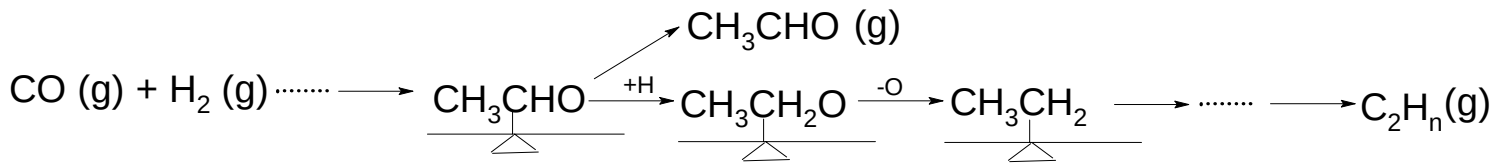

(b)

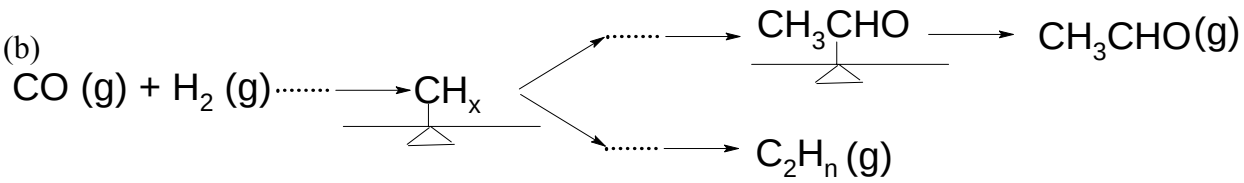

Figure 6.5 Recently proposed pathways of AcH and C_2 hydrocarbon formation during CO hydrogenation: (a) from reference [18], (b) from reference [33].

(a)

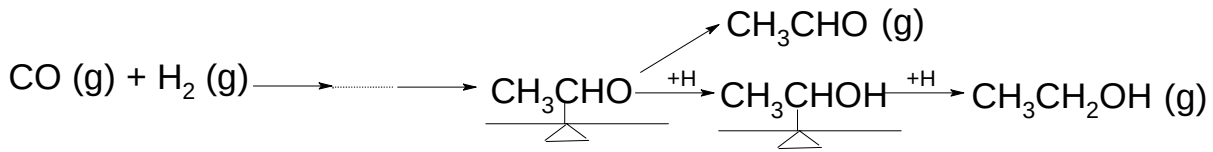

(b)

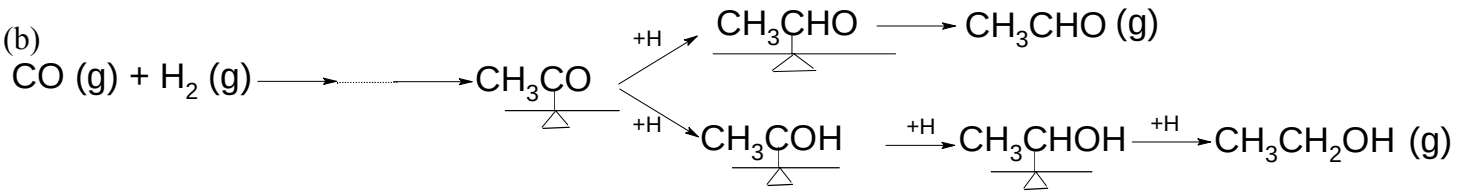

(c)

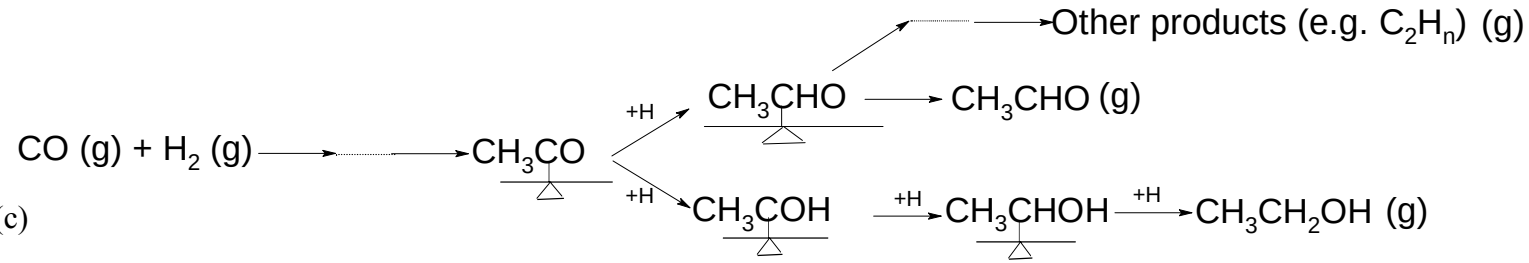

Figure 6.6 Recently proposed pathways of AcH and EtOH formation during CO hydrogenation: (a) from reference [33], (b) from reference [32],(c) from reference [18].

6.4.5 Relationship of EtOH and AcH formation

There has been disagreement as to the relationship between AcH and EtOH formation in the literature [6, 18, 32, 33, 60, 70, 79-82]. The SSITKA results obtained in this work, however, can be used to provide more insight regarding the mechanism for the formation of EtOH and AcH.

Figure 6.6(a) and (b) show two of the most popular and recently published routes for AcH and EtOH formation during CO hydrogenation. One possibility, 6.6(a), as proposed by Storsaeter et al. [18] and Mei et al. [33], is that some AcH formed on the surface desorbs, while the rest goes through two-step hydrogenation to form EtOH; and the other possibility, 6.6(b), as proposed by Choi and Liu [32], is more complex with EtOH and AcH sharing the same intermediates through -$COCH_3$, which is then hydrogenated to –$CHOCH_3$ and –$HOCCH_3$, precursors for AcH and EtOH, respectively.

If possibility 6.6(a) is true, it requires 2 hydrogenation steps to produce EtOH from AcH. This should result in a higher selectivity to AcH since τ_{AcH} is shorter than τ_{EtOH} ($\tau_{AcH} \approx$ 2.3 s, $\tau_{EtOH} \approx$ 10.4 s) - but this is contradictory to our reaction results since $S_{AcH} \approx S_{EtOH}$. It might be expected that EtOH could also be produced during the readsorption of AcH, but this does not appear to be the case since τ_{EtOH} did not vary with the amount of the catalyst used, within experimental error. This would have happened if readsorption and subsequent reaction played a significant role in the formation of EtOH.

Similarly, using the same reasoning, possibility 6.6(b) would appear not to be valid for our system either. With certain intermediates shared by both AcH and EtOH,

the expected selectivity to AcH should have been larger than that for EtOH because $\tau_{AcH} < \tau_{EtOH}$. Thus, both possibilities 6.6(a) and 6.6(b) can be ruled out with the same reasoning.

However, as is shown in Figure 6.6(c), if adsorbed AcH could further react to form other products, it would be reasonable that the selectivity for AcH was lower than expected, even close to the selectivity for EtOH. However, based on the detailed study of this possibility in Section 6.4.4, this is also unlikely to happen on Rh/SiO_2.

Thus, none of the popular mechanisms presented recently can explain our SSITKA results for the formation of EtOH and AcH. Although the secondary reaction of AcH to form EtOH by hydrogenation cannot be excluded since it is well known that hydrogenation of AcH can be carried out under mild conditions [81], under our reaction conditions, the secondary reaction of AcH to form EtOH on the same active Rh sites does not appear to be a dominant pathway for EtOH formation. Thus, it is highly likely that the mechanism for AcH and EtOH formation is much more complex than expected and cannot be resolved based on our results here.

6.5 Conclusions

In this study, the mechanistic pathways for different product formations in CO hydrogenation on Rh/SiO_2 were for the first time studied at the site level using

multicomponent SSITKA. Different from other products, it was found that neither MeOH nor AcH readsorption could be neglected on Rh/SiO_2 and had to be accounted for. It appears likely that, for Rh/SiO_2, MeOH and CH_4 are produced on different kinds of sites. Moreover, the number of sites producing CH_4 on such a catalyst surface is more than 100 times larger than those producing MeOH. It is also unlikely that MeOH shares any intermediates with C_2 products (hydrocarbons and oxygenates). By comparing different currently proposed possibilities for AcH and EtOH formation, it is concluded that the actual mechanism for the formation of these products is complicated and needs further investigation.

6.6 Acknowledgments

We acknowledge financial support from the U. S. Department of Energy (Award No 68 DE-PS26-06NT42801). We thank Drs. YongMan Choi and Ping Liu for their explanation about their cutting-edge microkinetic modeling work. Jia Gao also thanks Dr. Nattaporn Lohitharn for discussions about the SSITKA system set up.

6.7 References

[1] J.R. Rostrup-Nielsen, in "Catalysis-Science and Technology" (J. R. Anderson and M. Boudart, Eds.) Vol. 5. Springer-Verlag, Berlin / New York, 1984.

[2] I. Wender, Catal. Rev. Sci. Eng. 14 (1976) 97.

[3] J.J. Spivey, A.A. Egbebi, Chem. Soc. Rev. In Press (2007).

[4] M. Ichikawa, Bull. Chem. Soc. Jpn. 51 (1978) 2273.

[5] M. Ichikawa, J. Chem. Soc., Chem. Commun. 13 (1978) 566.

[6] R.P. Underwood, A.T. Bell, Appl. Catal. 21 (1986) 157.

[7] R.P. Underwood, A.T. Bell, Appl. Catal. 34 (1987) 289.

[8] F. Fischer, H. Tropsch, *Brennst.* Chem. 4 (1923).

[9] B. Sarup, B.W. Wojciechowski, Can. J. Chem. Eng. 67 (1989) 620.

[10] B. Sarup, B.W. Wojciechowski, Can. J. Chem. Eng. 67 (1989) 62.

[11] I.C. Yates, C.N. Satterfield, Energy Fuels 5 (1991) 168.

[12] J.M.H. Lo, T. Ziegler, J. Phys. Chem. C 111 (2007) 11012.

[13] G.P. van der Laan, A.A.C.M. Beenackers, Appl. Catal., A 193 (2000) 39.

[14] C.S. Kellner, A.T. Bell, J. Catal. 70 (1981) 418.

[15] C.G. Takoudis, Ind. Eng. Chem. Pro. Res. Dev. 23 (1984) 149.

[16] N. V. Pavlenko, Y.I. Pyatnitskii, Theor. Exp. Chem. 33 (1997) 254.

[17] A. I. Tripol'skii, N. V. Pavlenko, G.D. Zakumbaeva, Theor. Exp. Chem. 33 (1997) 165.

[18] S. Storsaeter, D. Chen, A. Holmen, Surface Science 600 (2006) 2051.

[19] O.R. Inderwildi, S.J. Jenkins, D.A. King, J. Phys. Chem. C 112 (2008) 1305.

[20] C. Mazzocchia, P. Gronchi, A. Kaddouri, E. Tempesti, L. Zanderighi, A. Kiennemann, J. Mol. Catal. A: Chem. 165 (2001) 219.

[21] B.H. Davis, Fuel Process. Technol. 71 (2001) 157.

[22] C.F. Huo, Y.W. Li, J.G. Wang, H.J. Jiao, J. Phys. Chem. C 112 (2008) 14108.

[23] M.A. Vannice, J. Catal. 37 (1975) 449.

[24] I.A. Fisher, A.T. Bell, J. Catal. 162 (1996) 54.

[25] K.J. Williams, A.B. Boffa, M. Salmeron, A.T. Bell, G.A. Somorjai, Catal. Lett. 9 (1991) 415.

[26] G.A. Huff, C.N. Satterfield, Ind. Eng. Chem. Res. 23 (1984) 696.

[27] Y. Mori, T. Mori, T. Hattori, Y. Murakami, Appl. Catal. 66 (1990) 59.

[28] E. Shustorovich, A.T. Bell, J. Catal. 113 (1988) 341.

[29] Y. Mori, T. Mori, T. Hattori, Y. Murakami, Appl. Catal. 55 (1989) 225.

[30] S. Shetty, A.P.J. Jansen, R.A. van Santen, J. Am. Chem. Soc. 131 (2009) 12874.

[31] M.K. Zhuo, K.F. Tan, A. Borgna, M. Saeys, J. Phys. Chem. C 113 (2009) 8357.

[32] Y. Choi, P. Liu, Journal of the American Chemical Society 131 (2009) 13054.

[33] D. Mei, R. Rousseau, S.M. Kathmann, V.-A. Glezakou, M.H. Engelhard, W. Jiang, C. Wang, M.A. Gerber, J.F. White, D.J. Stevens, J. Catal. 271 (2010) 325.

[34] S.L. Shannon, J.G. Goodwin, Jr., Chem. Rev. 95 (1995) 677.

[35] P. Biloen, J. Mol. Catal. 21 (1983) 17.

[36] C.O. Bennett, Acs Symposium Series 178 (1982) 1.

[37] J. Happel, Chem. Eng. Sci. 33 (1978) 1567.

[38] N. Lohitharn, J. G. Goodwin, Jr., J. Catal. 257 (2008) 142

[39] K. Sudsakorn, J.G. Goodwin, Jr., A.A. Adeyiga, J. Catal. 213 (2003) 204.

[40] C.A. Mims, L.E. Mccandlish, J. Am. Chem. Soc. 107 (1985) 696.

[41] C.A. Mims, L.E. Mccandlish, J. Phys. Chem. 91 (1987) 929.

[42] D.M. Stockwell, D. Bianchi, C.O. Bennett, J. Catal. 113 (1988) 13.

[43] S.H. Ali, J.G. Goodwin, Jr., J. Catal. 176 (1998) 3.

[44] S.H. Ali, J.G. Goodwin, Jr., J. Catal. 171 (1997) 333.

[45] S.H. Ali, J.G. Goodwin, Jr., J. Catal. 171 (1997) 339.

[46] S.H. Ali, J.G. Goodwin, Jr., J. Catal. 170 (1997) 265.

[47] S. Vada, B. Chen, J.G. Goodwin, J. Catal. 153 (1995) 224.

[48] V. Froseth, S. Storsaeter, O. Borg, E.A. Blekkan, M. Ronning, A. Holmen, Appl. Catal., A 289 (2005) 10.

[49] C.A. Mims, Catal. Lett. 1 (1988) 293.

[50] D.M. Stockwell, C.O. Bennett, J. Catal. 110 (1988) 354.

[51] D.M. Stockwell, J.S. Chung, C.O. Bennett, J. Catal. 112 (1988) 135.

[52] K.R. Krishna, A.T. Bell, J. Catal. 130 (1991) 597.

[53] P. Winslow, A.T. Bell, J. Catal. 86 (1984) 158.

[54] T.E. Hoost, J.G. Goodwin, Jr., J. Catal. 137 (1992) 22.

[55] A.M. Efstathiou, T. Chafik, D. Bianchi, C.O. Bennett, J. Catal. 148 (1994) 224.

[56] A.M. Efstathiou, T. Chafik, D. Bianchi, C.O. Bennett, J. Catal. 147 (1994) 24.

[57] A.M. Efstathiou, T. Chafik, D. Bianchi, C.O. Bennett, Stud. Surf. Sci. Catal. 75 (1993) 1563.

[58] A.M. Efstathiou, C.O. Bennett, J. Catal. 120 (1989) 137.

[59] A.M. Efstathiou, C.O. Bennett, Chem. Eng. Commu. 83 (1989) 129.

[60] S.D. Jackson, B.J. Brandreth, D. Winstanley, J. Catal. 106 (1987) 464.

[61] T. Koerts, W.J.J. Welters, R.A. van Santen, J. Catal. 134 (1992) 1.

[62] T. Koerts, R.A. van Santen, J. Catal. 134 (1992) 13.

[63] S.S.C. Chuang, M.A. Brundage, M.W. Balakos, Appl. Catal. A 151 (1997) 333.

[64] S.S.C. Chuang, R.W. Stevens, Jr., R. Khatri, Top. Catal. 32 (2005) 225.

[65] N.P. Socolova, Colloid Surface A 239 (2004) 125.

[66] H. Hayashi, M. Kishida, K. Wakabayashi, Catal. Surv. Jpn. 6 (2002) 9.

[67] J. Gao, X. Mo, A.C. Chien, W. Torres, J.G. Goodwin, Jr., J. Catal. 262 (2009) 119.

[68] A. Egbebi, J.J. Spivey, Catal. Commun. 9 (2008) 2308.

[69] J.G. Goodwin, Jr., S. Kim, W.D. Rhodes, Catalysis 17 (2004) 320.

[70] A. Takeuchi, J.R. Katzer, R.W. Crecely, J. Catal. 82 (1983) 474.

[71] J.T. Yates, P.A. Thiel, W.H. Weinberg, Surf Sci 84 (1979) 427.

[72] X. Mo, J. Gao, N. Umnajkaseam, J.G. Goodwin, Jr., J. Catal. 267 (2009) 167.

[73] A. Bertucco, C.O. Bennett, Appl. Catal. 35 (1987) 329.

[74] P.R. Watson, G.A. Somorjai, J. Catal. 72 (1981) 347.

[75] A.L. Borer, R. Prins, Stud. Surf. Sci. Catal. 75 (1993) 765.

[76] H. Arakawa, K. Takeuchi, T. Matsuzaki, Y. Sugi, Chem. Lett. 9 (1984) 1607.

[77] M. Ojeda, S. Rojas, M. Boutonnet, F.J. Perez-Alonso, F.J. Garcia-Garcia, J.L.G. Fierro, Appl. Catal., A 274 (2004) 33.

[78] H. Kusama, K.K. Bando, K. Okabe, H. Arakawa, Appl. Catal., A 197 (2000) 255.

[79] Y. Wang, H.Y. Luo, D.B. Liang, X.H. Bao, J. Catal. 196 (2000) 46.

[80] H. Orita, S. Naito, K. Tamaru, J. Catal. 90 (1984) 183.

[81] R. Burch, M.I. Petch, Appl. Catal., A 88 (1992) 61.

[82] M. Ichikawa, T. Fukushima, J. Chem. Soc., Chem. Commun. 6 (1985) 321.

CHAPTER SEVEN

SUMMARY

Ethanol, due to its low cost and low pollution emission in use, may be a viable gasoline alternative and a solution to the energy crisis in the future. Rh-based catalysts are known for their unique ability to catalyze ethanol synthesis from CO hydrogenation. Thus, there has been increasing interests in experimental and theoretical studies related to CO hydrogenation on Rh-based catalysts.

A study of the combined promoting effect of La and V oxides for ethanol formation during CO hydrogenation on silica-supported Rh catalysts was conducted. Non-promoted and La and/or V oxide promoted Rh/SiO_2 catalysts were prepared by sequential or co-impregnation methods and characterized by TEM, CO chemisorption and FT-IR. Their catalytic properties for CO hydrogenation were investigated using a differential fixed bed reactor at 230°C and 1.8 atm. It was found that, compared to non-promoted Rh/SiO_2, the singly promoted catalysts, $Rh\text{-}La/SiO_2$ and $Rh\text{-}V/SiO_2$, showed improved reactivity (3x) and better ethanol selectivities. However, the doubly promoted $Rh\text{-}La\text{-}V/SiO_2$ catalysts showed even higher activity (9x) and selectivity for ethanol and other C_{2+} oxygenates, with the selectivity of total C_{2+} oxygenates > 30% at these low pressure reaction conditions. The better performance of the $Rh\text{-}La\text{-}V/SiO_2$ catalysts appears to be due to a synergistic promoting effect of the combined La and V additions

through intimate contact with Rh. Use of just more of each promoter by itself was not able to produce the enhanced catalytic performance.

It has been reported widely that for Rh-based catalysts, promoters play an important role in catalyst activity and selectivities. Thus, the effects of the addition of La, V and/or Fe promoters on the kinetics of formation of various products were determined and the mechanistic pathways delineated using a Langmuir-Hinshelwood approach. It was found that, increasing H_2 pressure resulted in increased activities while increasing CO partial pressure had an opposite effect. However, the specific influence of H_2 or CO partial pressure on the activity and selectivities differed greatly with different promoters. There was a more significant change in activity of the La-V doubly promoted Rh catalyst with H_2 or CO partial pressure than for other catalysts, which may be due to a synergistic effect between La and V. The Fe singly promoted catalyst showed different trends in both rate and selectivity from other catalysts, suggesting a different promoting mechanism than La or V. Based on the fact that hydrogen-assisted CO dissociation has been reported to best describe the mechanism for Rh catalysts, Langmuir-Hinshelwood rate expressions for the formation of methane and of ethanol were derived and compared to the experimentally derived power law parameters. It was found that the addition of different promoters appeared to result in different rate limiting steps.

It has been suggested that the behavior of group VIII metal catalysts supported on transition metal oxides can be significantly affected by pretreatment conditions due to strong metal-oxide interactions. However, the origins for the SMOI effect are still in

debate. In this research, SMOI of Rh and vanadium oxide (as a promoter) supported on SiO_2 was studied at the site level for the first time, which provided an insight into the modification of surface properties after high temperature reduction. H_2 chemisorption, Fischer-Tropsch synthesis (FTS), and SSITKA were used to probe the SMOI effects. The catalytic properties of the catalysts for CO hydrogenation were investigated using a differential fixed bed reactor at 230°C and 1.8 atm, while for SSITKA, the reaction temperature was raised to 280°C and an excess of H_2 is used to maximize methane production. The addition of V to Rh/SiO_2 was found to suppress H_2 chemisorption, and high reduction temperature further decreased H_2 chemisorption on $Rh/V/SiO_2$ but had little effect on Rh/SiO_2. As reduction temperature increased, the activity for CO hydrogenation on Rh/SiO_2 remained essentially unchanged, but the activity of $Rh/V/SiO_2$ decreased significantly. It was found by SSITKA that the concentration of surface reaction intermediates decreased on $Rh/V/SiO_2$ as the reduction temperature increased, but the activities of the reaction sites increased. The results suggest that the decrease of amount of active sites due to the coverage of Rh by VO_x species is probably the main reason for the decreased overall activity induced by high reduction temperature. Surprisingly, new sites with higher activity appear to be formed probably at the Rh-VO_x interface.

Moreover, in this study, the mechanism of C_1 and C_2 hydrocarbon and oxygenate formation during CO hydrogenation on Rh/SiO_2 was for the first time investigated in detail using multiproduct SSITKA. This was also the first effort to explore at the site level the relationship between similar products [e.g., EtOH vs. AcH] on Rh/SiO_2. During

CO hydrogenation at 250°C and 1.8 atm, the selectivity to CH_4 was higher than any other product but the surface reaction residence time for CH_4 formation was not the shortest among all the products. The surface reaction residence time for C_2 hydrocarbons was longer than that for any other product (C_1-C_2). Even though the selectivities to AcH and EtOH were similiar, their surface reaction residence times differed significantly. Based on the SSITKA results, MeOH and CH_4 appear to be produced on completely different active sites. Moreover, C_2 hydrocarbons do not appear to be formed from adsorbed AcH. It is likely, however, that all C_2 products share at least one intermediate with CH_4, but none with MeOH. Several recently proposed pathways for EtOH and AcH formation are presented and compared to our results. The secondary reaction of AcH to form EtOH on the same sites does not appear to be a dominant pathway for EtOH formation. However, the precise mechanism for EtOH formation still needs further investigation.

APPENDICS

APPENDIX A

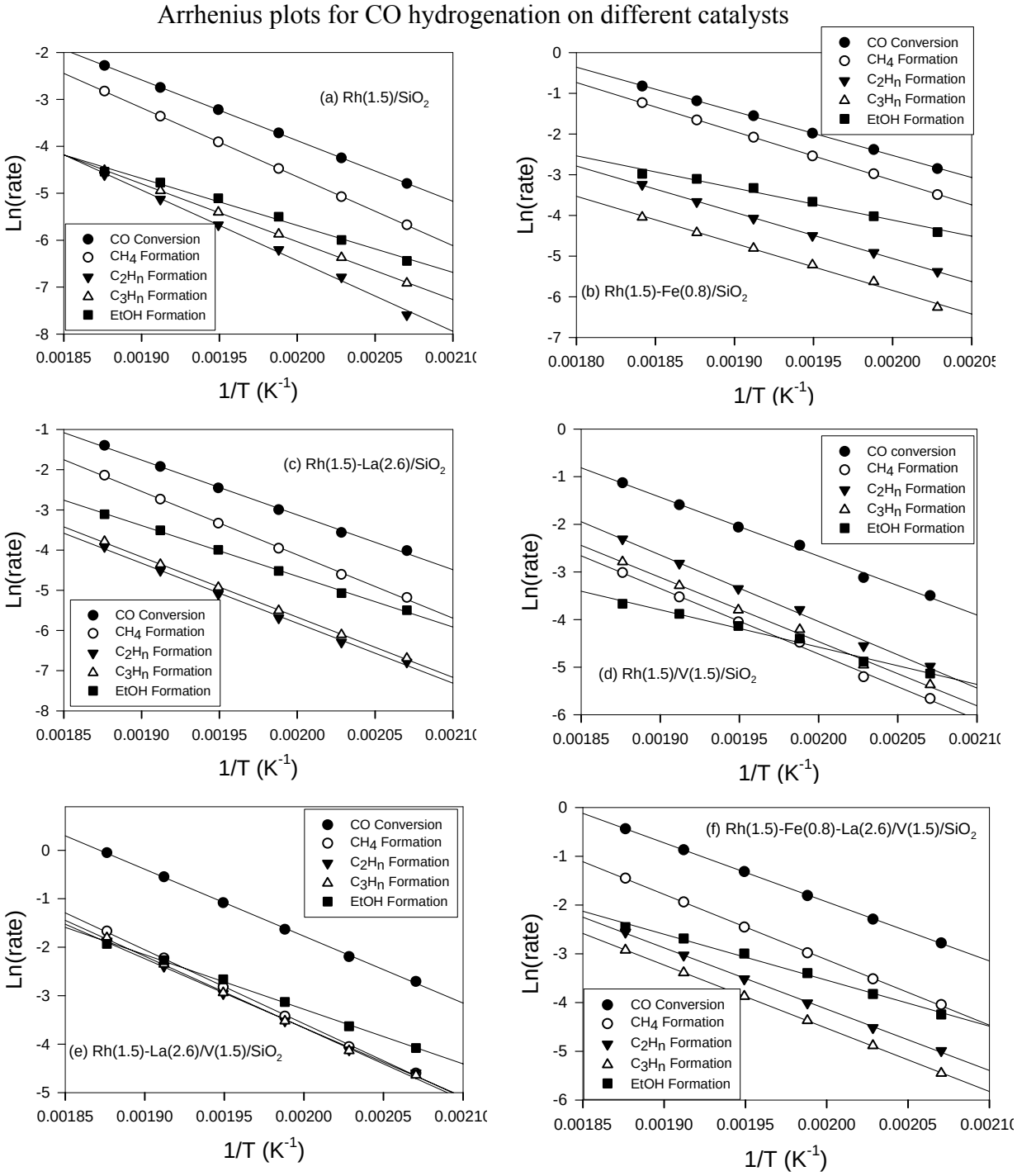

Figure A.1 Arrhenius plots for (a) $Rh(1.5)/SiO_2$, (b) $Rh(1.5)\text{-}Fe(0.8)/SiO_2$, (c) $Rh(1.5)\text{-}La(2.6)/SiO_2$, (d) $Rh(1.5)/V(1.5)/SiO_2$, (e) $Rh(1.5)\text{-}La(2.6)/V(1.5)/SiO_2$, and (f) $Rh(1.5)\text{-}Fe(0.8)\text{-}La(2.6)/V(1.5)/SiO_2$.

APPENDIX B

SSITKA results for different product formation on promoted Rh catalysts

Table B.1 The surface reaction kinetic parameters for different products on the Fe promoted Rh catalysts. [a]

$Rh(1.5)\text{-}Fe(0.8)/SiO_2$					
Product [h]	Rate [b] (μmol of C/g/s)	%HC Selectivity [c]	τ_i [d] (s)	$TOF_{ITK,\,i}$ [e] (s^{-1})	N_i [f] (mol of C/g)
CH_4	0.155	67.6	2.6	0.38	0.41
C_2H_n [g]	0.017	7.2	12.7	0.08	0.21
MeOH	0.013	5.6	5.6	0.18	0.07
AcH	0.005	2.3	8.1	0.12	0.04
EtOH	0.027	11.9	8.4	0.12	0.23
$Rh(1.5)\text{-}Fe(0.8)\text{-}La(2.6)/V(1.5)/SiO_2$					
Product [h]	Rate [b] (μmol of C/g/s)	%HC Selectivity	τ_i [d] (s)	$TOF_{ITK,\,i}$ [e] (s^{-1})	N_i [f] (mol of C/g)
CH_4	0.189	32.7	1.2	0.85	0.22
C_2H_n [g]	0.141	15.9	22.5	0.04	3.18
MeOH	0.019	3.2	5.5	0.18	0.10
AcH	0.034	5.9	6.2	0.16	0.21
EtOH	0.141	24.3	9.2	0.11	1.29

[a] 0.6 g catalyst was diluted by 2.4 g α-Al_2O_3. Reaction was carried out at 250 °C; P = 1.8 atm, flow rate = 30 mL/min (H_2:He:CO = 6:1:3). The analysis was done 15 h after reaction began and steady state was reached.

[b] Steady-state rate.

[c] Molar selectivity = $n_iC_i / \sum n_iC_i$.

[d] Residence time.

[e] $TOF_{ITK,\,i} = 1/\tau_i$.

[f] $N_i = Rate_i * \tau_i$.

[g] Hydrocarbons with 2 carbons.

[h] Experimental errors of all the results for CH_4 and C_2H_n are ±5%; experimental errors of all the results for MeOH and AcH are ±12%; Experimental errors of all the results for EtOH are ±8%.

Table B.2 The surface reaction kinetic parameters for different products on the La and/or V promoted Rh catalysts. [a]

$Rh(1.5)\text{-}La(2.6)/SiO_2$					
Product [h]	Rate [b] (μmol of C/g/s)	%HC Selectivity	τ_i [d] (s)	$TOF_{ITK,\,i}$ [e] (s^{-1})	N_i [f] (μmol of C/g)
CH_4	0.170	53.1	4.4	0.23	0.75
C_2H_n [g]	0.024	7.4	19.3	0.05	0.46
MeOH	0.006	1.8	5.1	0.20	0.03
AcH	0.011	3.4	4.9	0.21	0.05
EtOH	0.044	13.7	8.2	0.12	0.36
$Rh(1.5)/V(1.5)/SiO_2$					
Product [h]	Rate [b] (μmol of C/g/s)	%HC Selectivity	τ_i [d] (s)	$TOF_{ITK,\,i}$ [e] (s^{-1})	N_i [f] (μmol of C/g)
CH_4	0.063	18.2	1.8	0.55	0.12
C_2H_n [g]	0.087	25.1	19.1	0.05	1.66
MeOH	0.006	1.7	6.1	0.16	0.04
AcH	0.008	2.4	4.2	0.24	0.04
EtOH	0.032	9.3	8.6	0.12	0.27
$Rh(1.5)\text{-}La(2.6)/V(1.5)/SiO_2$					
Product [h]	Rate [b] (μmol of C/g/s)	%HC Selectivity	τ_i [d] (s)	$TOF_{ITK,\,i}$ [e] (s^{-1})	N_i [f] (μmol of C/g)
CH_4	0.351	26.8	3.2	0.31	1.13
C_2H_n [g]	0.182	13.9	19.1	0.05	3.47
MeOH	0.011	0.9	6.1	0.16	0.07
AcH	0.072	5.5	5.7	0.17	0.41
EtOH	0.169	12.9	8.8	0.11	1.49

[a] 0.6 g catalyst was diluted by 2.4 g α-Al_2O_3. Reaction was carried out at 250 °C; P = 1.8 atm, flow rate = 30 mL/min (H_2:He:CO = 6:1:3). The analysis was done 15 h after reaction began and steady state was reached.

[b] Steady-state rate.

[c] Molar selectivity = $n_iC_i / \sum n_iC_i$.

[d] Residence time.

[e] $TOF_{ITK,\,i} = 1/\tau_i$.

[f] $N_i = Rate_i * \tau_i$.

[g] Hydrocarbons with 2 carbons.

[h] Experimental errors of all the results for CH_4 and C_2H_n are ±5%; experimental errors of all the results for MeOH and AcH are ±12%; Experimental errors of all the results for EtOH are ±8%.